Master's Thesis

Supervisor: Associate Professor Dr. Yukio Koibuchi

An Integrated Approach in the Determination of Optimum Condition and Controlling Factors for Coral Reef Distribution in the Case of Ibaruma Coast, Ishigaki Island, Okinawa, Japan.

Desiree Eve Reyes MAAÑO

Student ID No. 47-126865

Graduate School of Frontier Sciences

Department of Socio-Cultural Environmental Studies

THE UNIVERSITY OF TOKYO

July 31, 2014

ABSTRACT

In the near shore areas of Ibaruma, Ishigaki Island, Okinawa Prefecture, Japan, the information about specific environmental parameters which significantly control the distribution of the reef, as well as identification of optimum condition for corals, is particularly important in its current restoration and coral transplantation activities. Using a methodological approach which integrates field observation, GIS mapping, numerical-wave simulation and SST remote sensing, it was identified that the most controlling factor in the case of Ibaruma is depth. Moreover, the correlations between the coral reef distribution and the range of environmental factors considered in this study (depth, PAR, sea surface temperature, total energy dissipation, significant wave height and orbital velocity near the bottom) were determined, as well as the optimum conditions for corals. The findings of this study have underscored and confirmed the possibility of overlaying and mapping the various environmental factors in order to understand the complex interaction happening in a coral reef ecosystem on a local scale.

ACKNOWLEDGEMENT

About two years ago, I came here in Japan, and was assigned to Westech Laboratory without any knowledge about foundations on coastal engineering, computer programming/numerical modeling and GIS. All I have with me were my minute skills in identifying marine organisms and keen interest in understanding them, as I thought I was entering into a marine biology laboratory. Little did I know that I will be later on dealing with stuff that all my life, I have always avoided with- math, physics, and engineering. But anyhow, there was no point in backing out then, since this time, I can't just easily run back to Philippines, it's just too far, and too costly. So I made a decision to continue my masters, take advantage of being able to be one of the "Todai" students, and learn something no matter what. I tried to embrace my research, even if I had to change my topic/direction for countless of times, cried over simple equations that I cannot derive, and learn the hard way most of the times.

That was two years ago. Today, I am nothing but thankful that I made that decision. As I hand in this thesis, I can't help but to feel a bit proud and grateful that I finally able to complete my research. Nevertheless, perhaps the most important thing is that, I was able to learn things way beyond I expected, i.e., GIS, numerical modeling, a bit of coastal engineering foundations, to name a few. But of course, this learning and the completion of my thesis wouldn't be possible without the help of numerous people who supported my journey in completing my masters' degree in Environmental Studies in The University of Tokyo, Graduate School of Frontier Sciences, under the Division of Environmental Studies, Department of Socio-Cultural Environmental Studies.

First and foremost, I owe my adviser, Dr. Yukio Koibuchi, a debt of gratitude that can never fully be repaid. He had changed my views about coral reefs and science of engineering, and he provided steadfast support, direction, and tremendous patience while I was doing my research. I am also equally thanking Dr. Jun Sasaki of our laboratory and Dr. Masahiko Isobe who is now in Kochi University, who imparted valuable insights to my research especially during the time that I was still learning about wave numerical modeling. I could never thank enough these three professors who had led me to appreciate the field of coastal engineering.

I am also expressing my special thanks to my co-advisers/ master's thesis committee, Dr. Takashi Mino and Dr. Hiroyasu Satoh, both from the Department of Socio-Cultural Environmental Studies of Division of Environmental Studies, The University of Tokyo, for providing additional support and critical view for the improvement of my research.

My appreciation is also extended to the members of my laboratory- Water Environment Science and Technology Laboratoty (Westech), especially to Mr. Hiroto Higa, who has been also my tutor, for always extending a hand and teaching me about basic research skills and some tools for analysis, as well as for all the research idea-discussions. The same is extended to Dr. HaeChong O, our post doc lab member, for providing additional insights about my research, and more importantly, for his endless encouragement.

Furthermore, I would like to extend the recognition to all the professors and experts in the field of oceanography, GIS, Statistics, and SWAN numerical model whom I met through online discussion groups and forums, as well as to my previous research advisers in the University of the Philippines. Thank you for all the patience and time answering all my technical queries and for providing additional inputs to my research.

Perhaps, I wouldn't be able to complete my thesis if without the remarkable help from my support group here in Japan. I would like to thank most especially, Ms. Tiffany Larraine Chua, my roommate and friend, for not only editing and proof-reading my thesis manuscript, but for always being able to be the source of light during the hard times I have had throughout my stay here in Japan. The same is extended to Ms. Johanna Cuadra, Ms. Shu Kuan Wong, Ms. Dyah Fatma, and to Mr. Victor Tumilba.

Despite the distance, I am also forever grateful to all my friends in the Philippines (Iris, Rachel, Arvin, Sir-Lolo Carlo Custodio, Ate Marianne Pan), who are always there virtually, as well as to those who are in the other parts of the world, Ms. Soulichan Lamxay of National University of Laos and Mr. James Patrick Santiago of Washington State University, for their endless support and encouragement, and for pushing and believing in me that I can finish this thesis.

Most importantly, I would like to sincerely thank the Asian Development Bank-Japan Scholarship Program (ADB-JSP) for their funding assistance so I can continue higher degree of studies here in Japan. This promising opportunity has led me to learn and experience things way beyond I expected here in Japan, which will surely be useful as I could apply all of these in the contribution to the development of my home country.

Lastly, I would like to thank my family, my parents and my five brothers, for their unselfish love and understanding, for all the support and advices, which always inspire me to never stop chasing my dreams.

Table of Contents

LIST OF FIGURES

LIST OF TABLES

CHAPTER 1: INTRODUCTION

1.1 General Introduction

Coral reefs are amongst the most invaluable ecosystems mostly found in the shallow waters of tropical regions. They bring colossal benefits that include provision of food and nutrition for coastal communities, coastal protection (Johnson & Marshall 2007), biodiversity, habitat to diverse aquatic species (Spalding, *et al*., 2001), cultural heritage, and income through fishing, tourism and recreation (Moberg & Folke, 1999; Ahmed, *et al*., 2005). A recent economic valuation reported by the United States agency NOAA (National Oceanic and Atmospheric Administration) estimated that the value of economic and ecological services that the coral reef ecosystem provides equals to about $375 billion per year.

However, coral reefs are depleting at an alarming rate. This has long been regarded as a worldwide issue as it brought tangible losses to global biological diversity and in socio-economic and ecological realms. Most of the world's coral reefs are damaged due to pressures brought by natural catastrophes (e.g., severe storms, tsunamis, ocean acidification, predation, diseases, and temperature stress) and anthropogenic activities (e.g., pollution, unsustainable fishing and tourism practices, dredging, and sedimentation) (McCulloch, *et al*., 2003; Belwood, *et al*., 2004; Harvell, 2002). It was estimated that 19% of the world's original coral reef areas are already lost and about 35% are critically at risk within the next 20-40 years if there are no countermeasures undertaken and if global climate threats continue to escalate (Wilkinson, 2008).

With the aforementioned risks faced by the coral reef ecosystem, several efforts have been made in order to conserve, sustain, and restore degraded reefs to prevent their extinction (Hoegh-Guldberg, 2006). Central to these efforts is the intent to sustain the coral reefs' ability to deliver ecosystem's goods and services. In order to achieve this outcome, it is therefore critical to have a better understanding of specific environmental drivers of coral reef distribution, as well as enhanced scientific concept of what comprises a healthy reef so it will be possible to predict coral community's responses to multiple ecosystems' stressors (Bauman, *et al*., 2013).

A sound knowledge about the precise description of spatial patterns and structure of reef system including the determination of optimum habitat condition for coral growth is necessary whether in assessing their condition, estimating the risks brought by ecosystems' stressors, or in coral reef restoration efforts (Andréfouët, 2006). Identification of which, among the myriad of environmental parameters in an area is the most influential to the reef biogeography has a profound implications for restoration of degraded reefs and will better enable researchers and local conservation managers to apply and design appropriate conservation measures. Although this question has long been pursued, it is only during this recent years that significant advances in terms of availability of environmental datasets and assessment methodologies reflecting technological improvements have been made (Couce, *et al*., 2012; Andréfouët, 2006) . These advances, including remote sensing, numerical simulations, as well as GIS (geographic information system) and mapping, coupled with field observation, have aided coral reef researchers and scientists in a better understanding of what controls the coral reef distribution.

1.2 Review of Related Literature

Before discussing the effects of different environmental variables to the corals, a background description of coral biology/ecology will be first explained, followed by the review of related studies. In this study, the scleractinian corals or the hard corals are the one considered for investigation as they are the one capable of reef building activities and can collectively form the primary structure of the coral reef in the tropical areas over time.

1.2.1 Corals and Coral Reefs, definition and biology.

Scleractinian corals, also known as the hard corals or stony corals, are animals which are capable of building coral reef structures in the ocean. They are mostly colonial, but some exist in solitary. A colony of coral is composed of tiny individual soft-bodied polyp animals, wherein when these colonies are combined together, it functions as a single organism connected by a transport of nutrients. A hard skeleton made up of calcium carbonate is found at the base of the polyps, which is known as calicle. This calicle forms the structure of the coral reefs and serves a a protective housing for the polyps. Those colonial corals are the ones which are capable of becoming the reef builders (Veron, 2011).

Corals, in general, exist symbiotically with algae, (mostly by zooxanthallae). These one-celled algae live inside the sac of each polyp. Since these algae are photosynthetic organisms, they require sunlight, which makes the corals, in general, dependent to sunlight. As a product of photosynthesis, zoonxanthallae provides oxygen and other nutrients to the polyps of the coral, which they need in order to survive. In return, the polyps provide the zooxanthallae the carbon dioxide which they need in order to perform photosynthesis together with sunlight. For these reasons, most of the reef building corals are found at the warm tropical areas in the world. Moreover, it is the zooxanthallae which gives the vibrant colors of the corals, and not the corals itself.

Coral reefs on the other hand, are large, robust marine structures, which usually form ridges or mounds, and are built as a result of the deposition of limestone (calcium carbonates) typically by corals, or by other living organisms, which can secrete $CaCO3$ as part of their metabolic activities. (INA & EC., 2010; Done, 2011). Fully formed coral reefs may take a geologic time scale to develop.

The formation of reefs start when the larval polyp attaches itself to a rock on the sea floor. Through the time, this polyp undergoes sexual and asexual reproduction and clones itself to a thousand replicates, creating colonies, which, as mentioned earlier, are regarded as a single organism. These colonies are connected to one another by the calicles. Over a geologic period of time, these colonies grow and connect and attach to each other, building to a what we call now coral reef.

1.2.2. Factors affecting the corals

For both local and geographical scales, the distribution and development of coral reefs are governed by various and frequently interacting environmental factors such as temperature, light, salinity, solar radiation, sedimentation, water quality and hydrodynamic variables (Bauman, *et al*., 2013; Kleypas, *et al*., 1999). A number of studies have been conducted to investigate how these individual factors independently influence the coral reef distribution (e.g., Risk, 2014; Edmunds & Gray, 2014; Hongo & Yamano, 2013; Margolin, 2012; Davies, *et al*., 2008; Glynn & Stewart, 1973). The most-discussed environmental drivers of reef function and distribution which are included in this study are briefly explained below.

1.2.2.1 Wave Energy / Water movement

Wave energy is one of the environmental factors which plays an important role in the characterization of the reef structure and key ecosystem processes in coral reefs (Gillis, *et al*., 2014; Yoshioka & Yoshioka, 1989; Dollar, 1982). Water fluxes can promote nutrient exchange and flushing of metabolic wastes and toxins (Hearn, 2001), dispersion and settlement of marine juvenile organisms (Abelson & Denny 1997), and reducing the thermal stress during the mixing of the water column thereby shielding the corals during bleaching events (Hearn, 1999). Cyclone waves, however, can be damaging to the reefs by causing abrasion and breakage, even up to the extent of displacement of large coral boulders (Massel, 1993).

Although waves are identified as a critical structuring factor in the reef communities, most of the corals and wave ecology studies classified waves qualitatively — "sheltered/closed" to "exposed" areas, or "high", "medium" or "low" wave energy regimes (e.g., Graham, *et al.*, 2014; Gourlay, 1996; Kilar, 1989). This is mainly because of limited availability of in situ wave data in most of the areas, especially in shallow coastal water regions where most of the corals are concentrated. It was then identified that the relationships comparing the wave energies exerted to the reef morphology and coral species distribution is needed to be investigated quantitatively (Storlazzi, *et al.,* 2002).

Works of Storlazzi, *et al.,* (2002) and Dollar, (1982) identified that the primary forces acting on a coral are drag, lift, weight, and inertia. In their previous studies, it was explained that these forces are a function of the horizontal components of wave orbital velocity, claiming that the data on wave height and period can provide a first order estimation of the forces acting upon coral reefs.

1.2.2.2 Temperature

Studies on the effects of temperature to the coral reef distribution and coral biology are well established. Most of the corals are stenothermal which is defined as organisms that are capable of living or growing within a limited range of temperature only (Glynn & Wellington, 1983). This is the reason why corals are mostly found in tropical regions only. With this, the species distribution and interaction, rates of growth and metabolism, dispersal and survival of marine larvae including susceptibility to diseases, are primarily controlled by temperature in the ocean (Thomas, *et al*., 2004; Harvell, 2002; Dunbar, *et al*., 1994). Prolonged exposure to extreme temperatures can cause thermal stress (~>30 °C) to corals, such as in the case of coral bleaching (Hongo & Yamano, 2013; Jokiels & Coles, 1977). Although most of the studies are concentrated on the effects of elevated temperature to the corals, some studies (e.g., Gates, *et al*., 1992; Jokiels & Coles, 1977) showed that exposing the corals to low temperature is more detrimental than in higher temperature. Their results showed that corals exposed to <18°C lived for only one to two weeks and showed no response of recovery after.

1.2.2.3 Light Intensity

The light intensity is identified as a major control in the presence and or absence of corals in the ocean, and has been the subject of most of the coral reef studies aside from temperature (Muscatine, 1990). Findings of these studies concluded that light intensity plays a crucial role not only in the photosynthetic activities of the coral symbiont, *Zooxanthallae*, but also in the calcification rates which is vital in reef building activities of corals (Rinkevich & Loya, 1984). In addition to that, light affects coral larvae settlement (Lewis, 1974), which subsequently controls and shapes the reef morphology (Mundy & Babcock, 1998).

In terms of light response studies in corals, one of the parameters being measured or investigated most is the PAR, or Photosynthetically Active Radiation. PAR is defined as the spectral range of visible light energy with wavelengths measuring from 400 to 700 nm which can be absorbed by photosynthetic organism (McCree, 1972). Studies revealed that PAR present in very high levels can be damaging to the corals (Lesser & Farell, 2004). Consequently, lower PAR inhibits the growth of corals since photosynthesis is limited (Kleypas, 1999).

Aside from the abovementioned controlling factors in the reef distribution, other environmental variables which are also elemental in the coral reef distribution are depth/bathymetry, turbidity, sediment/substrate type, water/ocean current including upwelling and or nearness to the deep water, water quality, and presence and frequency of destructive typhoons and cyclones in the area. These variables are somehow related to each other, for instance, Kleypas, (1999) explained that the light that reaches the coral reefs is a function of three major variables: (a) the direct light reaching the sea surface, which is then a function of the sun angle and atmospheric attenuation; (b) the light attenuation with water depth, which is a function of water clarity, (and can also be correlated with turbidity and sedimentation); and (c) depth. Insufficient light availability and high sediment deposition rates are controlling factors that limit the development of coral reef, which is in turn related to the type of substrate bottom in the area (Roy & Smith, 1970). During extreme cyclone or typhoon events, sediments can be carried horizontally or down the slope which can often cover a fraction or whole part of coral colonies (Fabricius, *et al*., 2008). The extent of the damage to the corals brought by storms and typhoons are associated to the magnitude of wave energy they transmit (e.g., Hongo, *et al*., 2012).

Though many studies have already been done to investigate the effects of these controlling factors to the distribution of coral reefs, as well as the identification of the optimum condition for coral reef growth/development, most of the studies are species-specific and the variables were considered in relative isolation. Some of which are limited to studying in a microenvironment or in a laboratory set-up which may not fully represent the conditions in a natural environment. Moreover, most of these studies merely consider the "presence-only" coral data, which does not account the quality or condition of the coral reef cover.

Currently, studies integrating all environmental factors that affect the coral reefs distribution are still limited (e.g., Kleypas, 1999; Couce *et al*., 2012; Bauman, *et al*., 2013) and to some extent, mostly covered regional scales only. The study of Kleypas, (1999) has been one of the seminal studies which revealed that the reef distribution globally is a function of interacting environmental factors, and that the lower limits of sea surface temperature (SST), light availability, and aragonite saturation state were identified as the main factors in determining the coral reef distribution. In addition, Kelypas' study has also enumerated the optimum conditions or the environmental limits to the presence, growth, and development of coral reefs, but in a global scale. Conversely, these various environmental factors that collectively affect the reef distribution patterns may be different from a regional scale to a local scale, and is driven by area-specific conditions (Huston, 1999).

1.3 Rationale of the study

In the near shore areas of Ibaruma, Ishigaki Island, Okinawa Prefecture, Japan, the information about specific environmental parameters which significantly control the distribution of the reef is particularly important in its current restoration and conservation activities. Investigating the most influential environmental factors where the corals are most abundant may be a useful tool for monitoring and management. In addition, through the process of determining the environmental controlling factors in a local area, optimum condition for the presence of coral reefs can be identified, as well as the environmental stressors present in the area (e.g., heat stress, damaging wave action, etc). The information that can be generated from this can be used in the establishment of habitat suitability indices which can be utilized later on to estimate and locate the most suitable area for transplantation or restoration activities.

The challenge now for the coral reef researchers and local managers is to gather and integrate all available resources for a local coral reef area where data sources are limited. In this study, the correlation between the range of environmental factors and coral reef distributions on a local scale will be investigated using a methodological approach which integrates field observation, GIS mapping, numerical-wave simulation and SST remote sensing.

1.4 Objectives

It is hypothesized in this study that the reef distribution is not always predominantly controlled by a single environmental factor, but it is dependent on the combination of different interacting environmental variables. Ultimately, the goal of this study is to determine where the corals are most abundant and what are the optimum conditions and the controlling factors of such distribution in the area.

To achieve this, the following specific objectives must be satisfied:

(1) to determine coral distribution along Ibaruma Coast;

(2) to identify, quantify, and plot various interacting environmental variables that affects the coral reef distribution: (wave energy, light attenuation, temperature data), and;

(3) to determine the optimum condition for corals based on the identified controlling factors, as well as the presence of environmental stressors in the area (e.g., heat stress).

1.5 Thesis Outline

All chapters in this thesis are self-contained with figures, tables and references. The thesis layout is as follows:

Chapter 1 is the *General Introduction* to this research including the *Rationale of the study* which lays emphasis to the purpose of this study with respect to previous *literature reviews*. This is followed by specific *Objectives.*

Chapter 2 explains in detail the location of the *Study Site* and the *Methodologies* used including brief theoretical explanations to the principles behind the approaches applied to achieve the objectives of this study.

Chapter 3 & Chapter 4 are the core chapters that explain the *Results & Discussions of the analysis*.

Finally, **Chapter 5** consists of *Conclusions and recommendations* of this study.

CHAPTER 2: STUDY SITE SETTING AND METHOD

This chapter provides the framework of the methodology in four sections. The first section outlines the description of the study area, as well as detailing the preliminary coral data collected from monitoring agencies. The second section describes the field survey done in the study area. The third section outlines the different environmental variables included in this study and how they were derived. The fourth section presents the methods used in analysis.

2.1 Study Site

Ibaruma is located on the northeast coast of Ishigaki Island (24° 30' 0" North, 124° 17' 0") which is situated in the southern Ryukyu Islands, Okinawa, Japan (Figure 1a-1b). Since Ishigaki Island is situated in an Asian monsoonal climate region, wind directions change seasonally: approaches from north during winter and from east to south during summer. The water flow pattern is significantly affected by northern winds which is the dominant wind direction throughout the year (Yamano, *et al*., 1998). The average sea-surface temperature (SST) is 24°C in winter and 28°C in summer (Japan Meteorological Agency website). The Ishigaki Island experiences an average of 1.9 typhoons per year (Yamano *et al*. 2000) with wave heights and wave periods greater than 10 m and 10 s, respectively (Hongo, *et al*., 2012), and occasional tsunamis once every 500-1000 years (Kawana & Nakata, 1994 as cited in Hasegawa & Yamano, 2004).

2.1.1 Ibaruma's initial water quality condition and physical environment

Since Ibaruma reefs are situated on the windward side of Ishigaki Island, the water circulation is primarily driven by wind, tidal current, and radiation stresses induced by waves breaking on the reef crest (Yamano, *et al*., 1998). According to the monitoring results facilitated by the Ministry of Environment, International Coral Reef Research and Monitoring Center (ICRRMC), the turbidity of the coral reef water is generally low, especially in Ibaruma coast where there is no outflow discharge (i.e. presence of a river) from adjacent terrestrial area.

The Ibaruma reef, characterized as a fringing reef, encloses a shallow lagoon (Figure 1c-1d) which is about 1000 m wide averaging to around 2.6 m deep during high tide (Hongo, *et al.*, 2012). Since Ibaruma reef faces the open ocean, it is greatly affected by monsoonal change of wind direction, and is exposed to large waves originating from the Pacific swell. It comprises of coral species that are typically windward-high- energy-forming reef (Hongo & Kayanne, 2009).

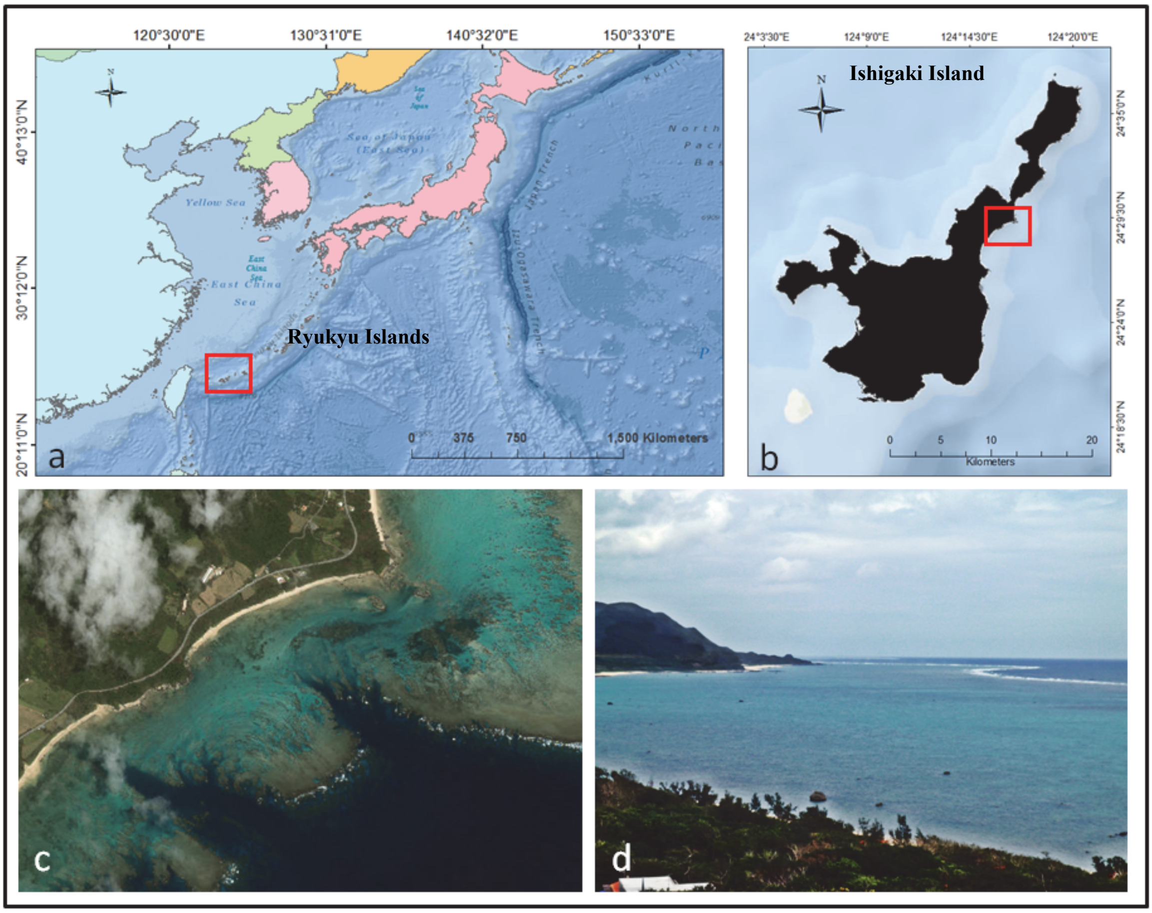

Figure 1. (a) Location map of Ishigaki Island situated at the southern part of Ryukyu Islands, Okinawa; (b) location of Ibaruma Coast in Ishigaki Island; (c) Aerial photo of Ibaruma, and; (d) Actual photo of Ibaruma Coast taken during field observation.

2.1.2 Status of Coral Reefs (Time Series Data)

Preliminary data on the time series coral cover (1998-2010) in Ishigaki Island from the Ministry of Environment-Japan, as well as the most recent coral cover distribution as analyzed from satellite images, were collected to be able to understand the patterns of its distribution.

The results of the coral reef monitoring program showed that relative to the other areas in Ishigaki Island (e.g., Miyara Bay, Sakieda Bay), Ibaruma shows a relatively stable and higher percentage of live coral cover at 70%.

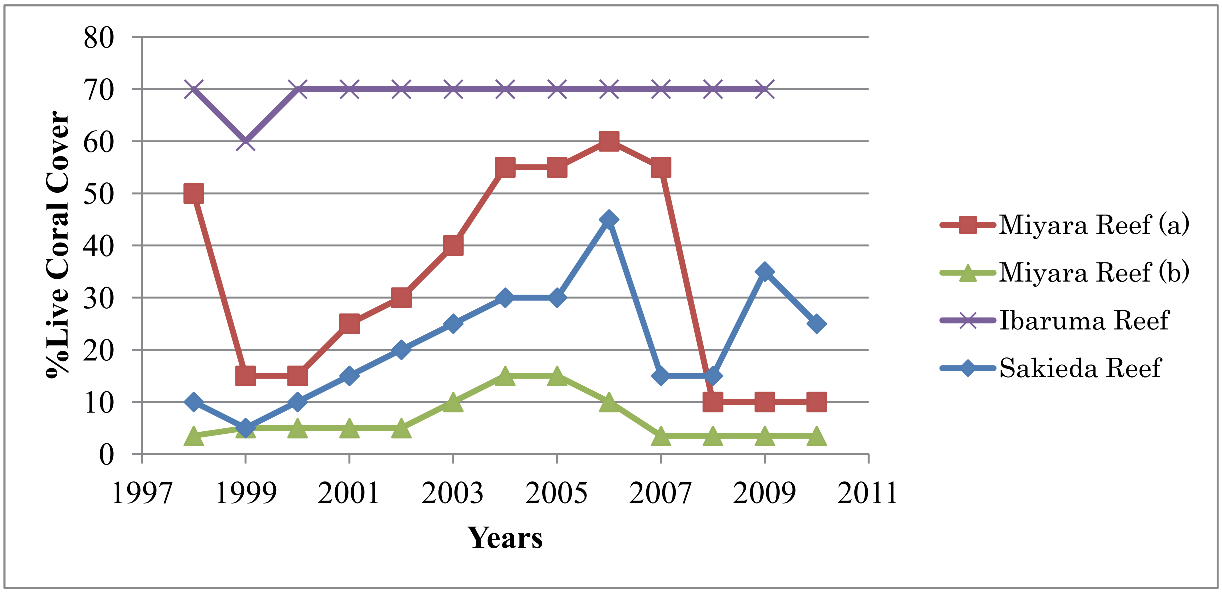

Figure 2. Time series data of % live coral cover at selected reef sites in Ishigaki Island as a result of ICRRMC in situ monitoring for the years 1998-2010.

2.2 Field observation

Field surveys to measure water depths and coral cover distribution in Ibaruma, as well as in situ measurement of photosynthetically active radiation (PAR) values were conducted in February, and June 2013 respectively. Water depths were measured using HydroSurveyorTM M9 (YSI) (Figure 5ab) where it collects bathymetry data and GPS positioning. This instrument has a bottom-tracking algorithm which is used for positioning. The unit is also equipped with depth transducers that operate at 1.0-3.0-MHz for measuring bathymetry. On the other hand, live coral cover was assessed by employing video-transect method (Figure 5c) over an area that is 1100 m along the coast by 800 m across the shore towards the reef crest (Figure 3). PAR values were measured using a light sensor; the measured amount of chlorophyll (ChL) approaches 0 μ mg/L Chl, and exhibits low turbidity.

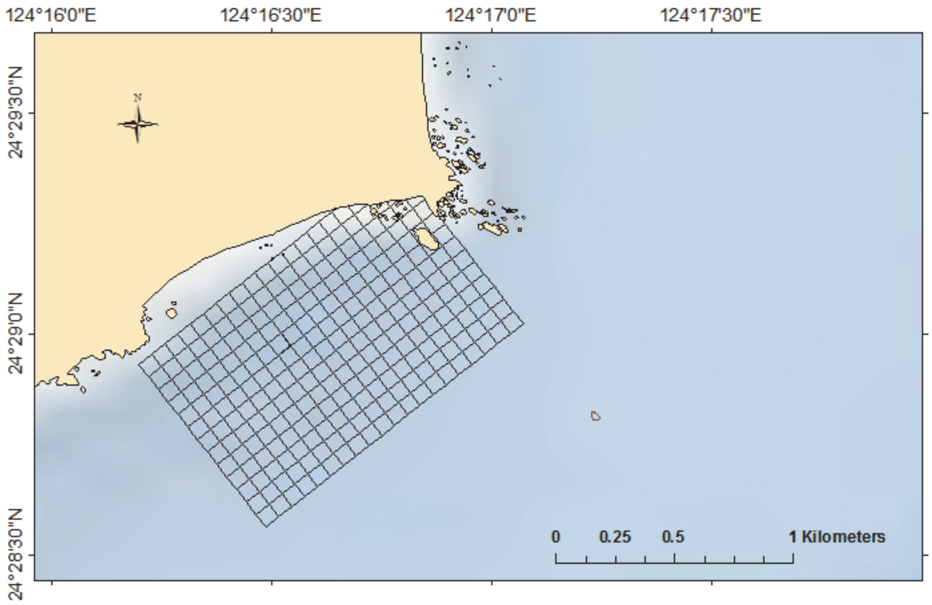

Figure 3. Location of observation site in Ibaruma Coast.

Figure 4. Observation points of coral cover survey
[*each pt ~60-70m transect*].

2.2.1 Coral Cover Survey

The percentage of hard live coral cover (HLCC) is considered as an indicator of coral reef health (Hill & Wilkinson, 2004). Using underwater video transect method, the HLCC in the observation site (Figure 3) were assessed. The camera used, Contour+2 (Figure 5d), which is equipped with high definition (HD) video and global positioning system (GPS) tracker, was immersed in the water for approximately 40-50 seconds at each observation points (Figure 4) while the boat was drifting at an average speed of 3 mph (1.3 m/s). The video footages were subsequently analyzed using the Contour Story Teller software (Figure 6) to extract quantitative coral data and corresponding GPS locations. The hard coral cover was determined based on their percentage cover using established visual estimation categories (Figure 7) by (English, *et al*. 1997).

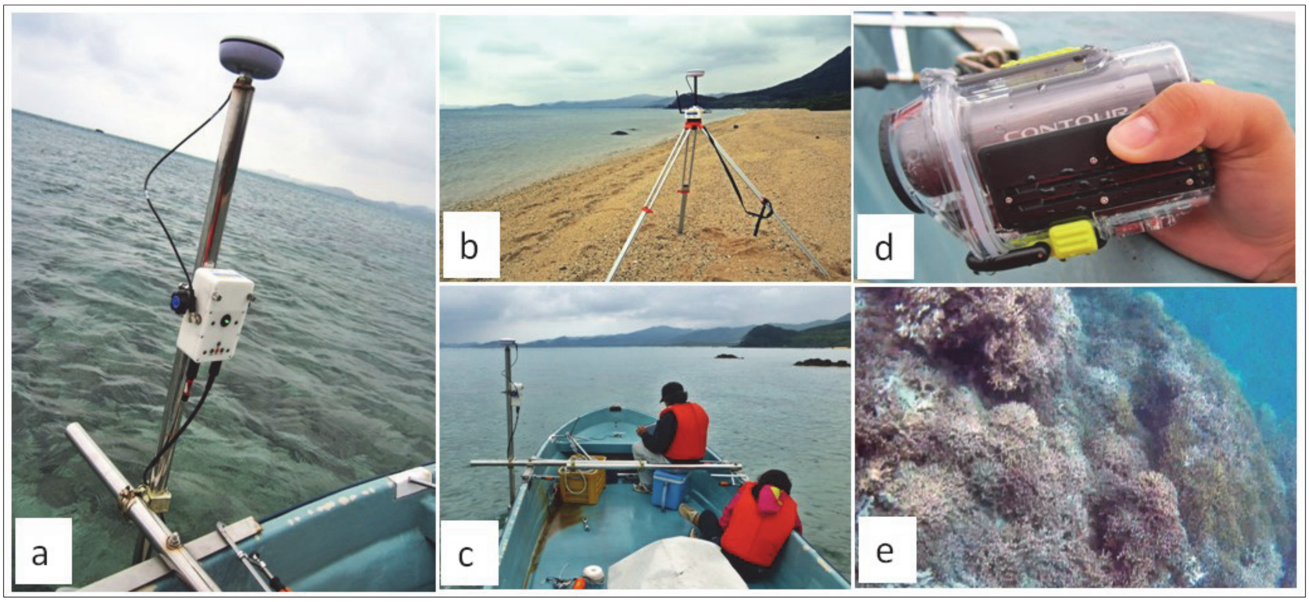

Figure 5. Coral Cover and bathymetry field survey: *(a-b) HydroSurveyorTM by Sontek used in bathymetry mapping; (c) Actual field survey-video transect method; (d) Countour+2 Video camera used for capturing coral cover, and; (e) actual snapshot of coral cover from video footages.*

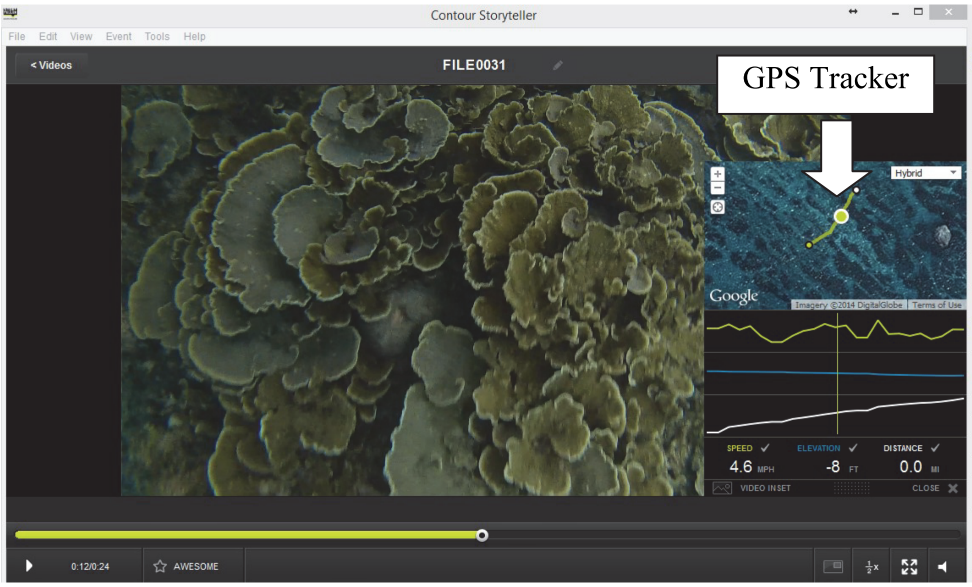

Figure 6. Video footage analysis using Contour Story Teller software.

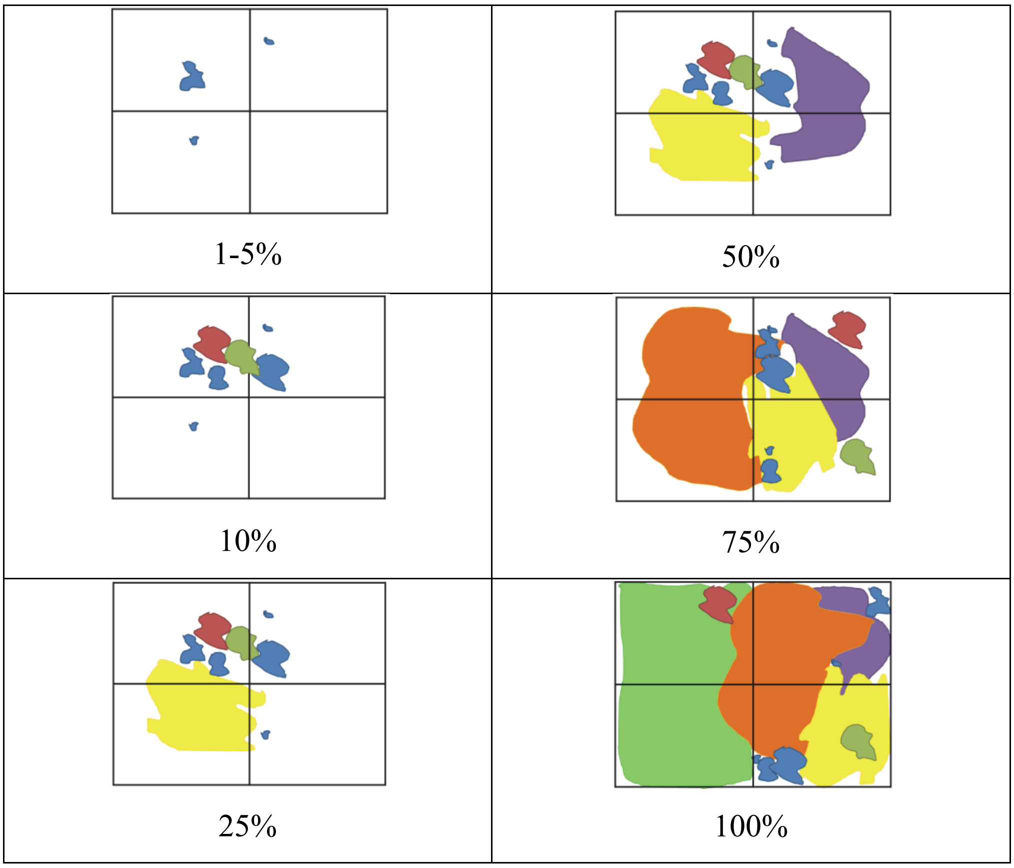

Figure 7. Visual Estimation Categories (English, *et al.*, 1997) used to analyze percent coral cover.

PAR measurement in the observation site was taken on the second field survey in June 2013 and the results were provided. PAR was measured using a light sensor at several observation points in the area and plotted against the depth to be able to get the light attenuation coefficient.

2.3 Environmental Variables

Aside from bathymetry and light attenuation (PAR) which were measured in situ, additional environmental parameters which have been examined in this study were SST, wave energy, orbital velocity near the bottom, and total energy dissipation. Except for SST which was calculated using remote satellite images, the latter three were determined using wave numerical simulation. The derivation of the said parameters is explained in detail in the following subsections.

2.3.1 Numerical Simulation: SWAN Model Cycle III version 40.91ABC

To reproduce important coastal processes in the reef areas of Ibaruma, a numerical wave modeling approach was applied in this study. For this reason, SWAN (Simulating WAves Nearshore) Model, developed by Delft University-Netherlands, was used to produce high-resolution and spatially extensive wave quantitative data, that will be later on be used to quantify the relation to coral reef distribution. The SWAN model which is free for the public domain, is a third generation phase-averaged, spectral wave model developed to acquire realistic parameters in shallow coastal areas for the given wind, bottom, and current conditions, (Booij *et al.,* 1999; and SWAN team, 2013). It has been widely used in different experiment and field cases, and is considered as one of the most reliable wave model worldwide. SWAN can handle physical phenomena such as wave propagation in time and space, shoaling, refraction due to current and depth, frequency shifting due to currents and non-stationary depth.

The SWAN model which is phase-averaging model, solves for the evolution of the shallow wave spectrum by using the action density spectrum. The governing equation of the SWAN model (i.e. action balance equation) in Cartesian coordinates is given by Equation 1.

$$\frac{\partial}{\partial t}N + \frac{\partial}{\partial x}c_x N + \frac{\partial}{\partial y}c_y N + \frac{\partial}{\partial \sigma}c_\sigma N + \frac{\partial}{\partial \theta}c_\theta N = \frac{S}{\sigma} \qquad \text{Eq. 1}$$

where x, y are horizontal Cartesian coordinates, t is time, Θ is the propagation direction of each wave component, c_x, c_y, c_σ, c_Θ stand for the propagation velocity in x-space, y-space, σ-space, Θ-space respectively. S is the source term in terms of energy density, which include the effects of generation, dissipation, and nonlinear wave-wave interaction.

In this study, the distributions of significant wave height (H_s), peak wave directions, orbital velocity near the bottom, and total energy dissipation were calculated and investigated. Simulations for both normal and stormy weather conditions were conducted since previous wave-coral studies showed that extreme weather events, such as storms and cyclones can significantly affect the coral reef distribution and morphology. Boundary conditions for the waves were obtained from Nationwide Ocean Wave Information Network for Ports and Harbours (NOWPHAS) since there is a port near the observation area (Ishigaki port) which measures a continuous observation of wave climate.

2.3.1.1 SWAN Model Set-up and Implementation for Ibaruma Coast

The SWAN Model Cycle III version 40.91 ABC for windows was used in this study for wave simulation within Ibaruma Coast. First, the model domain was specified in the SWAN input file (a data file with .swn extension) which includes some initial terms (Table 1) and variable parameters. The simulation was executed at a stationary, two-dimensional mode on a rectangular (regular) computational grid (Table 2). The input parameters, including the boundary conditions (Table 3) and physical processes (Table 4) employed in the simulation are summarized in the succeeding tables.

Table 1. SWAN initial input terms

Input Parameters	Input Values/ Command
Water level	0 m
Direction of north	90˚
Threshold depth	0.05
Gravitational acceleration	9.81 m/s^2
Water density ρ	1025 kg/m^3
Maximum wind drag coefficient	2.5 x 10^{-3}
Output calculation	Based on variance
Wind/wave direction	Cartesian (*the direction where the waves are going to or where the wind is blowing to*)
Power of high frequency tail (shape of spectral tail)	GEN3 Komen[1]
Maximum Froude number ($U/\sqrt{gd}$, where U is the current, and d is the water depth)	0.8
Mode	Stationary, Two Dimensional
Coordinates	Cartesian

[1]*Explained after Table 4*

Table 2. Details of computational grid and input bottom grid

Input Parameters	Input Values/ Command
Computational Grid	Regular and uniform
Origin (0 E, 0 N), direction of positive x-axis of computational grid	0, 0, 0 (used for small areas/Cartesian coordinates)
Length of computational grid (x, y)	3753 m, 2290 m
Number of meshes (x, y)	401, 248
Spectral direction	Circle
Number of mesh in θ space	36
Discrete frequency (lowest, highest)	0.05 Hz, 1 Hz
Grid resolution in frequency-space	31
Bottom Grid (input file)[2]	Regular and Uniform
Number of meshes (x, y)	401, 248
Δx, Δy (grid resolution)	10 m, 10 m
Exception Values (land area points which should remain dry in the computation)[3]	-999

[2]The bathymetry for all the model domains has been interpolated using ArcGIS 10.1 Spatial Analyst extension tools, from a combination of various sources from Japan Oceanographic Data Center (JODC) for the 500 m resolution bathymetry data and the sounding data collected from field observation last February 2013.

[3]All incoming wave energies are absorbed along the coastlines, hence the model assumes no wave generation in this area. In the case of open sea boundaries, it is assumed that waves can freely leave the computational domain.

Table 3. Details of boundary condition

Input Parameters	Input Values/ Command
Boundary spectral shape	BIN (The energy is located in one frequency bin)
Parametric spectra at the boundary	The boundary (where the spectra were given) was imposed at (constant) the East and South side. *It must be noted that only incoming wave components of these spectra are used by SWAN.*
Wave Spectra parameters (Normal condition)[4]	Significant Wave Height (Hs): 0.38m Peak Period: 4.8s Wave direction: 135° (NNW)
Wave Spectra parameters (Stormy condition)[5]	Significant Wave Height (Hs): 11.93 m Peak Period: 14.02s Wave direction: 60° (NE)
Initial Values for Stationary computation	Zero (0), The initial spectral densities are all 0

[4]For wave simulation during normal weather conditions, the input values for wave spectra parameters (Hs, peak period, and wave direction) reflected the month-long average data taken from the NOWPHAS website. (Representative period: May 2014 where no extreme weather events was observed, i.e., heavy precipitation, storms).

[5]In the case of wave simulation for stormy weather conditions, the input values for wave spectra parameters (Hs, peak period, and wave direction) reflected the recorded data during extreme cyclone/storm events which occurs once every 10 years.

Table 4. Physical processes employed in the SWAN calculation.

Input Parameters	Input Values/ Command
Wave-generation mode	GEN3 Komen[6]
Whitecapping	Calculation based on Komen[6]
Computation of quadruplet wave interaction	Turned OFF
Bottom friction	Activated using JONSWAP formulation, Friction coefficient: constant (0.067 m^2s^{-3} -wind sea condition)
Depth-induced wave breaking	Activated using constant breaker (Proportionality coefficient of the rate of dissipation, α=1.0; Ratio of maximum individual wave height over depth, γ=0.73)
Wave limiter	Activated; upper threshold = 10.0; Threshold for fraction of breaking waves = 1.0

[6]In this study, the SWAN ran in third-generation mode for wind input, quadruplet interactions, and whitecapping. Triads, bottom friction and depth-induced breaking are not-activated by this command. Komen was selected as an expression for exponential term for the wave growth by wind.

The output parameters (significant wave height (Hs), peak wave direction, orbital velocity near the bottom, and total energy dissipation) are requested in a two dimensional plot that can be opened and processed using MatLab software.

2.3.2 Sea-Surface Temperature Extraction from Landsat Satellite Images

Sea surface temperature (SST) is one of the identified controlling factors in the coral reef distribution. In this research, since in-situ temperature data are limited only to specific point locations, satellite images were utilized to derive the SST distribution in Ibaruma Coast.

Because the study area is relatively small and is very near the coastline area, the use of currently-available 1-km resolution data from multi-band thermal satellite sensors (NOAA-AVHRR, MODIS) is not appropriate. For this reason, Landsat thermal data which provide information up to 30-m resolution were utilized in this study. Although Landsat is more commonly used in deriving land-surface temperature (LST), there are already recent established studies (e.g., Raj & Fleming, 2008; Wloczyk, *et al.,* 2006; Fisher & Mustard, 2004; Trisakti, *et al.,* 2004) on how to extract the SST from the thermal bands of Landsat that is adopted in this research.

The Landsat Images were downloaded from the website of the United States Geological Survey (USGS) Landsat Imageries Archive. The following are the details and formulas used in the extraction of SST from Landsat Thermal Bands.

Table 5. Details of the Landsat satellite images downloaded

Sensor used	Landsat 8: Operational Land Imager (OLI) and Thermal Infrared Sensor (TIRS). Landsat 7 Enhanced Thematic Mapper Plus (ETM+)
Acquisition dates	April 5, 2014; September 9, 2013; September 25, 2013; August 24, 2013; October 11, 2013; October 2008; August 5, 2008,
Band used	For Landsat 8: Band 10/11, 100 meter resolution, Improved thermal mapping, with 11.5-12.51 μm wavelength For Landsat 7 ETM+: Band 6 (thermal IR), 60m resolution, with 10.4- 12.5 μm wavelength

The downloaded imageries were analyzed and the data images with the least cloud cover contamination were selected for analysis. In this study, the Landsat Images acquired on August 2008 and August 2013 were used as representatives for the SST distribution, since both showed zero cloud cover, and their distribution is the same. In addition, August is part of summer season in the study area, and so it experiences high temperatures. In this regard, the presence of heat stress that can be damaging to coral reefs was also investigated by combining the estimated SST from satellite images and the temperature point data provided by a private coral research company in Ibaruma.

2.3.2.1 Extraction of SST from Landsat Image

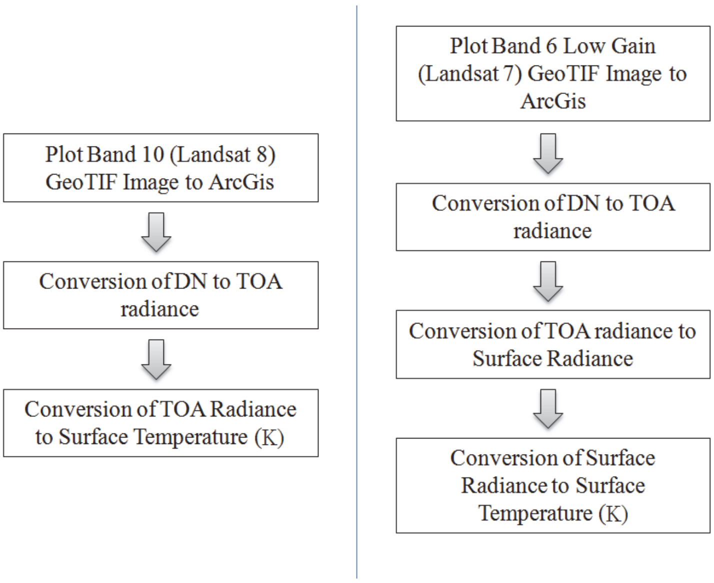

Figure 8. Procedural steps in extracting SST from Landsat image.

The GeoTIFF image file, Band 10 if Landsat 8; Band 6-Low Gain if Landsat 7, was plotted to ArcGIS to be able to extract the quantized and calibrated scaled Digital Numbers (DN) where the needed information was stored.

For Landsat 8, the DN values were first converted to TOA (Top of Atmosphere) Radiance, using the radiance rescaling factors provided in the metadata which is included in the downloaded Landsat product. The formula for the conversion as suggested by USGS is as follows:

$$L_\lambda = M_L\, Q_{cal} + A_L \qquad \text{Eq. 2}$$

Where,

L_λ = TOA spectral radiance (Watts/(m^2 *srad *µm))
M_L = band-specific multiplicative rescaling factor from the metadata
A_L =band-specific additive rescaling factor from the metadata
Q_{cal} = quantized and calibrated standard product pixel values (DN)

Using the thermal constants provided in the metadata file, the TIRS band data can be converted then from TOA spectral radiance (from Equation 2) to surface temperature using the following formula:

$$T = \frac{K_2}{\ln\left(\frac{K_1}{L_\lambda}+1\right)} \qquad \text{Eq. 3}$$

Where:

T = At-satellite brightness temperature (K)
$L\lambda$ = TOA spectral radiance (Watts/(m2 * srad * µm)) from Equation 2
K1 = band-specific thermal conversion constant from the metadata
K2 = band-specific thermal conversion constant from the metadata

In the case of Landsat 7, the process of SST extraction was based on the study made by Raj and Fleming, (2008), which incorporated the conversion from TOA spectral radiance to surface radiance, before being converted directly to surface temperature. The following formulas were used:

a. DN Values of Band 6 (low gain) to TOA Radiance:

$$L_\lambda = \left[\frac{[L_{MAX}-L_{MIN}]\times DN}{MaxGray} + L_{MIN}\right] - 0.31 \qquad \text{Eq. 4}$$

Where:

$L\lambda$ =TOA spectral radiance (Watts/(m2 * srad * µm))
L_{MAX}, L_{MIN} = maximum and minimum radiance values for a given band (available in the Metadata of the product).
MaxGray = maximum number of gray value
DN = digital number for a given band.
0.31 = (Wm^{-2} sr^{-1} μ m^{-1}) calibration constant for the calculated radiance

b. TOA Radiance to Surface Radiance

In this step, the effect of the atmosphere in the thermal region is removed, and the atmospheric parameters used to calculate the surface radiance were obtained using the Atmospheric Correction Parameter Calculator which can be found in the NASA website (http://atmcorr.gsfc.nasa.gov/). The formula for the conversion of TOA radiance to surface radiance was adopted from Barsi *et al.,* (2003a), as cited by Raj and Fleming, (2008).

$$L_T = \frac{L_\lambda - L_\upsilon - \tau(1-\varepsilon)\times L_D}{\tau \times \varepsilon} \qquad \text{Eq. 5}$$

Where:

L_T = surface radiance
L_λ = spectral radiance calculated from Equation 4.
τ = atmospheric transmission at the sensor's aperture
ε = surface emissvity
L_ν = upwelling spectral radiance between the surface and sensor (in $Wm^{-2}sr^{-1}\mu m^1$)
L_D =downwelling spectral radiance from the sky ($Wm^{-2}sr^{-1}\mu m^1$)

c. Surface Radiance to Surface Temperature

The final step was to convert surface radiance computed from Equation 5 to surface temperature using the following equation formulated by Barsi, *et al*., (2003b):

$$T = \frac{K_2}{\ln\left(\frac{K_1}{L_T}+1\right)} \qquad \text{Eq. 6}$$

Where:

T = surface temperature in Kelvin (K)
L_T = surface radiance from Equation 5
K_1, K_2 = pre-launched calibration constants (666.09 and 1282.71, respectively)

2.3.2.2 Development of Heat Stress Map

The presence of heat stress that can be damaging to coral reefs was also investigated. The results of the estimation of SST distribution extracted from the Landsat images were combined with the time-series temperature point data to be able to come up with the time-series data plots for the month of August. The areas which are exposed to temperature greater than 30˚C are identified, and the period (hours) were counted. ArcGIS 10.1 was used to visualize the areas where heat stress occurred. Figure 9 shows the procedural steps on how to develop the heat stress map.

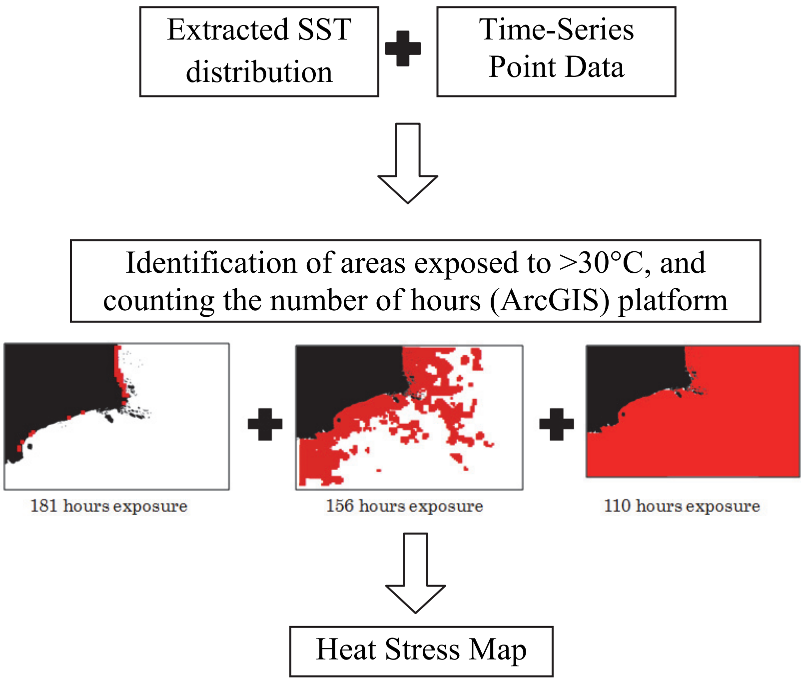

Figure 9. Procedural steps in developing heat stress map.

2.4 ArcGIS-Mapping, Spatial Analyst Tools and Data Analysis

After obtaining all the environmental variables that affect the distribution of corals, the data were plotted in a map using ArcGIS 10.1 software. Various spatial analysis tools such as interpolation, resampling, and data conversion and management tools were employed to achieve the appropriate resolution of the spatial distribution of the different environmental factors. The final resolution for each variable maps was 30m, and all vector data are converted to raster format. The converted raster data were overlaid in the map (Figure 10) and the relationship of each variable in relation to each other and to the coral reef distribution were calculated and analyzed using multi-variate analysis available in the Spatial Analyst tool of ArcGIS.

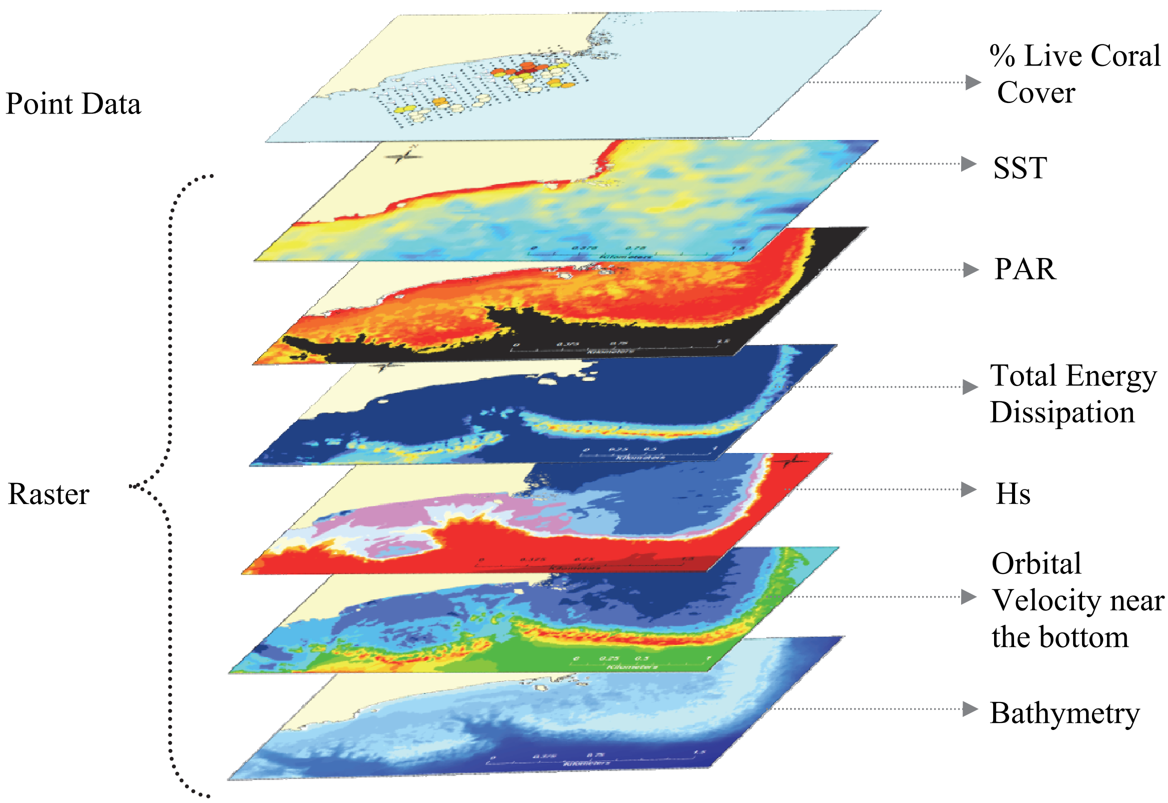

Figure 10. A graphic representation of the core GIS data types for the coral cover distribution and environmental factors.

2.4.1 Determination of Optimum Condition

In this study, it is assumed that the areas with the highest coral cover (100%) equate to the areas having the optimum condition for the presence of high coral cover. After plotting the coral cover distribution and each of the predictor variables in ArcGIS, the locations of the of the coral distribution were extracted along with the information from the overlaid raster data of environmental variables. The suitability indices were develop based on the extracted information with values ranging from 0 (unsuitable) to 1 (optimal conditions). The results were plotted into suitability index graphs.

2.4.2 Statistical Analysis and Determination of Controlling Factor

To quantify the relationship of each variables to one another and to the coral reef cover, the point data of coral cover and raw data extracted from each environmental raster layers (which were standardized first) were subjected to correlation test using Pearson statistical analysis. An array of scatter plots, correlation matrix, statistical summary, and the coefficient factor of determination were obtained.

After the statistical analysis test for correlation, the standardized environmental variables, which are regarded here as the predictor of coral cover variable (response) were subjected to regression analysis using the Partial Least Square Regression (PLSR) to quantify the contribution of each variable in predicting the coral cover. Data used for regression are standardized to have mean zero and variance one. PLSR was employed in this study since this model is best suited when there is numerous number of predictors (X variables) which exhibit multi-colinearity. This is useful in terms of identification of controlling factors/ important variable especially in the field of ecology since in many instances, most of the environmental gradients are non-independent (Carrascal et al., 2009), in this case, for example, light intensity is a function of depth. The PSLR analysis yielded a table of variable of importance in the projection of coral reef cover. The results were interpreted in the discussion part of this manuscript.

CHAPTER 3: RESULTS

3.1 Field Survey Results

3.1.1 Percent Live Coral Cover

The observation area covers approximately 1100 m parallel to the coastline and 800 m across the shore towards the reef crest. After the video footage analysis of the February 2013 coral cover survey, the percent live coral cover was plotted to a mesh with around 60-70 m resolution in ArcGIS to easily visualize and analyze the results. Figure 11 shows the percent live coral cover present in the area. It shows that the coral colony distribution is not evenly dispersed. Coral colonies, with high percent live cover, tend to occur in clumps at the eastern side of the observation area (124°16'45"E, 24°29'05"N) which is near some small islets. The red circle symbols show a 100% coral cover. As the gradient colour turns lighter (red to lighter yellow), the percent live coral cover decreases from 100% to 1-10%. The triangle symbols show areas with small patches of growing corals. The areas where coral transplants (in pink asterisk simbol) are situated were also observed during the survey.

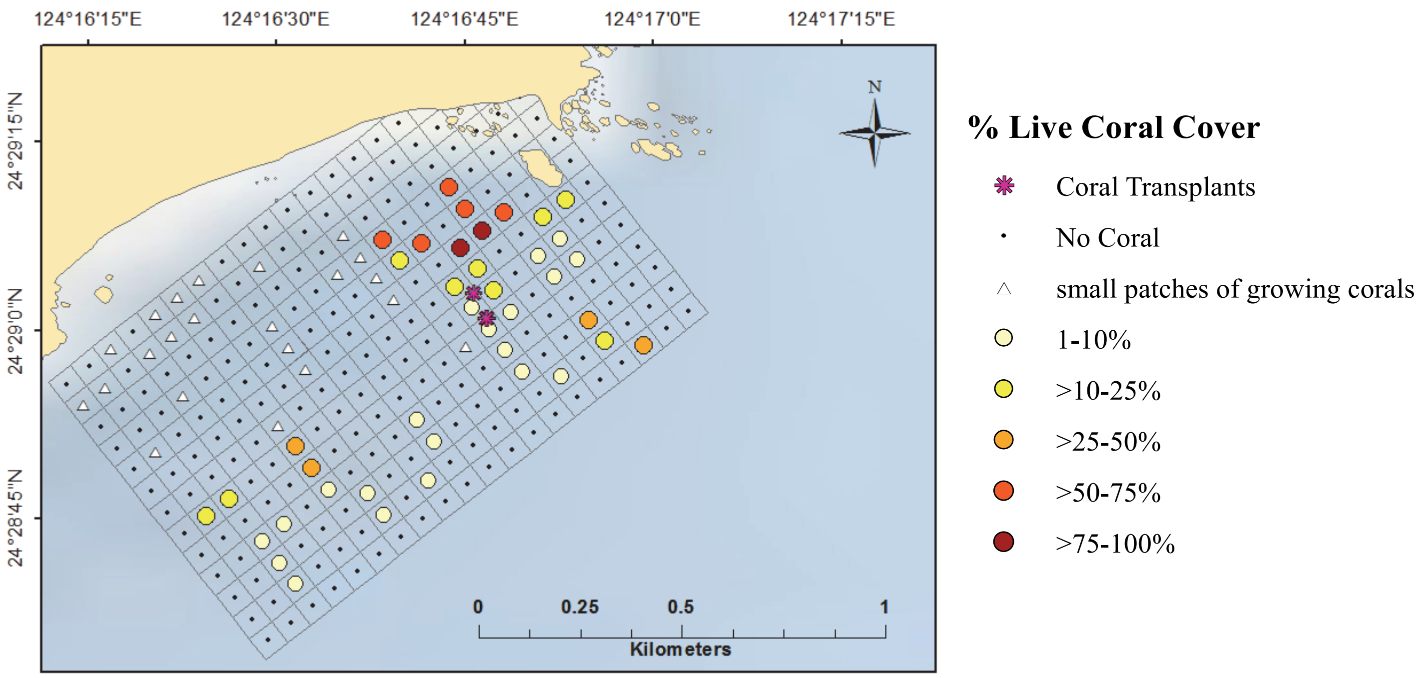

Figure 11. Percent Live Coral Cover present in the area.

Moreover, there is also a difference observed among the coral community structure present in the area. It is observed that more circular and massive corals are found near the inshore area, where the 100% coral cover is found. The most dominant species in this area are *Heliopora sp*. or the blue coral, and *Porites sp.* (Figure 12a). Meanwhile, more tabular, or in plate-form type of species are found in the offshore sites (near reef crest), such as *Montipora sp*. (Figure 12b).

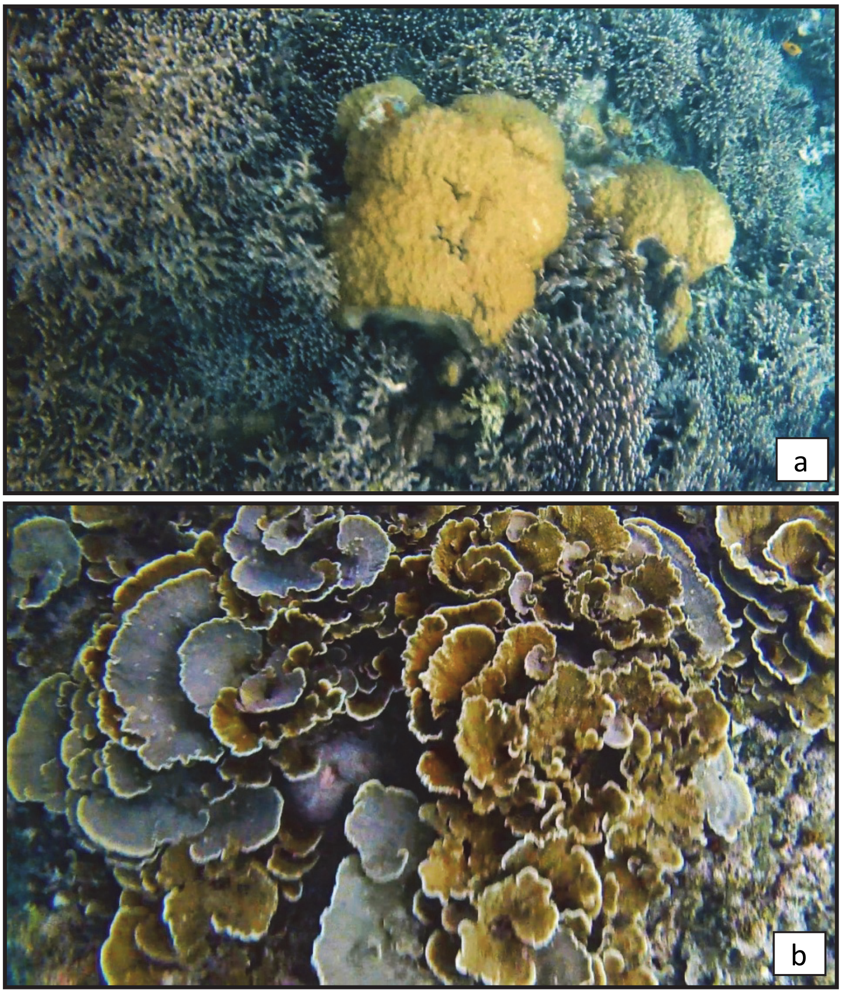

Figure 12 Coral Community Structure: (a) *Porites sp*. -most dominant in the inshore part; (b) *Montipora sp*.-most dominant near the reef crest

3.1.2 Bathymethry/ Depth

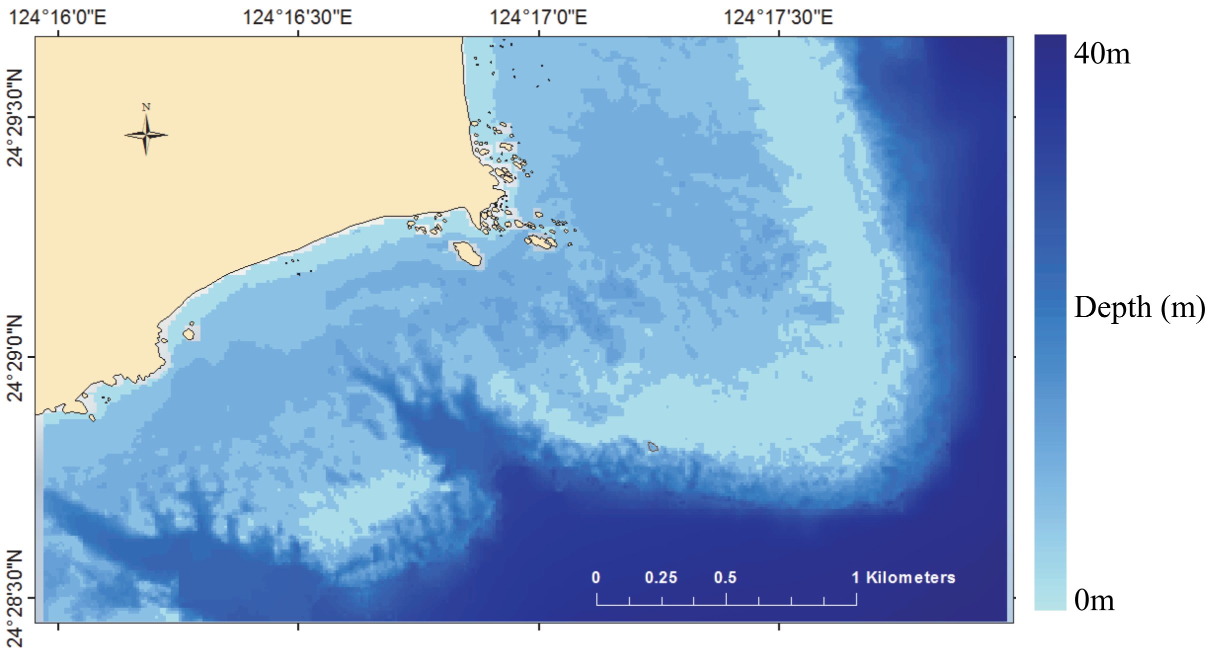

Figure 13. 10-meter resolution bathymetry map of Ibaruma Coast.

Figure 13 shows a 10-meter resolution bathymetry map of Ibaruma as a result of the combined sounding data collected during the field survey and the bathymetry data with 500 m resolution from JODC. Both data has to be used and should be combined because the bathymetry input file needed to run the wave simulation requires a larger area extent. The lighter blue color indicates areas with shallower parts while the darker blue for the deeper parts (~40 m). From the resulting image, the location of the reef crest (relatively in lighter blue, which is closer to the deeper sea) can be easily located because it is the highest point of coral reef. It is also apparent that Ibaruma's topography contains a spur and groove system which extends from the reef crest to the reef slope.

3.1.3 PAR

As a result of the field observation conducted on June 2013, the light attenuation coefficient, 2629.2 $e^{-0.325x}$ (Figure 14) was calculated and was used in plotting the PAR distribution in Ibaruma (Figure 15).

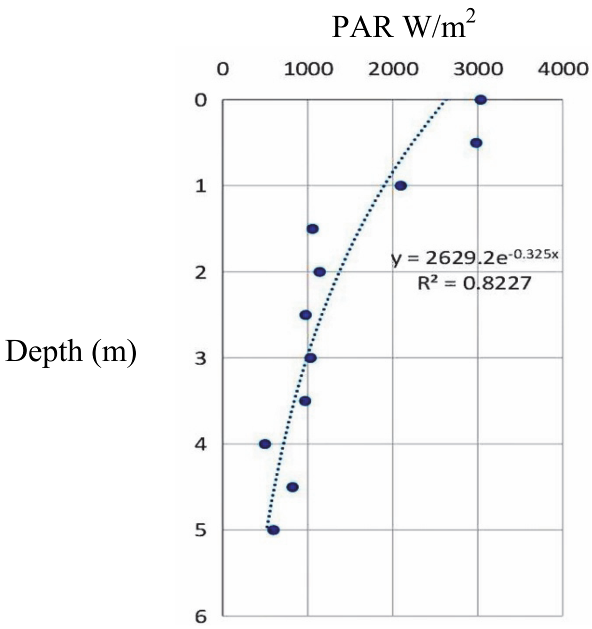

Figure 14. PAR distribution vs. depth.

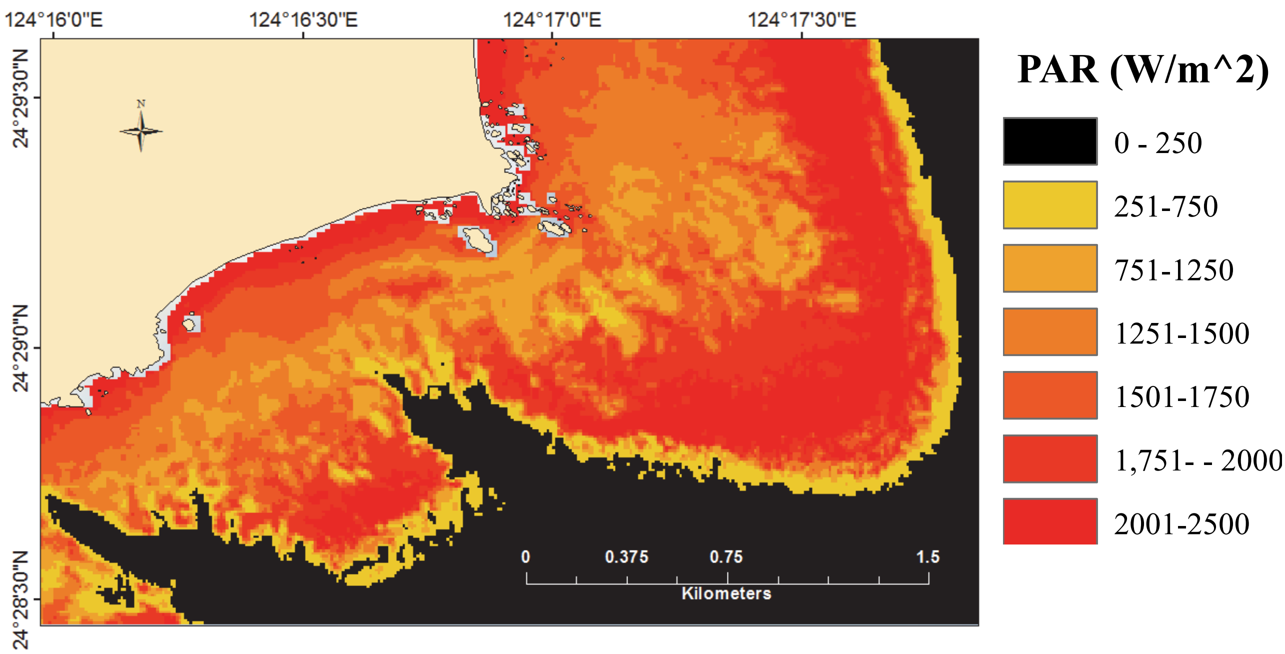

Figure 15. PAR Distribution over Ibaruma Coast.

In Figure 15, higher PAR values are illustrated by red color while lower values in yellow. Black areas show very low (0-250 W/m^2) light attenuation. In this result, it is clearly obvious that the light attenuation or the distribution of PAR is a function of depths in the area.

3.2. Environmental Variables and Coral Distribution

3.2.1 Coral Cover and Depth

The percent coral cover distribution was overlaid to the depth and shows the following distribution:

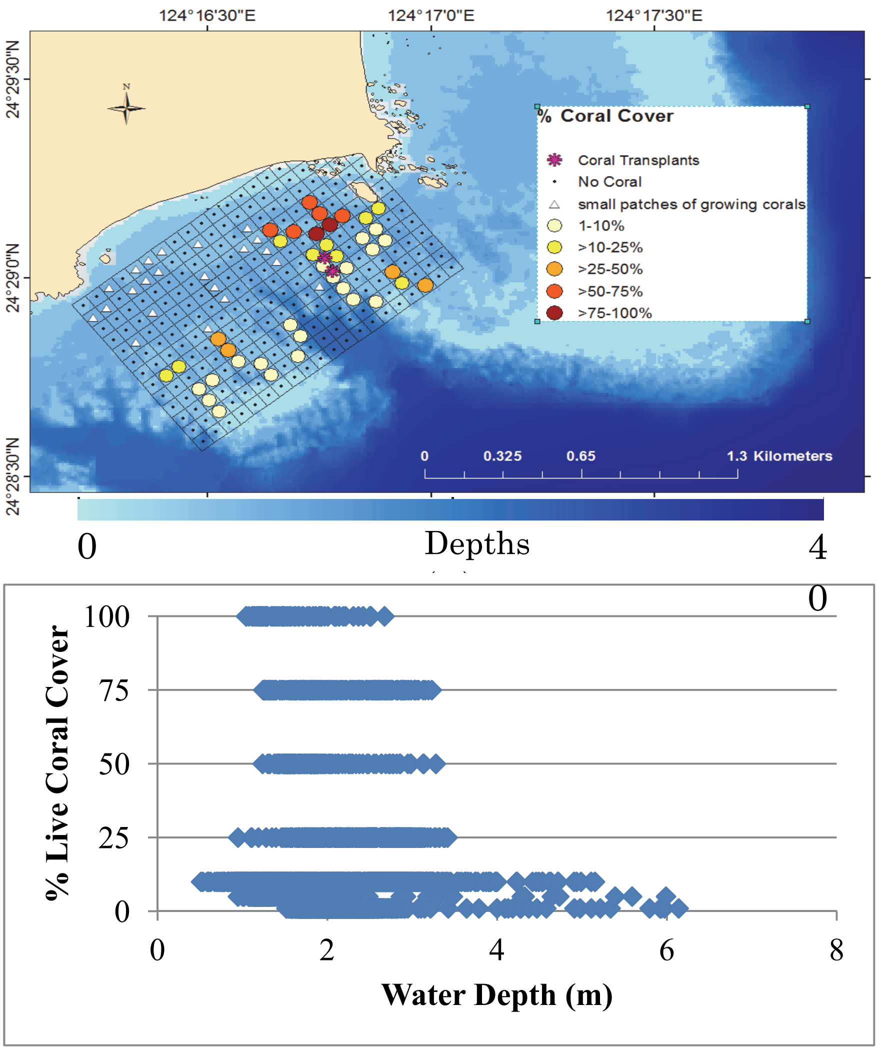

Figure 16. Percent Live Coral Cover Distribution at Certain Depths.

This result in Figure 16 shows that the coral distribution is restricted within certain depths only, which starts from 0.5 m, up to 6 m for the deepest part. It also shows that high coral cover density (80-100%) was found at depths 1.044 ~ 2.673 m.

3.2.2 Coral Cover and PAR

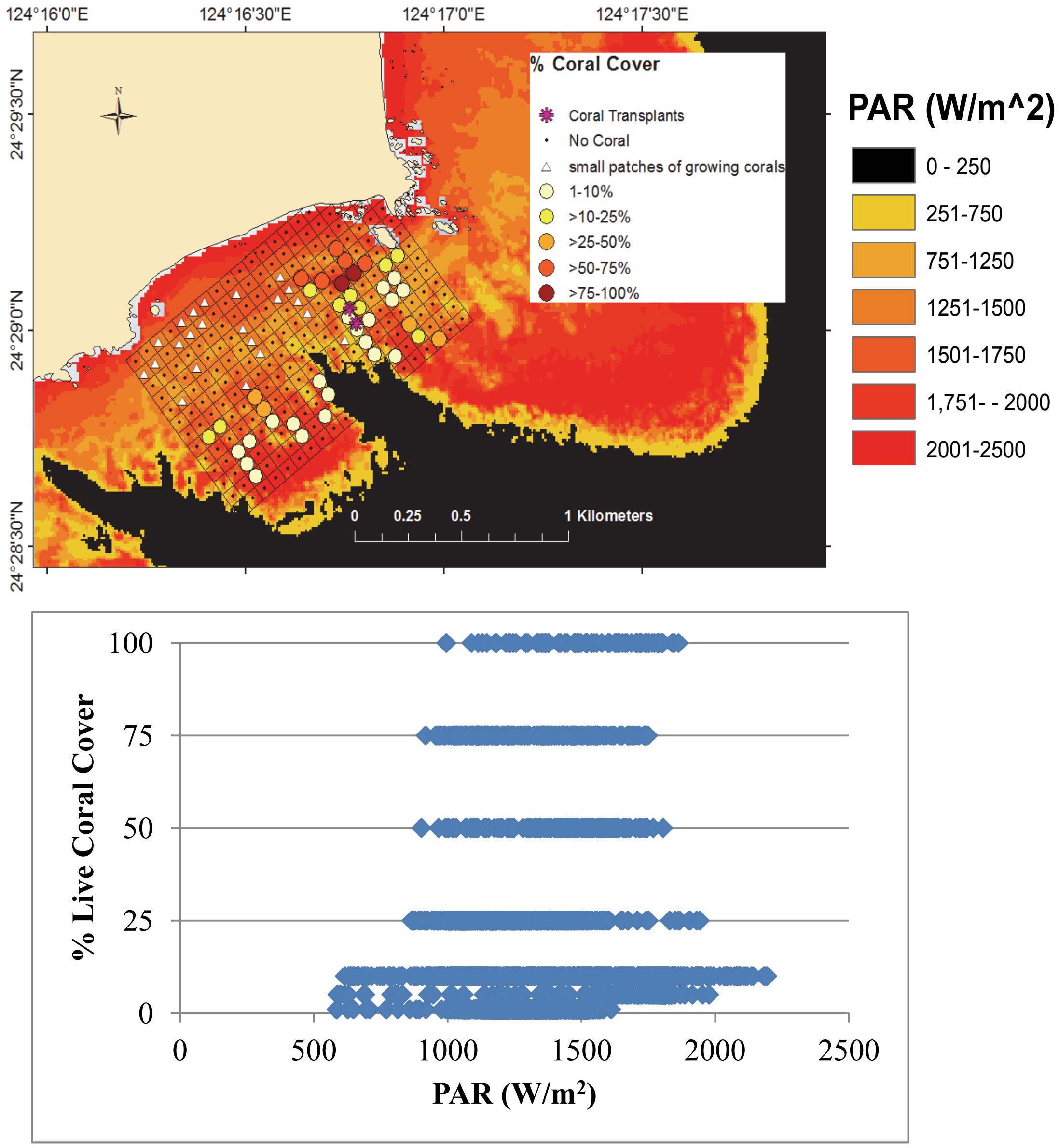

Figure 17. Percent Live Coral Cover vs. PAR distribution (W/m^2).

Figure 17 shows the percent coral cover distribution when overlaid to the light attenuation in terms of PAR. PAR values at locations with high coral cover density (75-100%) ranges to 900 W/m^2 to 1800 W/m^2. It clearly shows that presence of corals is also limited by the amount of PAR available in the area. Since PAR is a function of water depth, assuming that the turbidity approaches to zero, then the relationship of PAR vs coral cover distribution is the same with those of depth.

3.2.3 Results of SWAN simulation: Calculation of Significant Wave Height

A. Significant wave height for normal weather condition

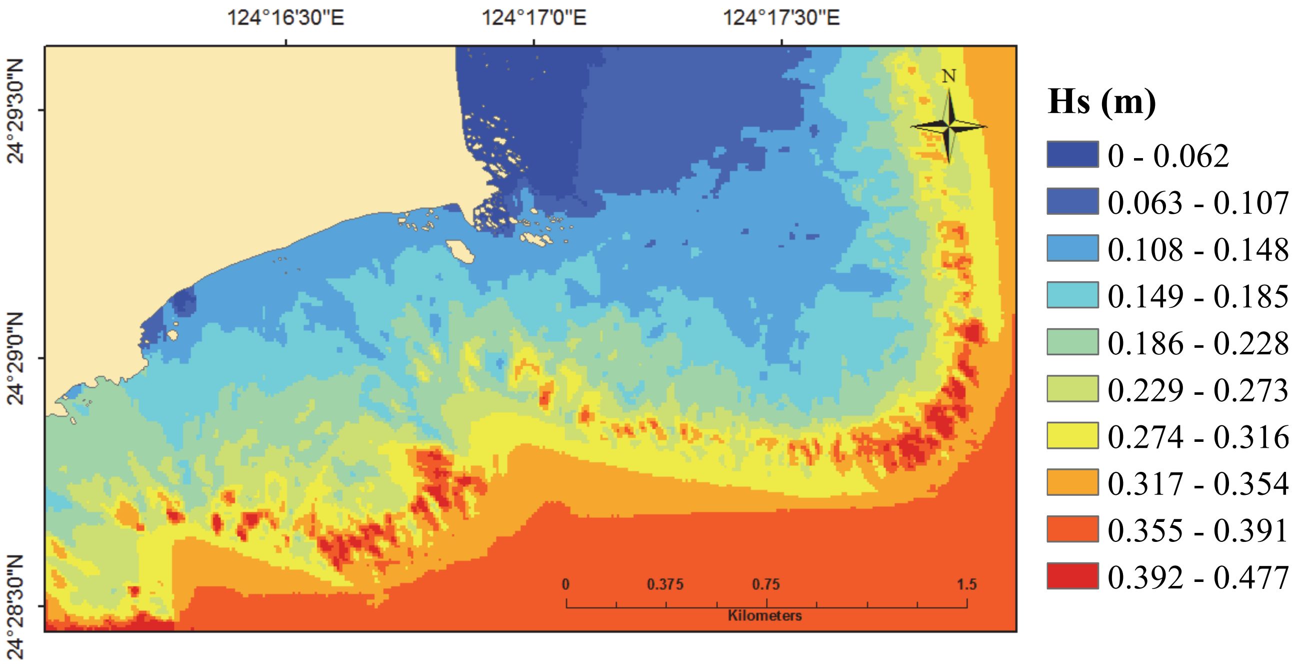

Figure 18. Significant wave height distribution during normal weather condition.

Figure 18 shows the results of SWAN simulation for the significant wave height (Hs) distribution during normal weather condition over Ibaruma. It showed here that high Hs which range to 0.39~0.48 m occurred over the reef crest. However, Hs decreases as the waves propagate near shore. Results also showed up to 50% reduction in the incident wave energy (~Hs) from intermediate to shallow waters.

When the coral cover is overlaid to the Hs distribution (Figure 19), it shows that Hs at the areas with high coral cover ranges to 0.15 m ~ 0.19 m. This is relatively lower compared to the Hs found near the reef crest with 0.27 m ~ 0.32 m and where there is only 10-25% live coral cover.

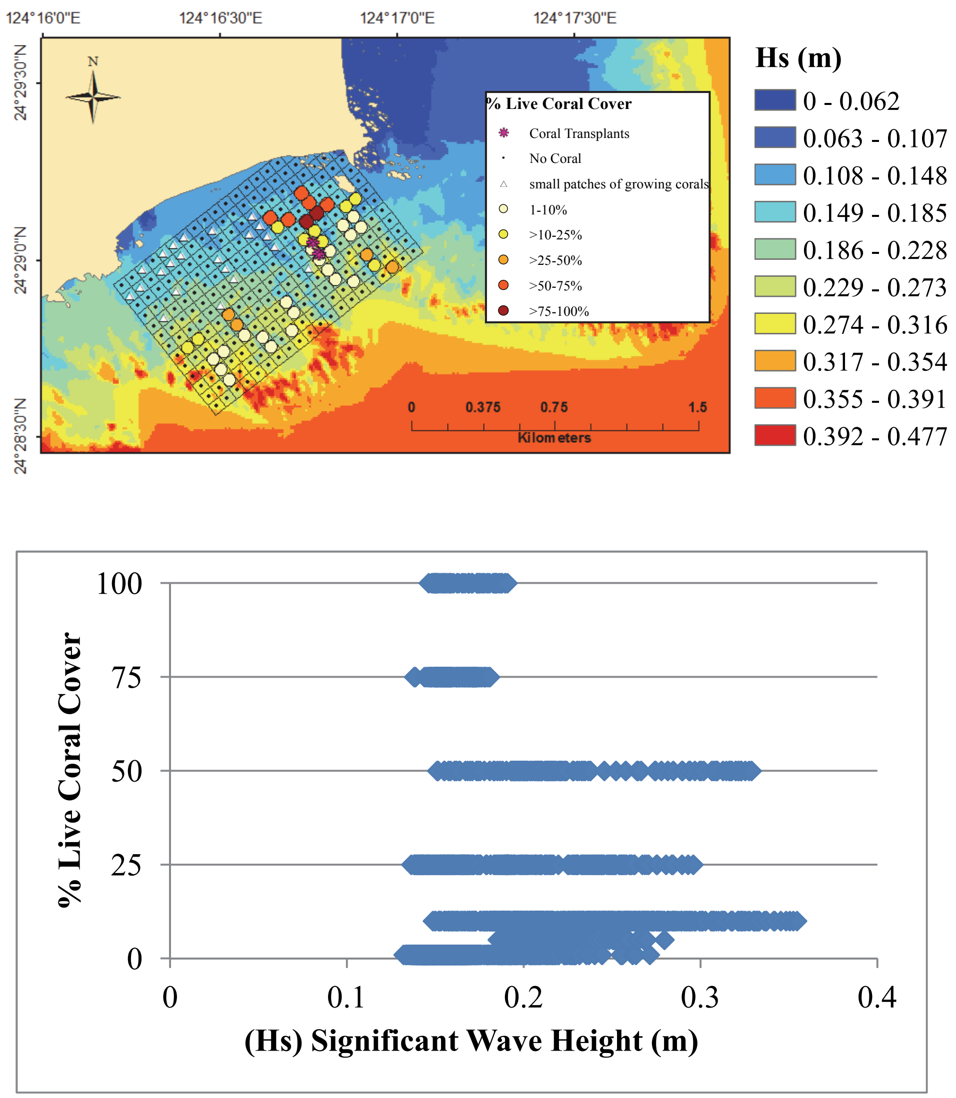

Figure 19. Percent live coral cover vs significant wave height distribution during normal weather condition.

B. Significant wave height for stormy weather condition.

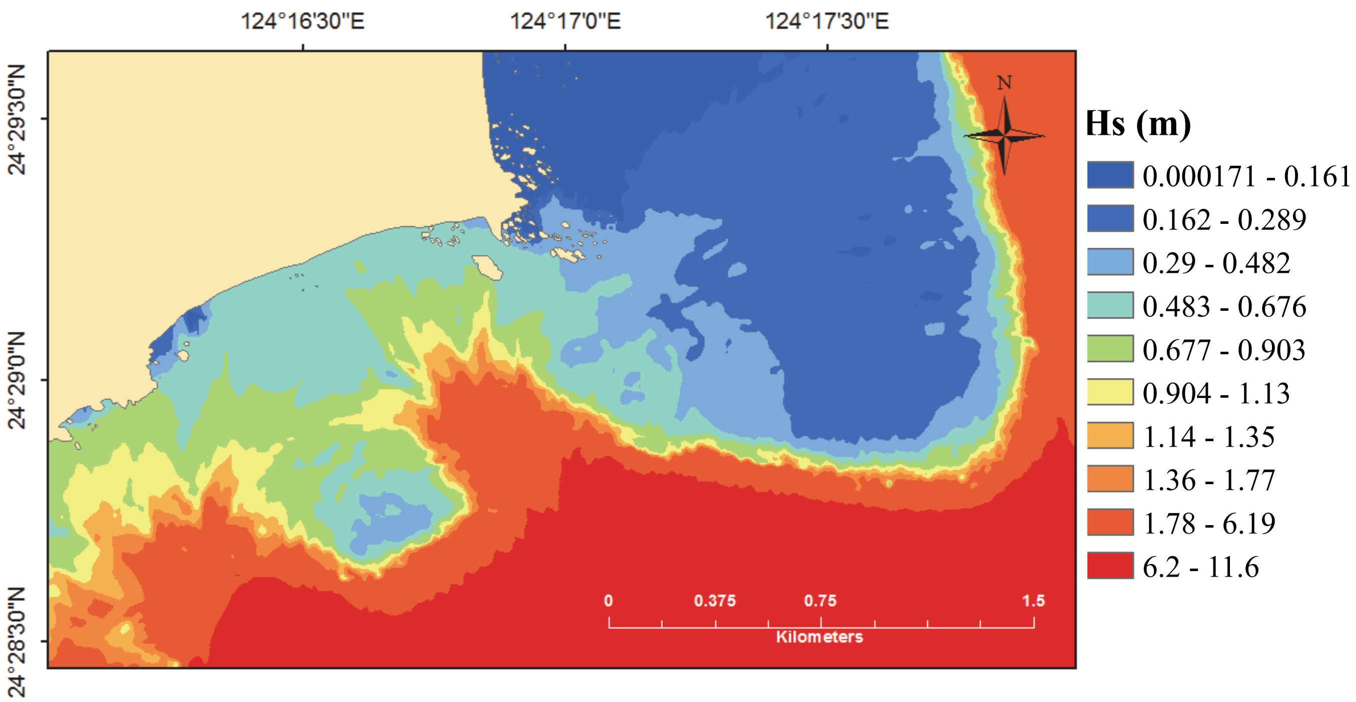

Figure 20. Significant wave height distribution during stormy weather condition.

Figure 20 shows the results of SWAN simulation for the significant wave height (Hs) distribution during stormy weather condition. This is a simulation for an extreme weather event which occurs only once in ten year-period. When the coral distribution is overlaid to the map (Figure 21), it clearly shows that corals experiences intense wave energy with Hs up to 5 m and that can be damaging enough to the coral branches or can overturn small boulder of coral.

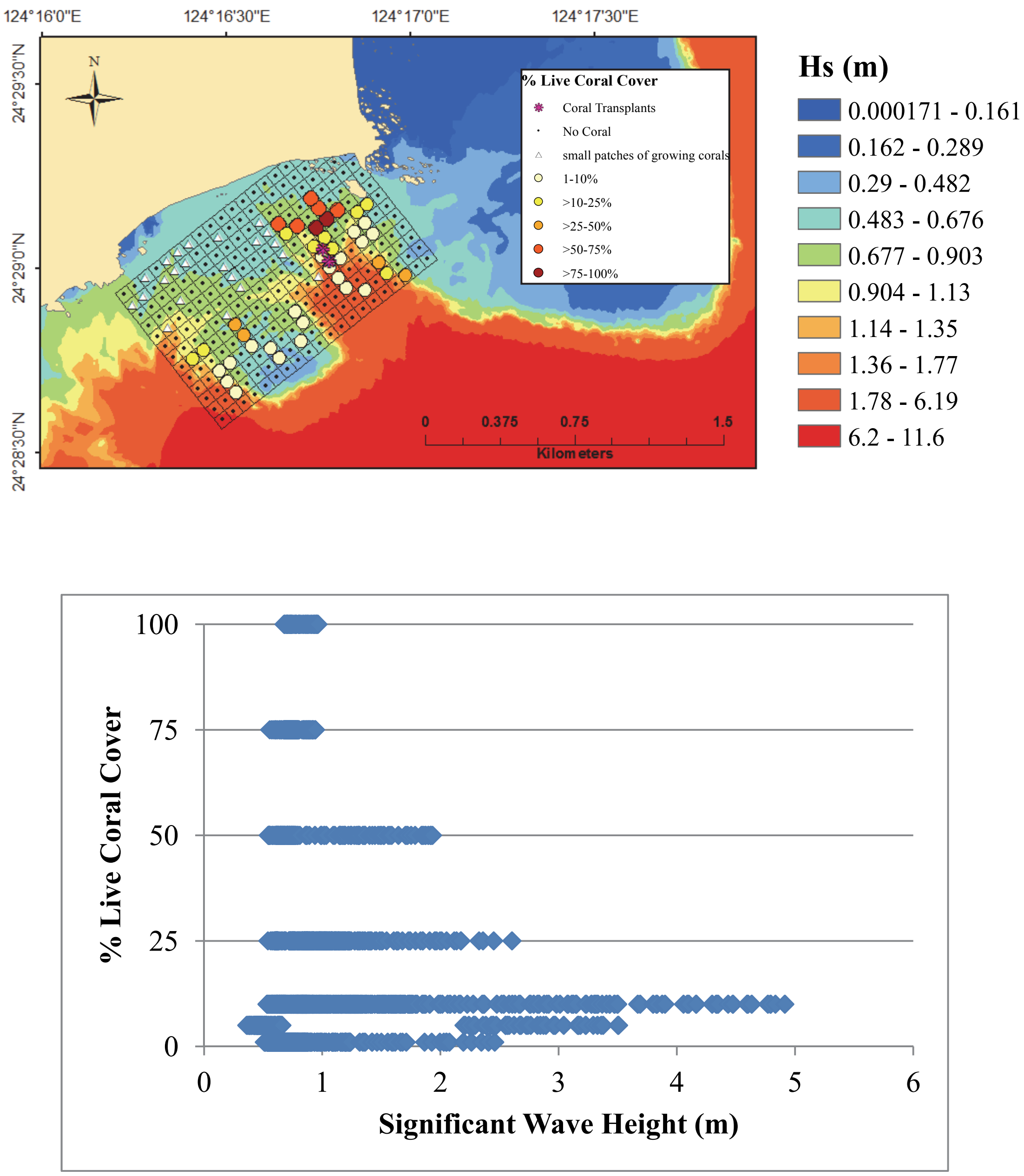

Figure 21. Percent live coral cover vs significant wave height distribution during stormy weather condition.

3.2.4 Results of SWAN simulation: Calculation of Orbital Velocity near the Bottom

A. Orbital Velocity near the Bottom (in m/s) Distribution during Normal Weather Condition

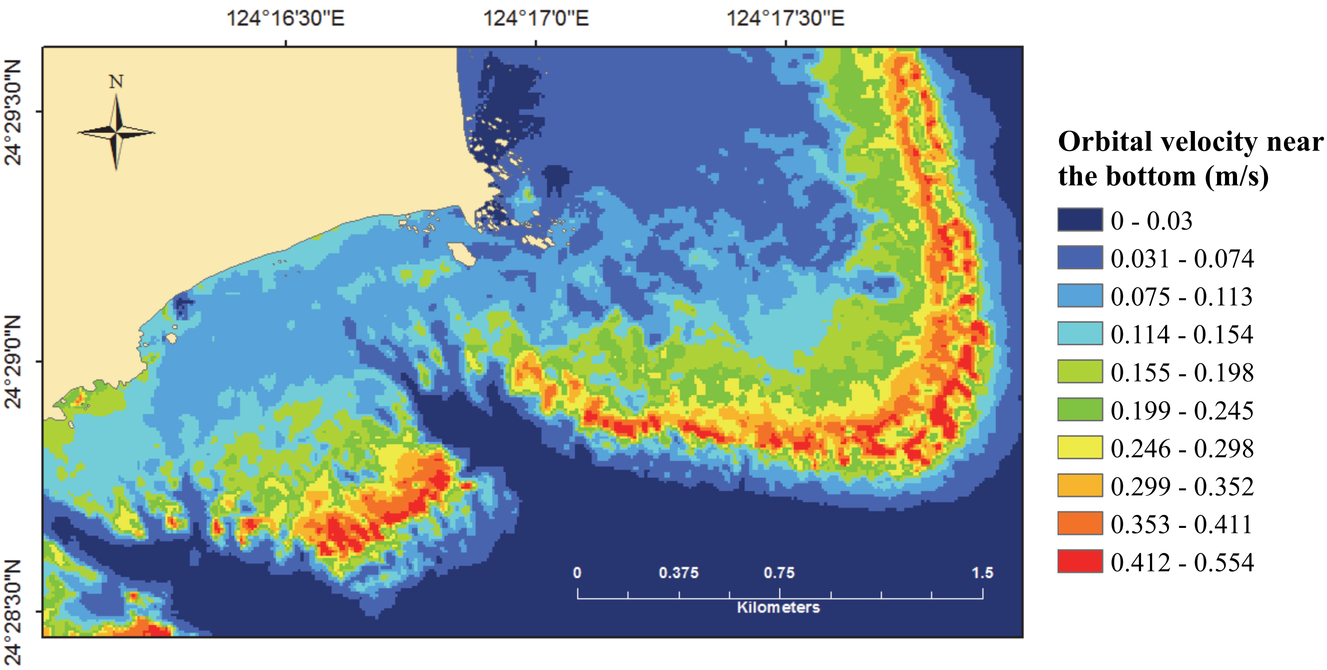

Figure 22. Distribution of orbital velocity near the bottom (in m/s) during normal weather condition.

The SWAN Model, aside from calculation of significant waveheight, can also calculate the orbital velocity near the bottom (U_{bot}). Figure 22 shows the results of SWAN simulation for the U_{bot} (in m/s) distribution during normal weather condition over the study area. It showed here that there is a high orbital velocity occurring at the reef crest which ranges to 0.412 m/s ~0.554 m/s occurred over the reef crest. The U_{bot} decreases as it approaches the coastline. It is also apparent in the figure that U_{bot} is a function of the depth since very low values of U_{bot} were observed at deeper areas.

Figure 23 shows the percent coral cover distribution when overlaid to the distribution of orbital velocity near the bottom in the area. The U_{bot} at locations with high coral cover density (75-100%) ranges to 0.072 to 0.138 m/s. It is also evident that the values of U_{bot} are higher at the reef edge. Moreover, two peaks are observed, because the location where the 50% coral cover showed different orbital velocities near the bottom, and this may be accounted to the different roughness of the bottom which will be explained in detail in the discussion part.

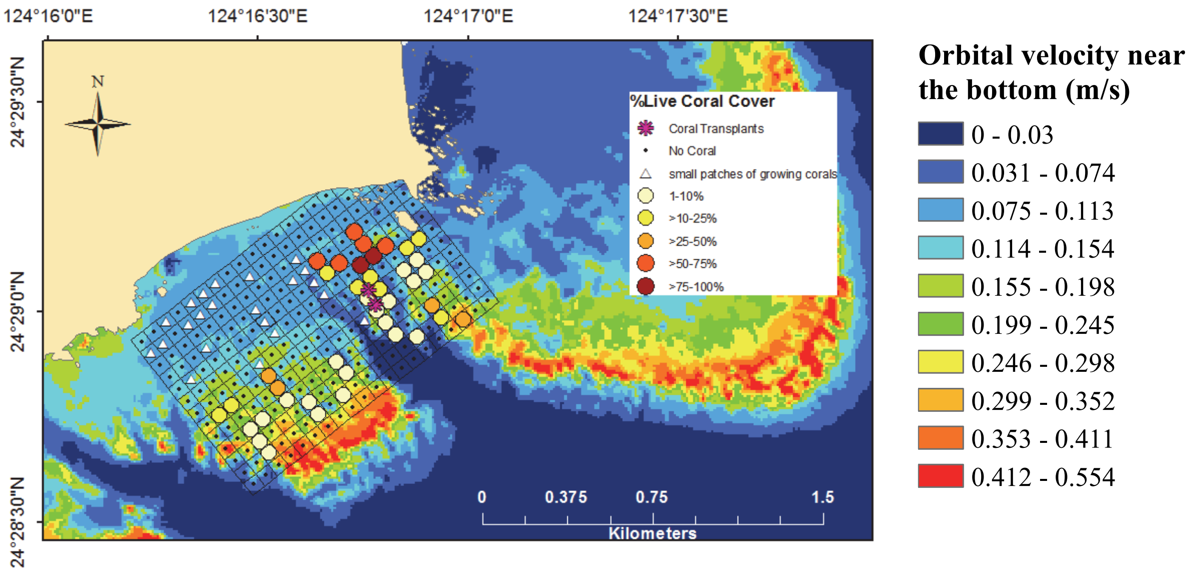

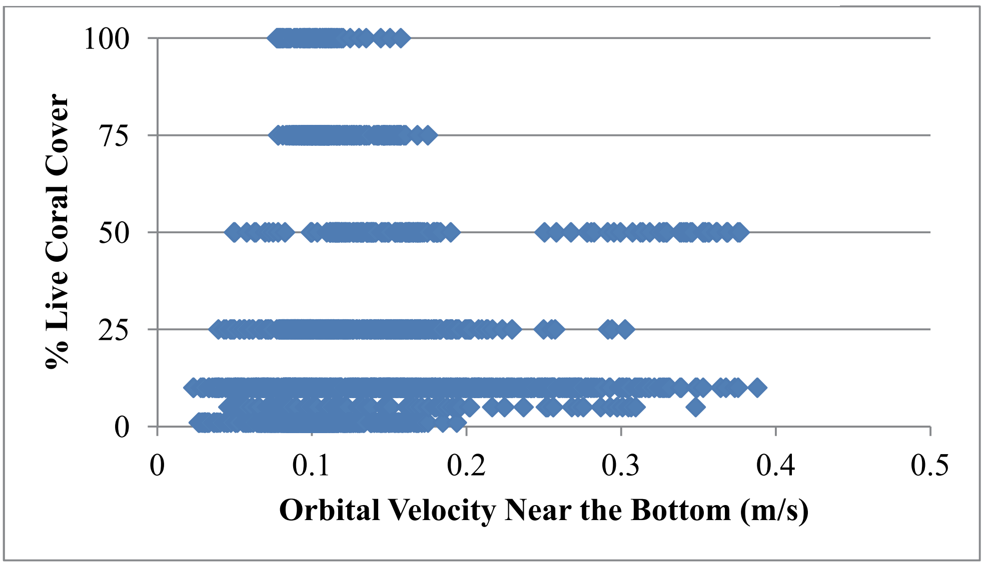

Figure 23. Percent live coral cover vs. distribution of orbital velocity near the bottom (m/s) during normal weather condition

B. Orbital Velocity near the bottom (in m/s) distribution during stormy weather condition

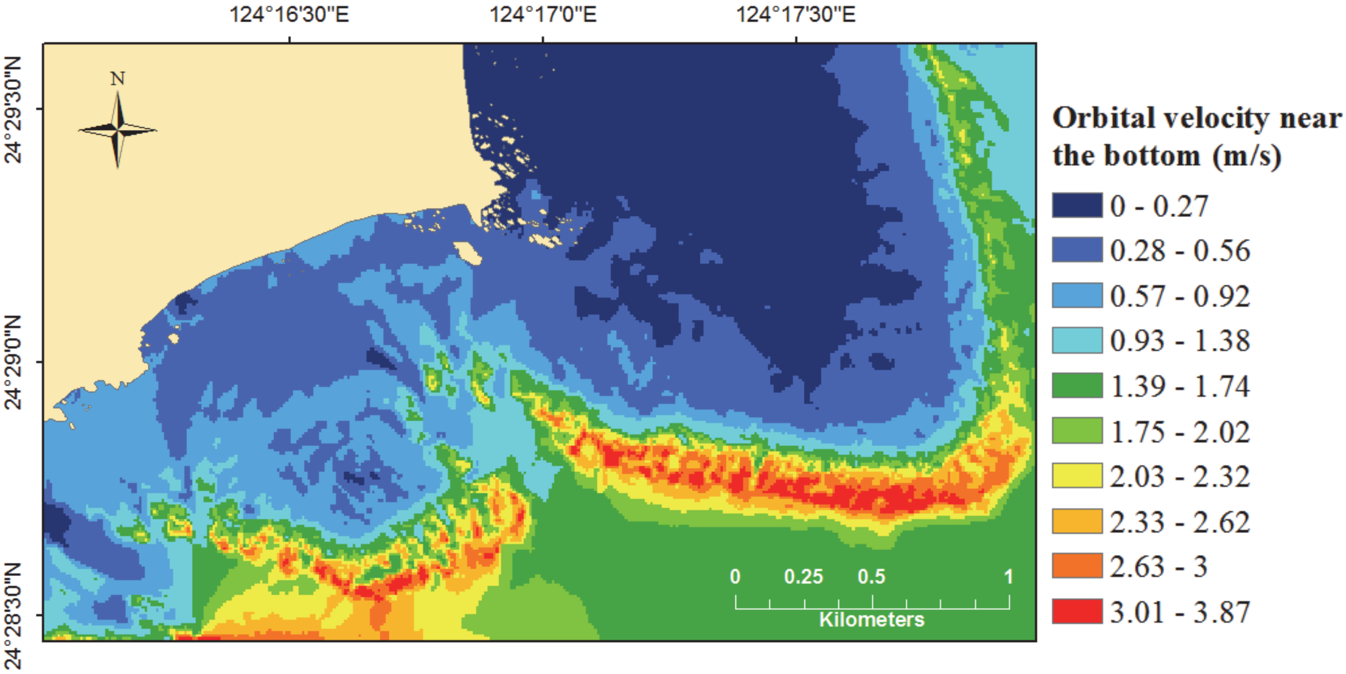

Figure 24. Distribution of orbital velocity near the bottom (in m/s) during stormy weather condition.

Stormy wave conditions with Hs = 11.93 m and T = 14.02 s were propagated with the SWAN model over the study area for dominant southerly and easterly wave conditions with the aim of evaluating the amount of total wave energy dissipation. Figure 24 shows the results of SWAN simulation for U_{bot} distribution during stormy weather condition. This is a simulation for an extreme weather event which occurs only once in ten year-period. When the coral distribution is overlaid to the map (Figure 25), it clearly shows that corals experiences high orbital velocity up to almost 1m/s and that can be damaging enough to the coral branches or can overturn small boulder of coral.

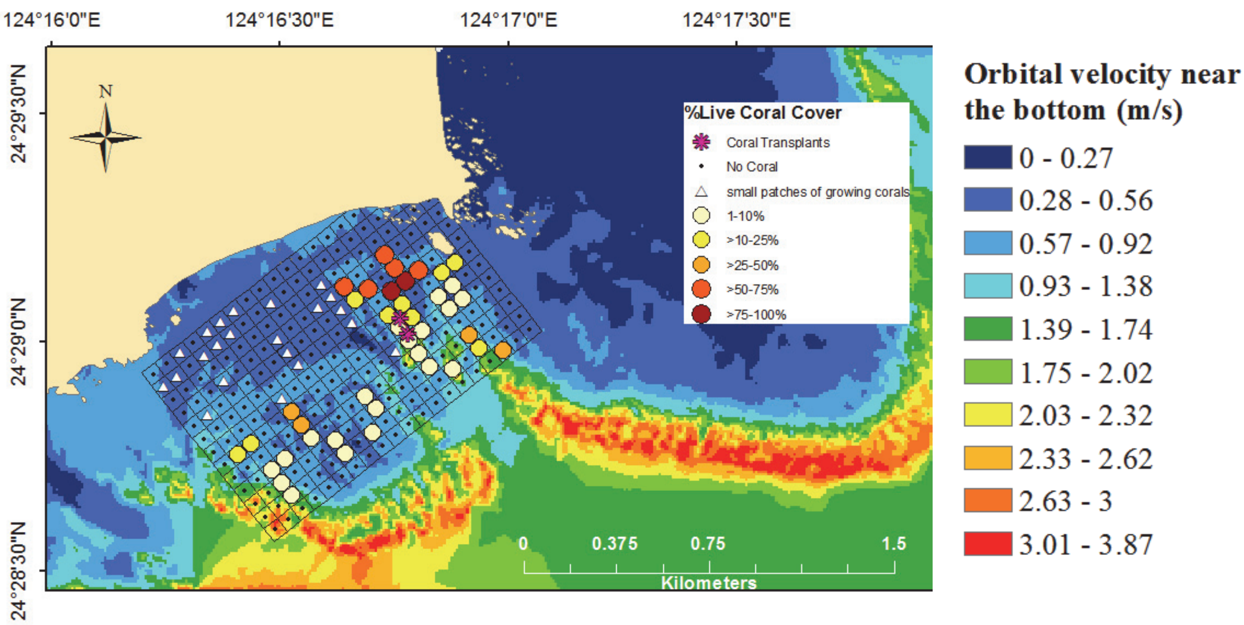

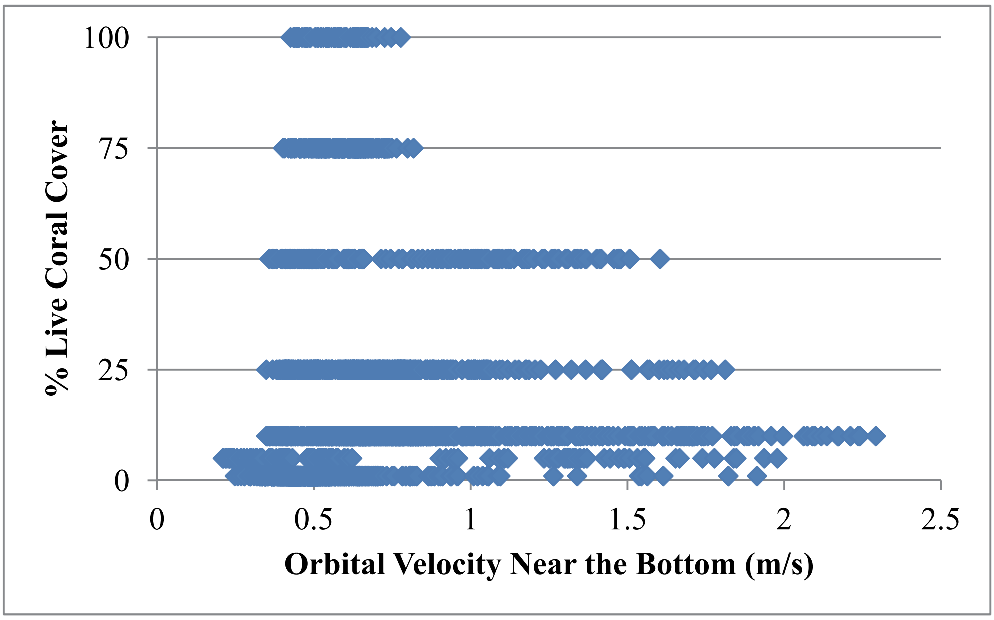

Figure 25. Percent live coral cover vs. distribution of orbital velocity near the bottom (m/s) during stormy weather condition.

3.2.5 Results of SWAN simulation: Calculation of Total Energy Dissipation (W/m2)

A. Total Energy Dissipation (E_{Total}) (W/m^2) during normal weather condition

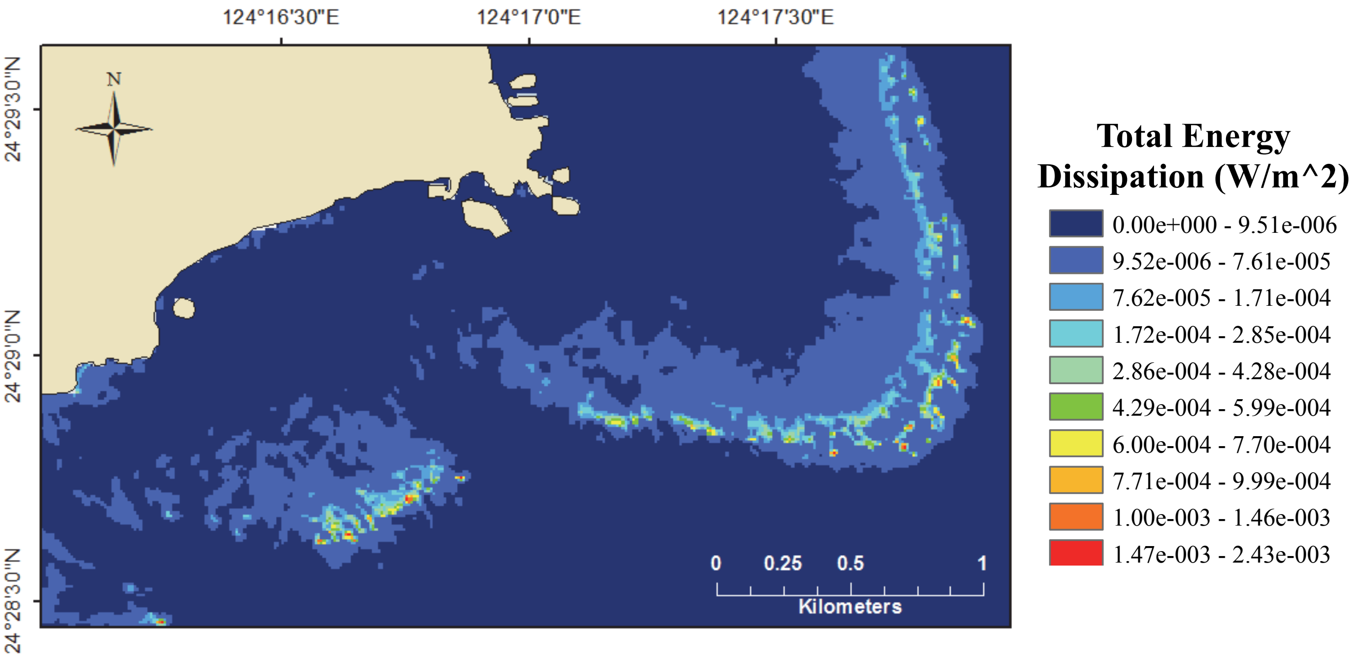

Figure 26. Distribution of total energy dissipation (W/m^2) during normal weather condition.

The total energy dissipation (E_{Total}) was the last variable calculated in SWAN. Figure 26 shows the result of the simulation to calculate E_{Total} in the study area during the normal weather condition. It clearly shows here that similar to the results obtained in the calculation of orbital velocity near the bottom, high energy dissipation is observed over the reef crest area. When the coral cover distribution is overlaid (Figure 27), the E_{Total} in the areas where there are high coral cover density (75-100%) were already very small (2.2e-6 ~8.2e-6 W/m^2).

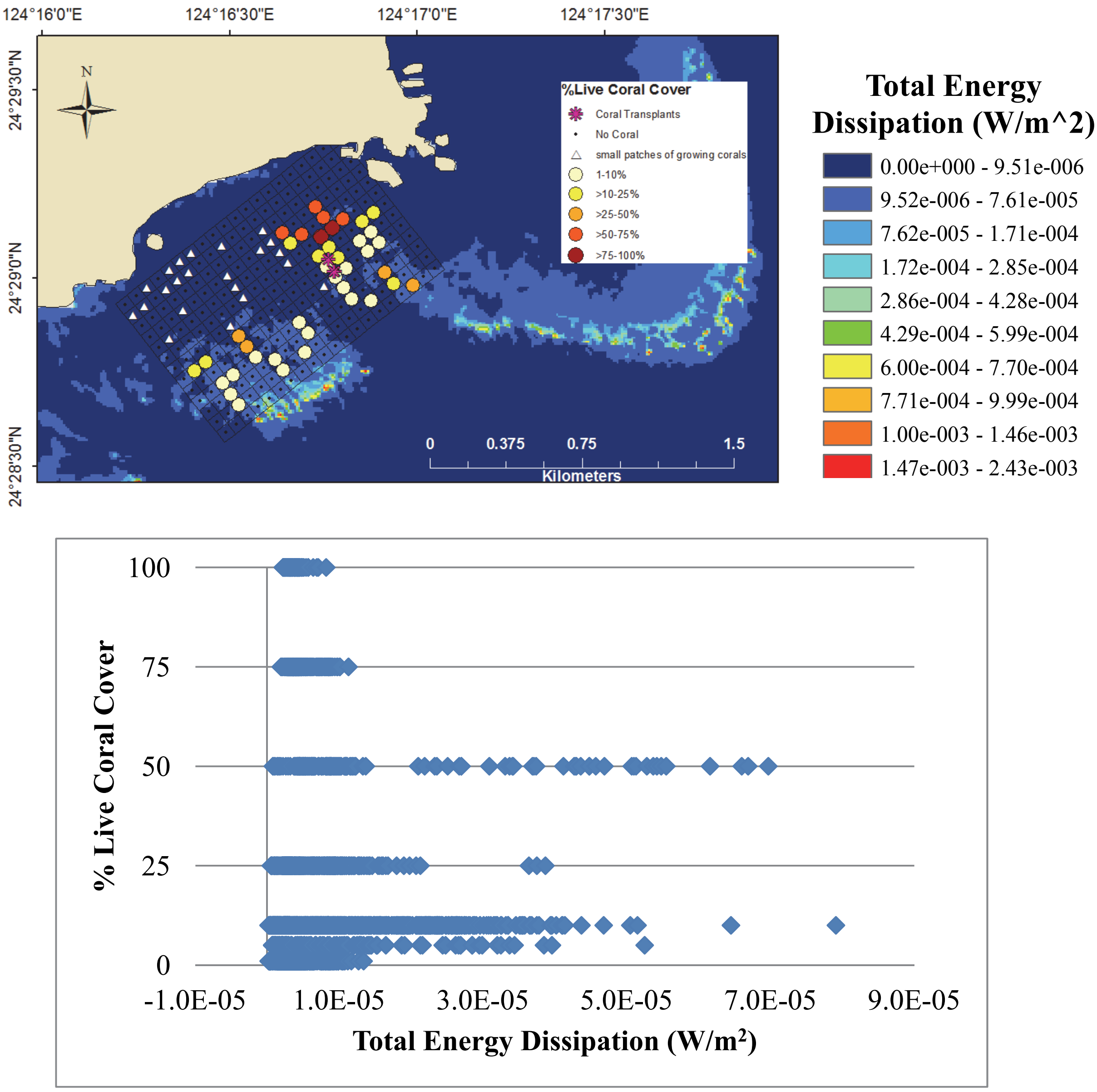

Figure 27. Percent live coral cover vs. distribution of total energy dissipation (W/m^2) during normal weather condition.

B. Total Energy Dissipation (E_{Total}) (W/m^2) during stormy weather condition

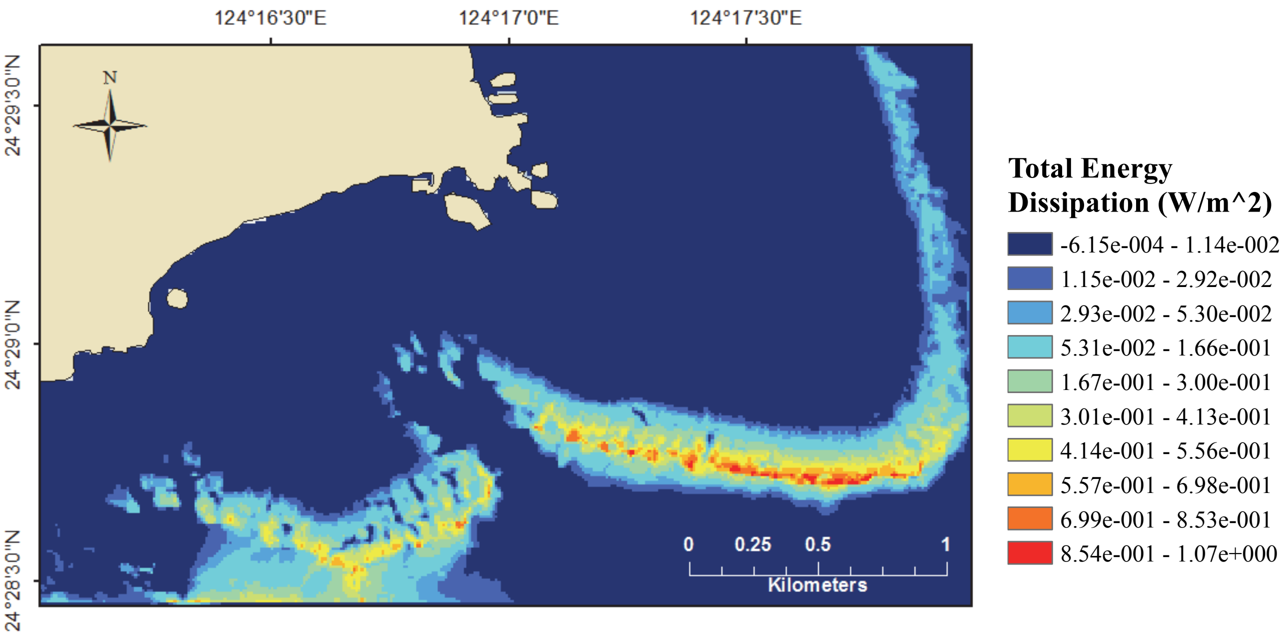

Figure 28. Distribution of total energy dissipation (W/m^2) during stormy weather condition.

For the simulation of E_{Total} during the stormy weather condition, the results showed that almost all wave energy (90%) is absorbed at the reef crest area (Figure 28). When the coral cover distribution is overlaid (Figure 29), the E_{Total} in the areas where there are high coral cover density (75-100%) were already very small (6.6e-5- ~1.4e-3 W/m^2).

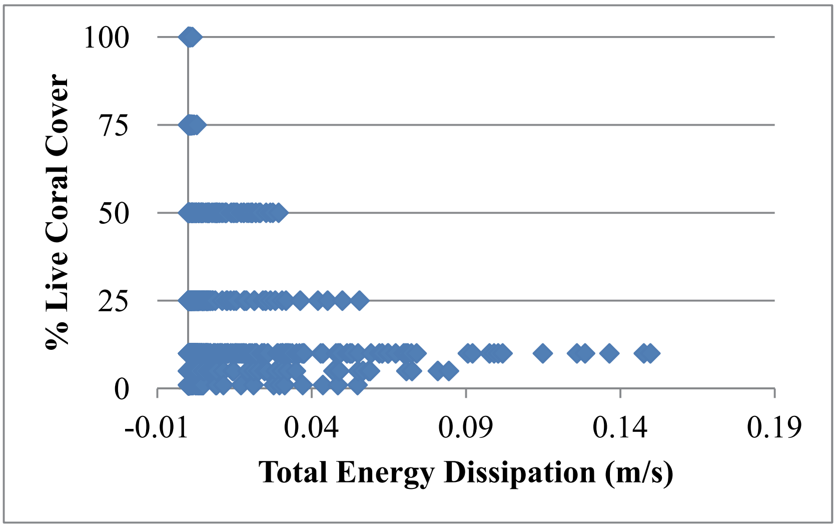

Figure 29. Percent live coral cover vs. distribution of total energy dissipation (W/m^2) during stormy weather condition.

3.2.6 Coral Cover and SST

For the distribution of sea surface temperature (SST), Figure 30 shows the extracted SST from Landsat images (in ˚C) at the study area for the month of August 2013. The extracted temperature range results which is from 26.4 ˚C to 30.0 ˚C (highest) falls within the reported temperature ranges in literature as well as with the direct temperature point data available in the study area. It is evident based on the results of extraction that higher SST (in red to yellow color) occurs in the areas near the coastline, as well as in the shallower part of the study area. In this light, it is possible that some parts of the study area experience heat stress (> 30 ˚C) for a certain period of time, hence, a predictive heat stress distribution map was also developed for this study.

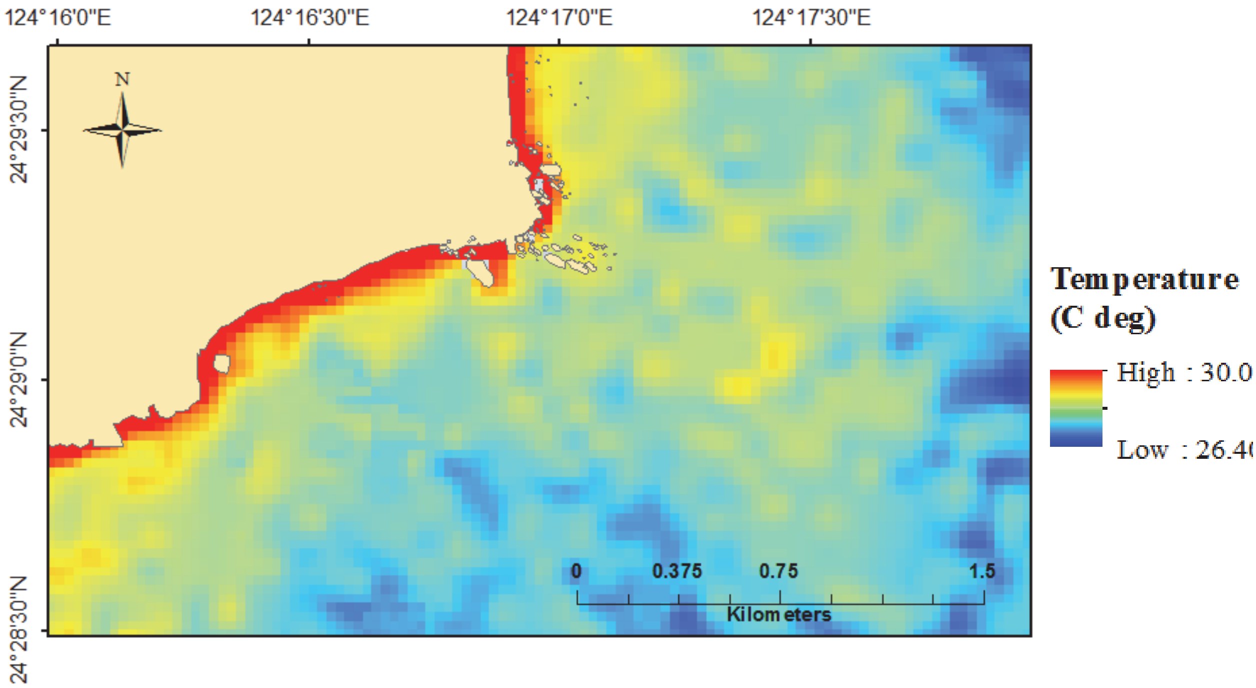

Figure 30. Extracted sea surface temperature distribution from Landsat image for the month of August, 2013.

Overlaying the coral cover to the SST layer as shown in Figure 31, it shows that the temperature ranges within the coral reef areas are within 26.9˚C to 28.6 ˚C. This temperature range falls just within the right temperature limit for the coral reefs in general.

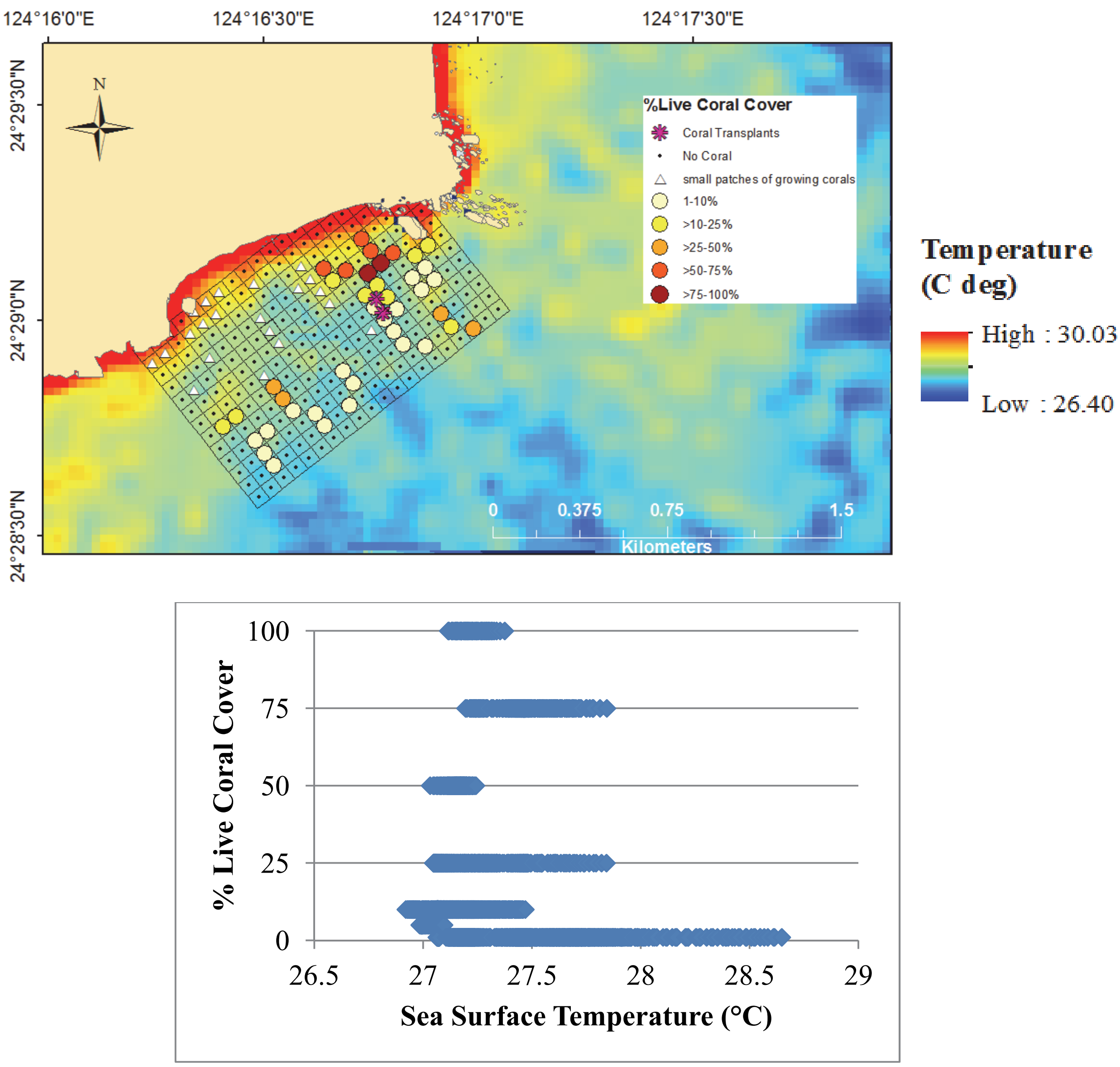

Figure 31. Coral Cover Distribution vs. SST Distribution.

3.2.6.1Development of Heat Stress map

Since the extracted SST represents a month within the summer period in Ibaruma, a heat stress map was developed in order to determine the susceptibility of the corals to be exposed on a high temperature which could be damaging to them. The time-series temperature point data (Figure 32) provided by a private coral research company was utilized in combination with the SST distribution map. The location where the temperature was taken was in the area where the coral transplants are located. Figure 33 shows results of combining the time series point data with the temperature distribution.

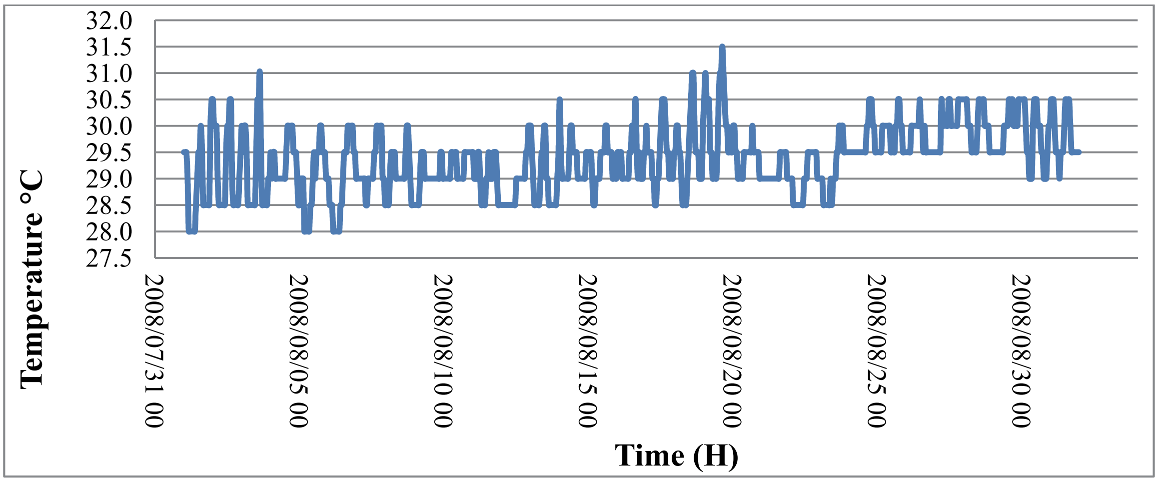

Figure 32. Time series temperature data point for the month of August 2008 at coral transplanted areas.

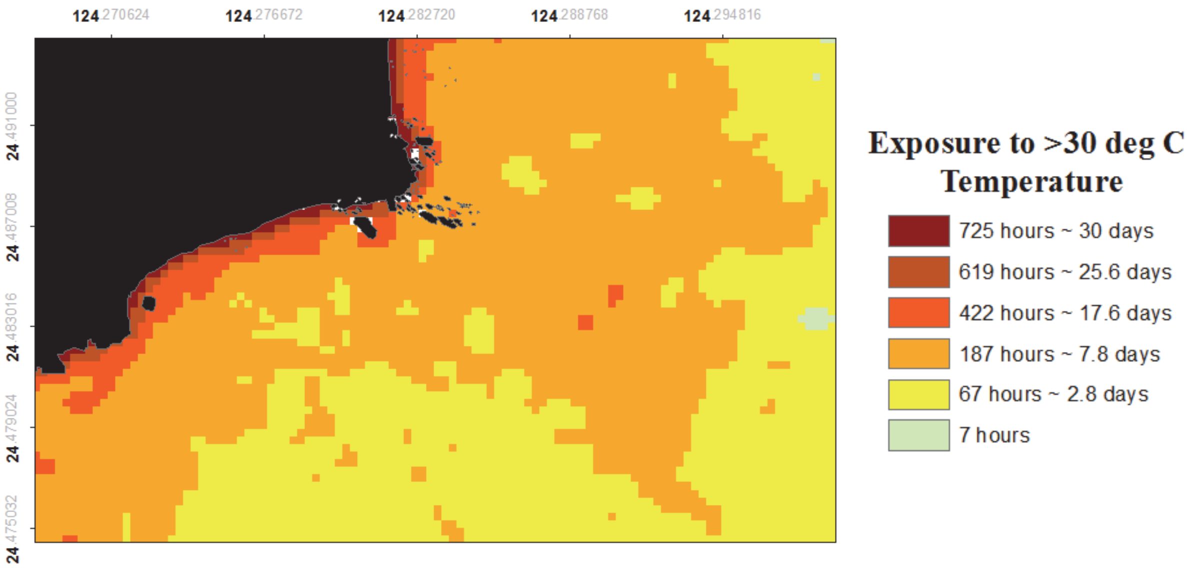

Figure 33. Representative heat stress map for the during summer month (August)

Figure 33 shows the representative heat stress map for the summer period (August, 2013) in the study area. It shows that the areas near the coastline areas experience a constant month-long high temperature with greater than 30°C.

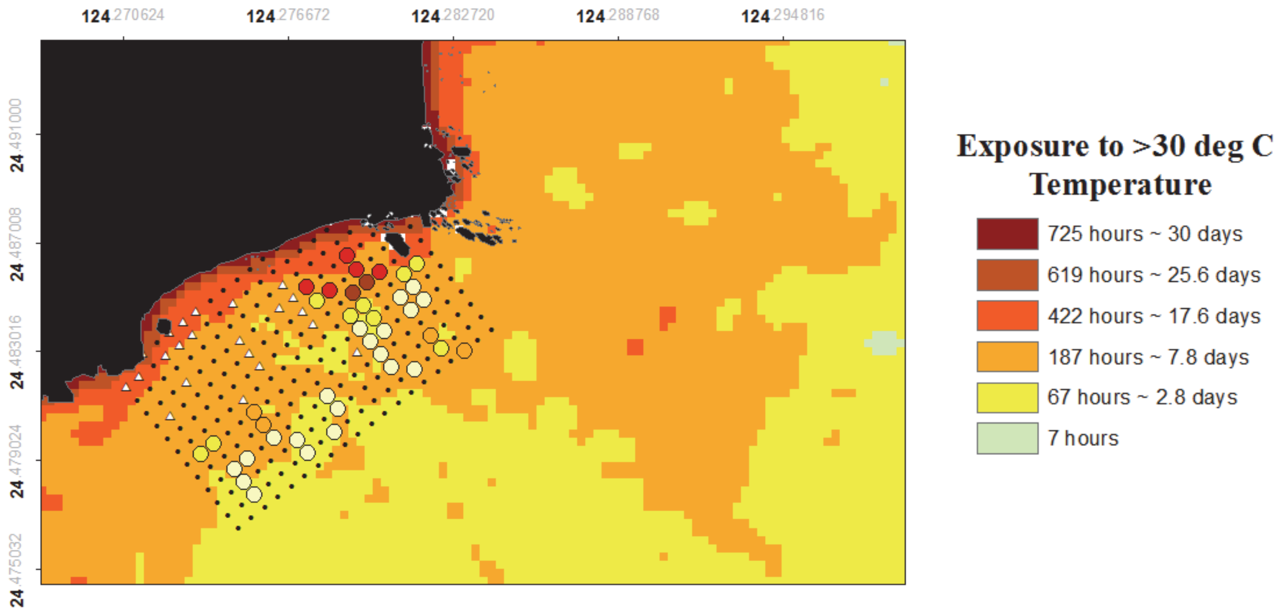

Figure 34. Heat stress map for the coral reef distribution area.

When the coral distribution was overlaid to the map, the resulting image is shown in Figure 34. It shows here that the area with 75% coral cover may be exposed to heat stress for approximately 25 days, and those areas with 100% cover may experience high temperature for a approximately 17 days. The results indicated that the scenario wherein the corals may be exposed to high temperature for a quite period of time maybe detrimental to them and could lead to coral bleaching. However, since the temperature is also regulated with the wave action, this kind of scenario is mitigated.

3.3 Identification of Optimum Condition (Suitability Indices)

The suitability indices were developed based on the extracted information from the areas that exhibit the optimum condition for the presence of coral reefs. The values for the associated environmental predictor in the areas that are optimally suitable are normalized and converted to values ranging from 0 (unsuitable) to 1 (optimal conditions). In this context, the most suitable area equates to the characteristics of areas with high coral cover (100%). Graphic representations of the relation between environmental variables and suitability are shown in the following section. All variables are associated with the coral cover.

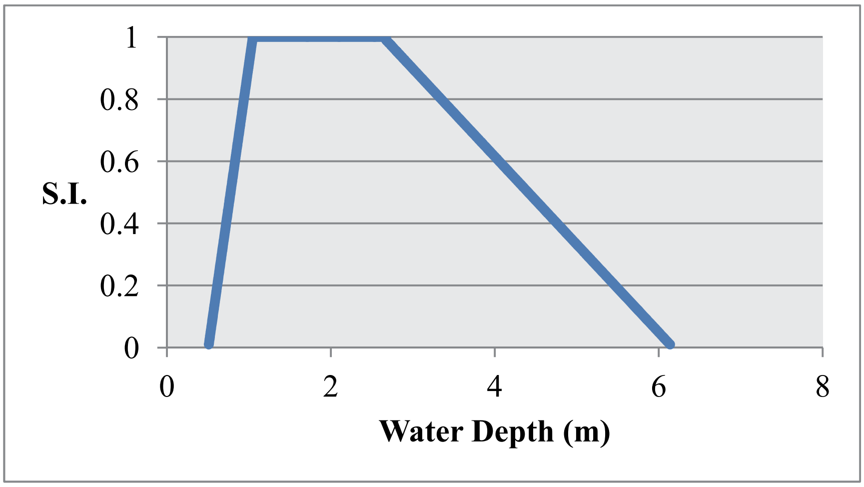

Figure 35. Suitability Index graph for the optimum water depth condition for corals in Ibaruma.

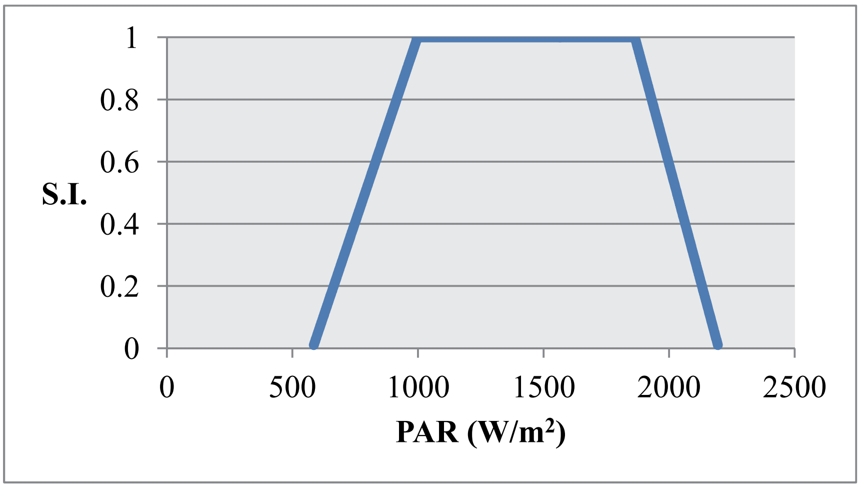

Figure 36. Suitability Index graph for the optimum PAR levels for corals in Ibaruma.

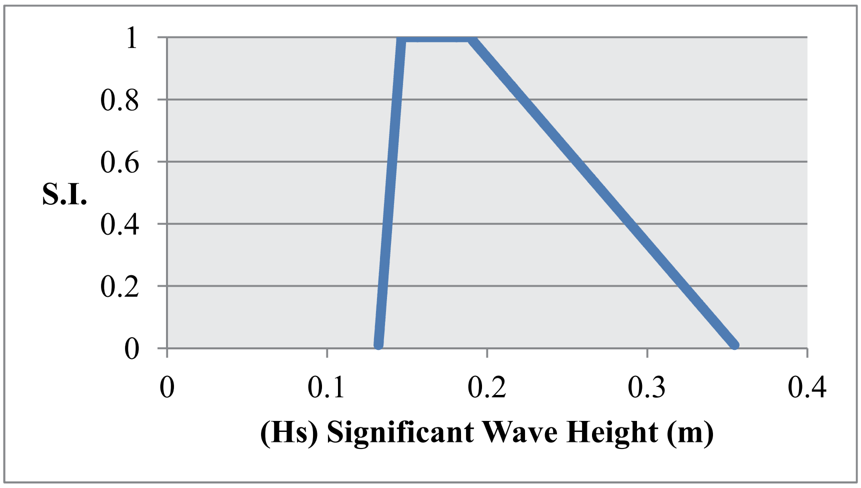

Figure 37. Suitability Index graph for the optimum wave height condition for corals in Ibaruma during normal weather condition.

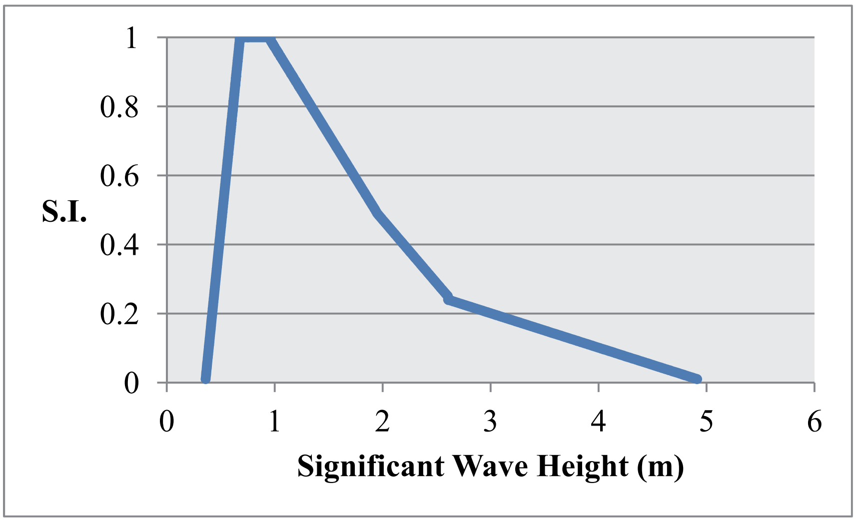

Figure 38. Suitability Index graph for the optimum wave height condition for corals in Ibaruma during stormy weather condition

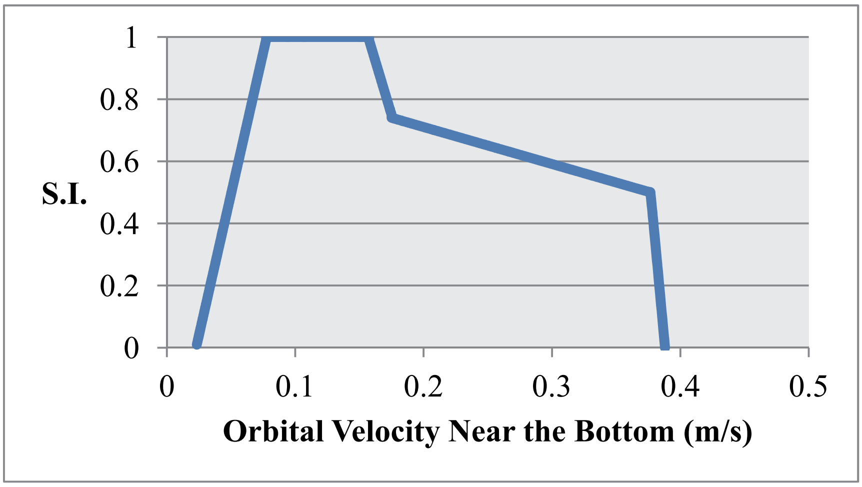

Figure 39. Suitability Index graph for the optimum orbital velocity near the bottom condition for corals in Ibaruma during normal weather condition.

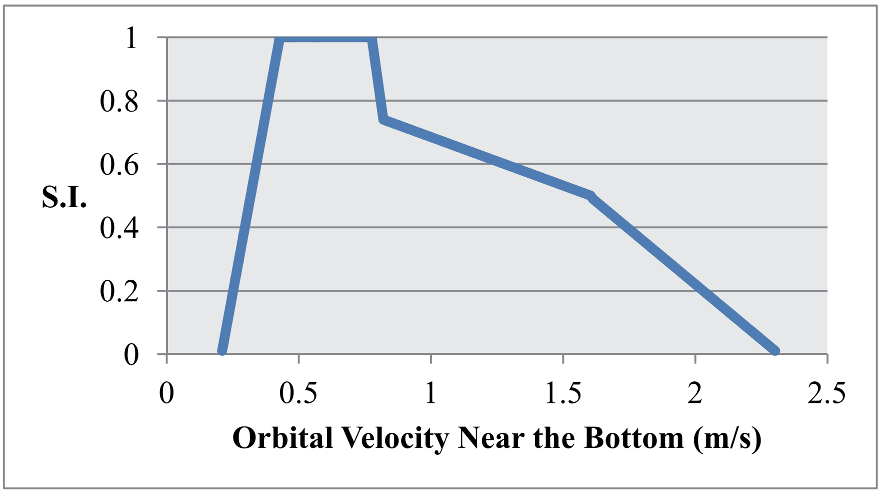

Figure 40. Suitability Index graph for the optimum orbital velocity near the bottom condition for corals in Ibaruma during stormy weather condition.

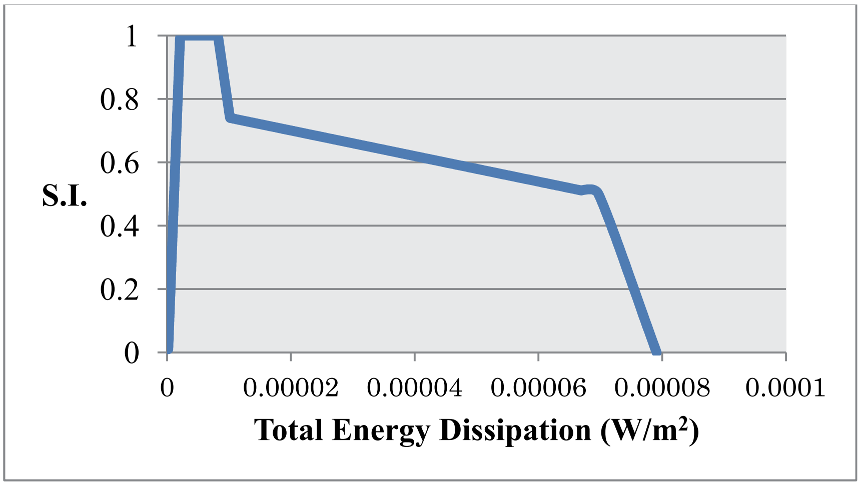

Figure 41. Suitability Index graph for the optimum total energy dissipation condition for corals in Ibaruma during normal weather condition.

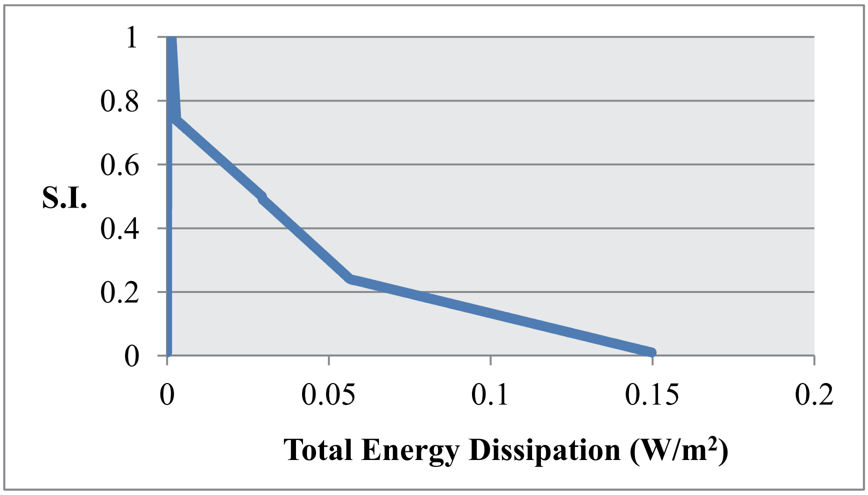

Figure 42. Suitability Index graph for the optimum total energy dissipation condition for corals in Ibaruma during stormy weather condition

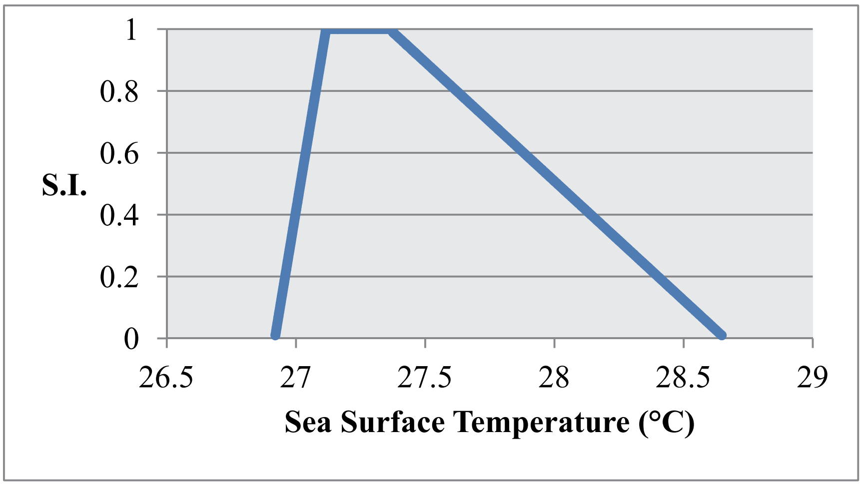

Figure 43. Suitability index graph for the optimum sea surface temperature condition for corals in Ibaruma.

The summary for the values of optimum condition for each environmental variable illustrated in Figures 35-43 is shown in Table 6. The values obtained for the optimum condition for each of the environmental factors exhibit a narrow range of condition especially in the case of U_{bot}. It also shows that the shape of suitability index graph of U_{bot} and E_{Total} is similar.

Table 6. Summary of the values for the optimum condition for coral cover distribution in Ibaruma

Environmental Variables	**Optimum Condition** (**100%**)	**Stormy Condition** (**On areas where Coral Cover are 75%-100%**)
Depth (m)	1.04 ~ 2.67	
Light attenuation (PAR) (W/m^2)	995 ~ 1863	
Significant wave height (Hs) during normal condition (m)	0.146 ~ 0.191	0.556 ~ 0.963
Orbital velocity near the bottom (m/s)	0.077 ~ 0.156	0.402 ~ 0.777
Total energy dissipation (W/m^2)	2.20e -06 ~8.21e -06	6.58e -05 ~ 1.42 e -03
Sea surface temperature (SST) (°C)	27.1 ~ 27.4	

3.4 Identification of the Controlling Factor

To finally achieve the goal of this study in determining the controlling factor of the distribution of corals in the study area, the raw data for each factors and the coral cover were standardized first and subjected to correlation test using Pearson statistical analysis. This statistical test can quantify the relationship of each variable to the coral reef cover, as well as identify the significance (p-value) of the results of the correlation. Afterwards, the standardized variables were subjected to Partial Least Square regression to identify which among the variables can best predict the coral cover in the area. The results of the analysis are as follows:

Table 7. Summary of statistics for the coral cover distribution (response/Y variable) and environmental predictors (X variables)

Variable	Obs.	Obs. with missing data	Obs. w/out missing data	Minimum	Maximum	Mean	Std. deviation
Coral Cover (%)	8947	0	8947	0.00	100	4.97	15.78
PAR (W/m^2)	8947	0	8947	29.0	2268	1279	435
Depth (m)	8947	0	8947	0.485	13.9	2.615	2.20
SST (˚C)	8947	0	8947	26.8	29.7	27.3	0.400
U_{bot} Normal (m/s)	8947	0	8947	0.017	0.448	0.133	0.072
U_{bo}t stormy (m/s)	8947	0	8947	0.200	3.06	0.694	0.383
H_s Normal (m)	8947	0	8947	0.116	0.423	0.200	0.051
H_s Stormy (m)	8947	0	8947	0.363	7.6	1.04	0.867
E_{total} stormy (W/m^2)	8947	0	8947	-1.40e-04	0.502	0.007	0.034
E_{total} Normal (W/m^2)	8947	0	8947	1.01e-07	4.15e-04	9.50e-06	2.10e-05

Table 7 showed the summary of basic statistics (i.e., minimum, maximum, mean and standard deviation values) used in this study for the environmental variables (predictor variables) and the coral cover, regarded here as the dependent/response variable. The number of observation for the coral cover which has ~65 m x 65 m mesh resolution was achieved by employing the resampling tool using nearest neighbor interpolation method available in ArcGIS. The points for all the data where resampled to 10 m resolution. The statistics showed that the mean percent coral cover distribution in the observation area is relatively low (~5%), and could be accounted to the high number of interpolated "no coral" and "small patches of coral" (~1%) data points. It is also the reason why there is higher standard deviation for coral cover distribution (15.78). In the case of environmental variables, the calculation of PAR in the area shows a maximum of 2268 W/m^2 which is the condition found in shallower area, while 29 W/m^2 for the minimum value which is the condition in the more deeper part of the observation area. The mean depth in the observation site is found to be 2.6 m, while the temperature during summer season averages to 27.3 °C. For the results of the numerical simulation of waves, it shows a significant difference in the simulation results between stormy and normal weather conditions. For the wave height distribution the mean significant wave height averages to 1 m during stormy weather condition, while 0.694 m/s for the orbital velocity. The results of simulation for the total energy dissipation yield very small values, with 1.0E-07 W/m^2 as the minimum for the energy dissipation during normal weather condition.

The results of the correlation tests are shown in Table 8, and are illustrated in Figure 41.

Table 8. Correlation matrix (Pearson)

Variables	Coral Cover	PAR	Depth	SST	U_{bot} Normal	U_{bot} stormy	H_s Normal	H_s Stormy	E_{total} stormy	E_{total} Normal
Coral Cover	**1**	**0.070**	**-0.081**	**-0.028**	-0.010	-0.007	**-0.075**	**-0.046**	**-0.041**	**-0.027**
PAR	**0.070**	**1**	**-0.838**	**0.326**	**0.339**	**-0.078**	**0.023**	**-0.269**	**-0.073**	**0.247**
Depth	**-0.081**	**-0.838**	**1**	**-0.282**	**-0.178**	**0.141**	**0.111**	**0.290**	**0.078**	**-0.104**
SST	**-0.028**	**0.326**	**-0.282**	**1**	**-0.250**	**-0.300**	**-0.551**	**-0.277**	**-0.163**	**-0.187**
U_{bot} Normal	-0.010	**0.339**	**-0.178**	**-0.250**	**1**	**0.245**	**0.730**	**-0.198**	**0.068**	**0.696**
U_{bo}t stormy	-0.007	**-0.078**	**0.141**	**-0.300**	**0.245**	**1**	**0.619**	**0.819**	**0.755**	**0.151**
H_s Normal	**-0.075**	**0.023**	**0.111**	**-0.551**	**0.730**	**0.619**	**1**	**0.400**	**0.354**	**0.483**
H_s Stormy	**-0.046**	**-0.269**	**0.290**	**-0.277**	**-0.198**	**0.819**	**0.400**	**1**	**0.677**	**-0.080**
E_{total} stormy	**-0.041**	**-0.073**	**0.078**	**-0.163**	**0.068**	**0.755**	**0.354**	**0.677**	**1**	**0.046**
E_{total} Normal	**-0.027**	**0.247**	**-0.104**	**-0.187**	**0.696**	**0.151**	**0.483**	**-0.080**	**0.046**	**1**

Values in bold are different from 0 with a significance level alpha=0.05

The Pearson correlation matrix as shown in Table 8, shows the degree of how one variable is associated to one another, where the closer the value gets to 1, the higher the positive correlation (0.5 ~ 1.0); and if the value gets closer to -1, the stronger the negative correlation. If the value is nearer to zero, there is no linear relationship between the variables. In this study, there is no strong linear relationship found in the case of coral cover vs. all the variables although the degree of association for each variable can still be measured. In this scenario, the depths (-0.081), followed by significant wave height (-0.075), and PAR (0.070), are the variables most correlated with coral cover distribution in Ibaruma, while both orbital velocity during normal and stormy weather conditions showed the least correlation (-0.010, -0.007 respectively). The highest and most significant correlation is exhibited by relationship between PAR and depths with r = -0.838. Moreover, significant wave height during normal condition is strongly associated with many variables such as SST (-0.551) and orbital velocity near the bottom under normal and stormy weather condition (0.730, 0.619, respectively). For the stormy weather condition, the significant wave height is obviously strongly correlated with the orbital velocity near the bottom under stormy weather condition (0.819), while the latter is strongly associated with the total energy dissipation during the stormy weather condition (0.755). For the total energy dissipation under normal weather condition, it is correlated with orbital velocity near the bottom and significant wave height both under normal weather condition (0.696 and 0.483, respectively).

Figure 44 illustrates the relationships through scatter plots representation across all the variables and coral cover as discussed earlier in Table 8. It also shows here the confidence ellipses or the 95% confidence region of the points/variables where the estimated solution to the problem is found. The values of the variables for horizontal and vertical axis were standardized so that they are dimensionless and easier to compare from one another. The red and blue colour represents the positive and negative relationship respectively.

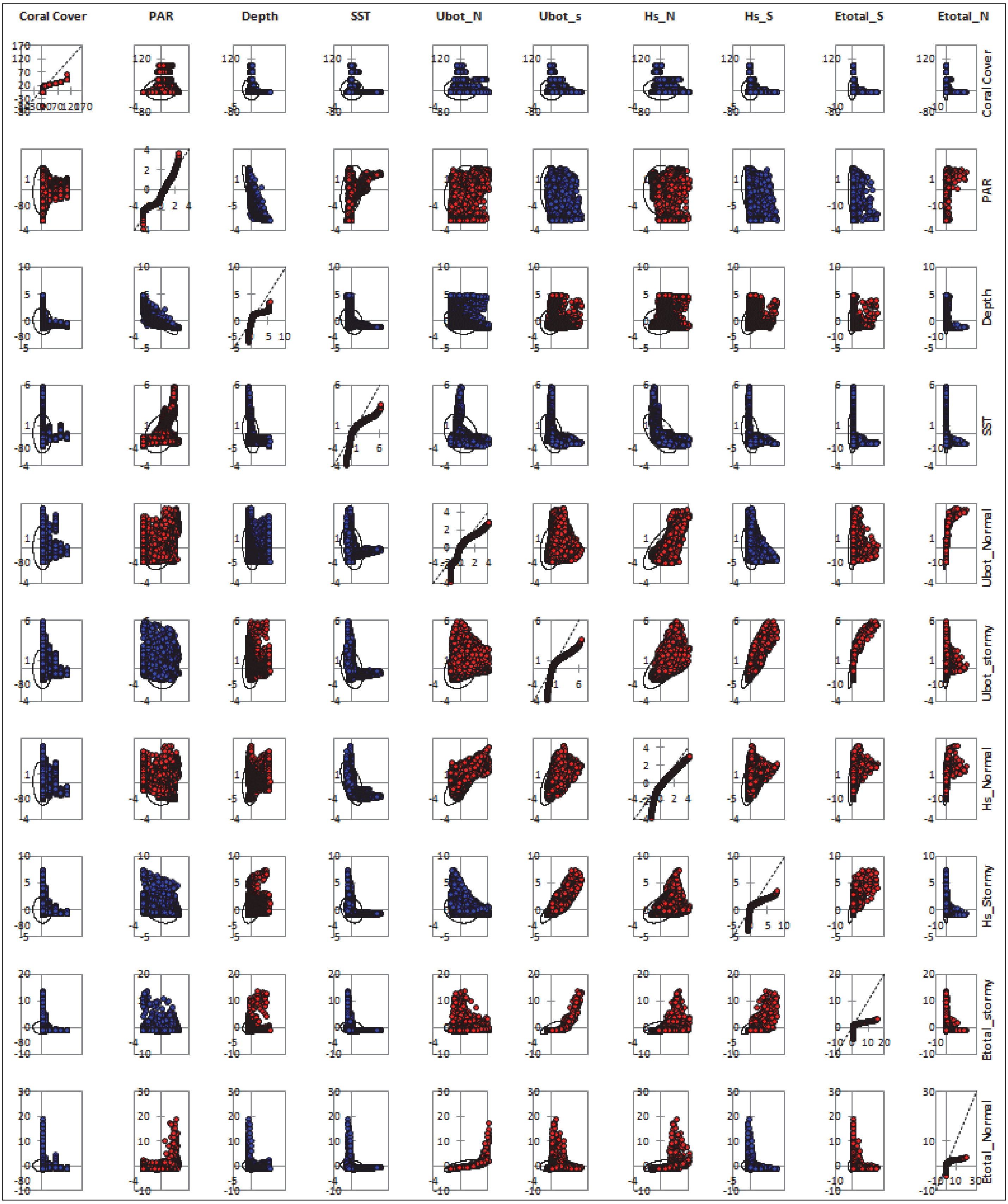

Figure 44. Scatter plots showing the relationship of each environmental factors and coral cover.

Table 9. P Values.

Variables	Coral Cover	PAR	Depth	SST	Ubot Normal	Ubot stormy	Hs Normal	Hs Stormy	Etotal stormy	Etotal Normal
Coral Cover	**0**	**0.000**	**0.000**	**0.007**	0.342	0.490	**0.000**	**0.000**	**0.000**	**0.011**
PAR	**< 0.0001**	**0**	**< 0.0001**	**< 0.0001**	**< 0.0001**	**< 0.0001**	**0.027**	**< 0.0001**	**< 0.0001**	**< 0.0001**
Depth	**< 0.0001**	**< 0.0001**	**0**	**< 0.0001**	**< 0.0001**	**< 0.0001**	**< 0.0001**	**< 0.0001**	**< 0.0001**	**< 0.0001**
SST	**0.007**	**< 0.0001**	**< 0.0001**	**0**	**< 0.0001**	**< 0.0001**	**< 0.0001**	**< 0.0001**	**< 0.0001**	**< 0.0001**
Ubot Normal	0.342	**< 0.0001**	**< 0.0001**	**< 0.0001**	**0**	**< 0.0001**	**< 0.0001**	**< 0.0001**	**< 0.0001**	**< 0.0001**
Ubot stormy	0.490	**< 0.0001**	**< 0.0001**	**< 0.0001**	**< 0.0001**	**0**	**< 0.0001**	**< 0.0001**	**< 0.0001**	**< 0.0001**
Hs Normal	**< 0.0001**	**0.027**	**< 0.0001**	**< 0.0001**	**< 0.0001**	**< 0.0001**	**0**	**< 0.0001**	**< 0.0001**	**< 0.0001**
Hs Stormy	**< 0.0001**	**< 0.0001**	**< 0.0001**	**< 0.0001**	**< 0.0001**	**< 0.0001**	**< 0.0001**	**0**	**< 0.0001**	**< 0.0001**
Etotal stormy	**< 0.0001**	**< 0.0001**	**< 0.0001**	**< 0.0001**	**< 0.0001**	**< 0.0001**	**< 0.0001**	**< 0.0001**	**0**	**< 0.0001**
Etotal Normal	**0.011**	**< 0.0001**	**< 0.0001**	**< 0.0001**	**< 0.0001**	**< 0.0001**	**< 0.0001**	**< 0.0001**	**< 0.0001**	**0**

Values in bold are different from 0 with a significance level alpha=0.05

The significance of the test results is shown in Table 9. P values or the statistical significance indicates the practical significance, or the importance of the data in the applied setting, in this case, the significance of the correlation test analysis of the variables to the coral cover. A small p value (typically $p \leq 0.05$ (alpha significance level) indicates high significance of the test results, while higher p values ($p \geq 0.05$) indicates otherwise. In this study, the correlation results showed that all data/test results showed that they are statistically significant ($p \leq 0.05$) except for orbital velocity near the bottom for both normal and stormy weather day condition. Relatively higher p values are also observed for SST and total energy dissipation during normal weather condition when plotted against the coral cover. Similarly, the relationship of significant wave height and PAR shows a higher p values ($p \leq 0.027$) than the rest of the results ($p \leq 0.0001$).

For the last step, in order to determine which among the variables significantly affects/ or can predict the coral cover, the standardized data of the environmental variables and the percent coral cover were subjected to partial least square regression, a type of multiple regression which can accommodate data with multi-colinearity. Based on the results of the Pearson correlation test, there are many among the environmental variables that are correlated with each other, i.e., depths and PAR, depths, and significant wave height, etc.

The results of the PSLR analysis yielded one significant component explaining the variance in the response variable (coral cover). Among the results is the table of variable of importance to the prediction (VIP) which gives scores to each of the variable in terms of its importance/ weight when predicting the coral cover. The results are shown in Figure 45, and Table 10.

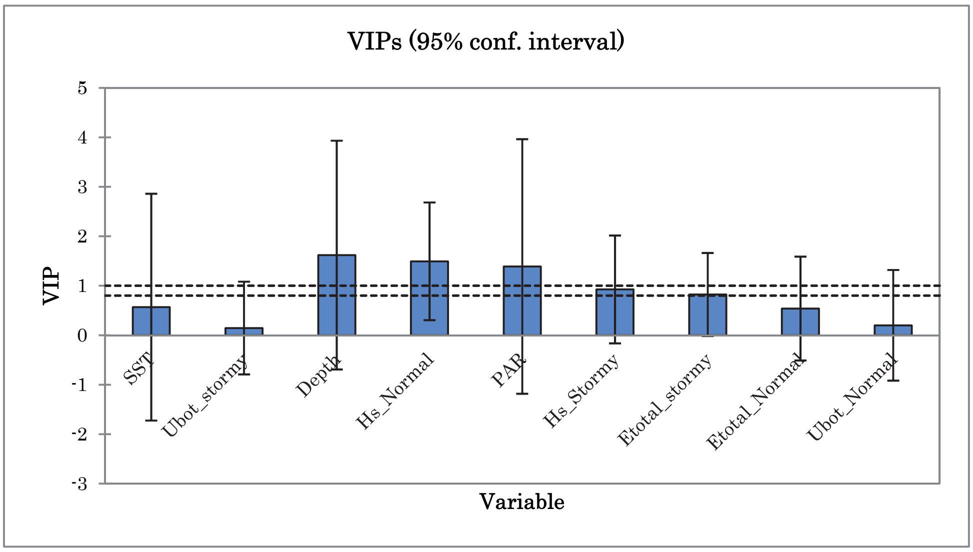

Figure 45. Variable of importance in the projection of coral cover.

Table 10. Variable Importance in the Projection (VIP).

Variable	VIP	Standard deviation	Lower bound(95%)	Upper bound(95%)
SST	0.568	1.17	-1.725	2.86
Ubot_stormy	0.146	0.478	-0.791	1.08
Depth	1.62	1.18	-0.692	3.93
Hs_Normal	1.49	0.607	0.304	2.68
PAR	1.39	1.31	-1.182	3.96
Hs_Stormy	0.926	0.556	-0.164	2.02
Etotal_stormy	0.823	0.428	-0.016	1.66
Etotal_Normal	0.540	0.535	-0.510	1.59
Ubot_Normal	0.201	0.571	-0.918	1.32

In Figure 45, the vertical bars show the magnitude of influence of each environmental factors in the projection of coral cover, and the vertical line in the middle of the bar is the standard deviation. The results showed that the depths, followed by significant wave height during normal weather condition and PAR have the highest VIP score (1.62, 1.49, and 1.39 respectively), while orbital velocity near the bottom both during normal and stormy conditions yielded the lowest score (0.201, 0.146 respectively). The total energy dissipation during normal weather condition and SST showed almost equal scoring in the VIP, (0.540 and 0.568), as well as the significant wave height and total energy dissipation both during stormy weather conditions (0.926 and 0.823 respectively).

CHAPTER 4: DISCUSSION

In natural coastal environment, it is often difficult to treat in isolation the effects of different environmental factors in the coral reef distribution. Rather, the distribution is influenced by a variety of interacting factors, and that, it may be possible to quantify which among these factors dominantly affects the distribution. This study has attempted to investigate the contribution of each factors, and the optimum condition in relation to the percent coral cover in the case of Ibaruma Coast. Such information will be useful in the area's conservation and restoration activities.

Each layer of the environmental variables in relation to the coral distribution prepared for this study will be discussed in detail in the following subsection. It is clear from the obtained results that when an environmental factor is plotted against the coral cover, there is a certain peak observed, which in this study, is regarded as the optimum condition for the coral distribution. The interpretation of the statistical analysis to determine the contribution of each factor will be discussed in the last part of this chapter.

4.1 Coral Cover and Topographic profile of Ibaruma Reef

The results of the coral survey in this study appear typical of a fringing coral reef of the Ibaruma Coast. The study area spans across the shallow lagoon up to the portion of reef crest. Reefs in this area are composed of corals and other benthic organisms which are not evenly dispersed. It is typical that corals in shallow lagoon areas occur in patches, which has been also observed in this study. The coral colony with high percent cover tends to aggregate in one area (124°16'45"E, 24°29'05"N) of the observation site. The results shown in Table 6 provide the quantitative description of the different environmental variables in the area where 100% coral cover is observed. In addition, coral community structure varied most between inshore and offshore sites (near reef crest), where more circular and massive corals are found near the inshore area (i.e., *Porites sp.*), and more tabular, plate-form and foliaceous (*Montipora* sp.) in the near reef crest areas. This observation follows the same distribution patterns observed by Hongo, *et al.,* (2012) which has also conducted coral survey study in Ibaruma, but on the adjacent northern part of this study area. This kind of variation is controlled by different factors, (i.e., temperature, wave action, light intensity, water quality, sedimentation, species interaction) as suggested by most of the coral reef community and assemblage studies that showed similar coral community patterns (Hongo, *et al.,* 2012; Iryu, *et al*., 1995; Dai, 1993; Done, 1982).

4.2 Environmental factors affecting the coral distribution and determination of optimum condition

The determination of the optimum condition for corals is considered an utmost importance since the quantitative information that will be gathered can be very much useful for coral reef management and monitoring. In most of the field studies, the optimum condition for coral reef environment are described qualitatively, for instance, the environmental factors correlated with healthy reef coral growth are described as conditions having "low" turbidity, "low" sedimentation rates, "low" inorganic nutrients, "warm tropical shallow" waters, "enough" light intensity, and "moderate" wave action. However, followed by these descriptions are questions such as, "*How moderate is moderate?*", "*How low is low?*", and or "*How much is enough*?". This study has attempted to answer such kind of issues and quantified the environmental parameters that are associated with a healthy coral reef environment. The results shown earlier are discussed in detail in the following subsections.

4.2.1 Depth

Generally, reefs are recognized as being limited to shallow water areas. For most of the coral reef distribution studies, the context of shallow coastal water is defined as having enough light that reaches the corals which they use for their photosynthesis. Depending on the location, corals can exist at depths up to 50 m, and rarely up to 100 m. This study has revealed that the coral reef in Ibaruma exists at depths ranging from 0.5 m up to 6 m. The highest coral cover is found at 1 m ~ 2.7 m deep. This depth range is found to be most suitable for corals in the study area. Aside from having enough available light for its primary production, one reason that could be accounted for its high cover at this depth range is that corals are not totally being exposed even at low tides. The tides in Ishigaki is semi-diurnal wherein it experiences two high and two low tides at every lunar day, which ranges from 2.5 m during spring tide (high tide) to ~0.8 m below the mean sea level during low tides (Japan Meteorological Agency, http://www.data.jma.go.jp/gmd/kaiyou/db/tide/gaikyo/nenindex.php). Provided that the ambient temperature does not exceed 30°C and there is enough water movement during low tide, the corals will be able to withstand short period of exposure due to low tides. This is because corals are able to develop a mechanism to adapt in such condition, i.e., secretion of protective mucus in order to stay wet, and retraction of polyps (Wild, *et al.,* 2004).

Depth is considered as a separate factor affecting the coral distribution apart from light intensity, though both are related to each other, since the primary purpose of this study is to locate and quantify the optimum condition where high coral cover exist.

4.2.2 Light Intensity

In this study, the light intensity or irradiance available to corals was measured in terms of photosynthetically active radiation (PAR), which is defined previously as the spectral range of solar radiation that photosynthetic organisms can use in order to perform photosynthesis. The results showed that the PAR is evidently higher in shallower areas and decreases with depth. Additionally, the findings of this study showed that the most suitable condition in terms of PAR for corals in Ibaruma ranges to 995 ~ 1863 W/m^2. It must be noted that in this study, the PAR were measured as a function of depth, or we can also say, "PAR reaching the bottom". On that account, the results might not be comparable to the findings of other coral studies wherein light conditions, or PAR levels were measured differently. In reality, the obtained PAR values for the optimum condition are not absolute. It will always be a case to case basis. Since PAR is a function of depth and water turbidity, and turbidity is a function of type of sediment present in the area, it will almost be unlikely to set a fixed benchmark of optimum condition of PAR values for corals in general. Moreover, there is no standardized methods on how to assess/ measure PAR levels in coral reef areas, which is apparent, for example on the varying unit of measurement used, and in the wide range of differences of the obtained results. For instance, the study of Kleypas (1999) focused on the determination of environmental limits of corals in a global scale, where reef limits for the light intensity is 50-450 μ $Em^{-2}s^{-1}$, while the study of Kayanne (1996) in Shiharo reef, Japan, showed that light intensity which varies seasonally ranges from 552 to 864 μ mol $m^{-2}s^{-1}$. Thereupon, however, it is possible to agree on at some extent about the optimal condition when the coral reef area of concern is on the same location or share the same geographical and environmental features. In this study, the water turbidity in Ibaruma is generally, and most of the time - low, as supported by the field measurement conducted where the measured chlorophyll (μ m/ L) approaches to zero.

As discussed earlier, light intensity plays a key role in the presence and or absence of corals. PAR controls the presence and amount of xoozanthallae, chlorophyll, and other photosynthetic pigments (Rodolfo-Metalpa et al., 2008) which are crucial in the coral symbionts' photosynthetic activities. When these factors are combined, as well as the known effects of by-products of photosynthesis, it will in turn indirectly affect the coral growth, and consequently, the reef building/calcification activities of hard corals. At low level of light condition, zooxanthallae are inhibited to photosynthesize, though, there are still coral symbionts which are adapted in this type of conditions, such as some species of soft corals. On the other hand, excessive irradiance can be damaging to corals. This has been clearly shown in the results of this study, where a decline in the presence of corals and reef condition is evident succeeding a certain peak of PAR levels in the area. The effects of excessive light intensity to corals are well documented. When corals are exposed to high light conditions which are way higher than normal, it may cause stress to corals. For instance, one of the factors triggering the occurrence of coral bleaching is increased solar irradiance. Stressed corals exposed to a very high light intensity, coupled with increase in sea surface temperature, and low water exchange, can cause the host corals to expel their symbiotic algae. Since the zooxanthallae, aside from living symbiotically with the host corals, are the one providing color/ pigment to the corals, the abandoned host will start to bleach and lose their vibrant colors, and eventually ceased if exposed for a prolonged period of time.

Knowing the vital effects of what light intensity can do to corals, the quantitative information then about its distribution in a local coral reef area is very important. Coral reef managers will be able to locate the areas where coral bleaching, for example, are possible to occur.

4.2.3 Significant Wave Height, Orbital Velocity near the Bottom, Total Energy Dissipation

This subsection will mainly elaborate the results obtained from the SWAN simulation of significant wave height, orbital velocity near the bottom and total energy dissipation during normal and stormy weather day conditions.

In the natural environment, coral reefs are constantly subjected to the forces exerted by water movement created by current and waves. This phenomenon is essential to create a healthy reef environment as it increases the corals' uptake of nutrients and oxygen, aids in washing off certain metabolic wastes and toxins, as well as relieves the corals from possible thermal stress. However, similar with the other environmental factors, wave action can be beneficial up to certain extent only. Destructive waves brought by strong typhoon and cyclones can bring significant damage to the reef structure and morphology, disabling them from their usual metabolic activities. In this study, the water movement or wave action were represented by three separate factors: significant wave height, orbital velocity near the bottom, and total energy dissipation simulated both under normal and stormy weather condition.

4.2.3.1. Simulation under normal weather condition

In this study, significant wave height is chosen as one of the parameters representing the contribution of water movement and wave action in the area. Defined as the average height of the one-third largest waves (Dollar, 1982), significant wave height is a well-known measure of energy in a wave field (Lugo-Fernandez et al., 1998).

During normal weather day condition, the results have shown that significant wave height in the areas where hundred percent coral cover is observed ranges from 0.15 to 0.2 m. The result of the simulation follows the same pattern/ranges with the results obtained from other studies which conducted actual wave height measurement in shallow coastal water areas (i.e. Lowe et al., 2005; Gillis et al., 2014). In addition, this optimal wave height condition for corals in the specified location is a result of the pressure gradient or radiation stress created from the wave breaking at the reef crest, which consequently drives the reef circulation in the shallower part of the area (Longuet-Higgins & Stewart, 1962). It has been identified that this wave-driven circulation plays a major role in the cross-reef transport of food and nutrients, as well as juvenile settlement (Lowe et al., 2005).

Furthermore, with a 0.38 m as an initial significant wave height approaching the reef crest, it is evident that the coral reefs are able to reduce or "break" the waves to about 40% of the incoming waves which indicates the ability of coral reefs to reduce wave heights. The reduction of depth can cause the alteration of wave height, which in the case of Ibaruma, about 40 m deep from the open ocean to 13 m at the reef edge, and then to about 2-3 m deep in the shallow lagoon area. This is the reason why an increase in wave height distribution is observed around the reef crest area (Figure 18).

When the coral cover was overlaid with the results of wave height simulation, the percentage of live coral cover around the areas where waves are breaking are relatively low, ranging to about 10%-25% live coral cover only. Although reef structure is present, it was observed that most of the corals near the reef crest are composed of fragments of broken dead corals (Figure 43). This situation might be attributed to increased shear stress and the strong attenuation of hydrodynamic energy in the area including the increased orbital velocity near the bottom which can break or damage coral branches.

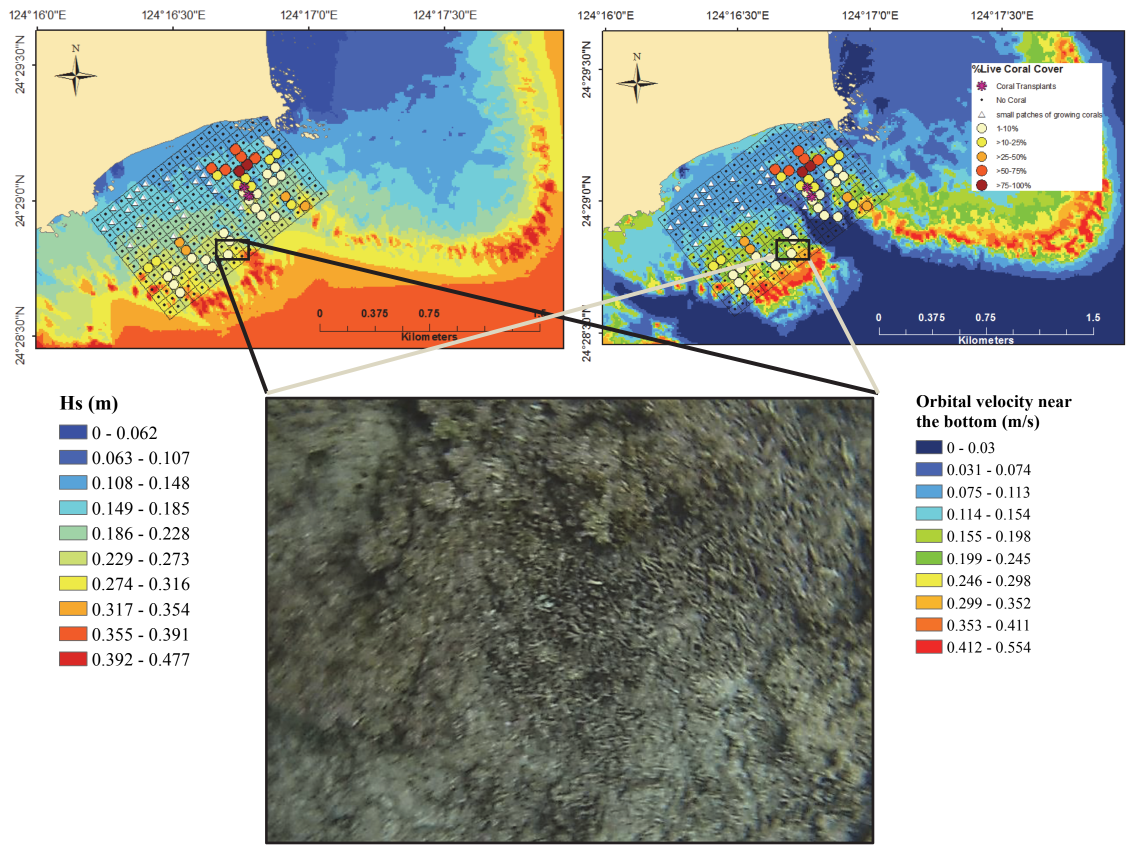

Figure 46. Snapshot of condition of corals near the reef crest of Ibaruma, and the significant wave height and orbital velocity near the bottom distribution.The area is composed of broken fragments of corals.

Orbital velocity near the bottom, on the other hand, is the velocity of water particles due to wave motion that is particularly brought by surface waves. Investigating orbital velocities near the bottom is mostly associated with sediment transport studies (i. e. Storlazzi et. al., 2002; Hsu et. al., 2006) and is therefore another important factor to look at in this study. Since measurement of sedimentation rates is not part of this study, the information about the distribution of orbital velocities near the bottom will somehow give an indication about what might be happening with the sediment particles in the area. Results have shown that orbital velocities at the reef crest area are particularly high, and coral cover is low. As the waves pass through the reef crest and go through the shallow back reef lagoon, the orbital velocity tends to decrease and become more evenly distributed. At the areas where high coral cover is found, the orbital velocity ranges from 0.08 to 0.16 m/s, which is about 70% decrease from the reef crest areas where wave breaking occur. It must also be noted that at the deeper part of the study area (towards the offshore), the orbital velocity is very little and approaching almost to zero. This is because orbital velocities decline with increasing depth (Baldock et al., 2014) and shorter wavelengths. This means that at the deeper part of the ocean, orbital velocities near the bottom are almost negligible. The result of a recent study of Baldock et al., (2014) showed similar trend where orbital velocity near the bottom increases to a maximum depth of 1 m to 1.2 m at the reef flat, and then decreases with an increase with depth.

On this account, the results of the wave simulation have explained the reason why the condition of coral cover near the reef crest is relatively low. This finding is supported with the video transect file collected, wherein fragments of broken corals and high amount of sediment and rubbles are present in the area (Figure 43). The same results were obtained from the studies of Storlazzi et al. (2002) in which, he suggested that in high-energy environments, (reef crest area), the reef could be less well-defined, and the coral cover could be relatively lower composing of more wave-tolerant species. The coral breakage and abrasion maybe accounted to high bottom orbital velocities around the reef crest areas which may trigger high suspension of sediment in the coastal water (especially during stormy weather condition).

The last factor associated with the water movement and wave action that is considered in this study is the total energy dissipation. The total energy dissipation is defined as the “dumping” or “transmittal” of energy from the surface gravity waves over time due to bottom friction, or roughness of benthic communities that causes water turbulence (Hearn et al., 2001). By turning on the option for the presence of bottom friction, as well as providing relevant input parameters in the SWAN wave simulation, the total energy dissipation was calculated. Results showed that energy dissipation mainly occurs at the entrance of reef crest area, and as the waves go to the shallow lagoon, the energy dissipation decreases and tends to distribute evenly at the shallow lagoon area where the higher coral cover are present. The Ibaruma's spur and groove system which is evident at the reef crest and reef slope area creates a rough bottom friction which induces the energy dissipation. As it enters the shallower part of the lagoon, where the bottom is relatively even and smoother, the dissipation decreases.

A study of Hearn et al., (2001) showed that energy dissipation is proportional to the nutrient uptake of corals, as well as to the bottom shear stress and speed, creating high rates of mass exchange. This finding is particularly important in understanding the reason on why, even with low nutrient levels of the warm tropical seas, the corals still manage to flourish.

Henceforward, it must be taken into account that the bottom friction is one of the most important aspects to create energy dissipation. For instance, a rough bottom, in this case may be composed of reef ridges, or simply just by coral cover. It should follow then that areas covered with corals or spur bottom will create energy dissipation that is essential in mass-nutrient exchange.

4.2.3.1. Simulation under stormy weather condition

Evidences from various studies on how cyclones, storms, and extreme weather events affect the coral distribution and morphology are already well-established. Since Ibaruma, Ishigaki Island is situated on the tropical warm waters of the pacific side; it is therefore prone to frequent storm and typhoon events. Hence, this study has also attempted to simulate the three wave-related factors during stormy weather conditions in Ibaruma.

With an initial boundary conditions of 11.93 m significant wave height and a period of 14.02 s, simulation of distribution of significant wave height, orbital velocity near the bottom, and total energy dissipation under the stormy weather condition were carried out. Results showed significant increase for all the parameters, with almost the same pattern of distribution, which may pose a major threat to the corals especially to those that are located in the reef crest.

For all the three parameters, the corals that are located on the edge of the crest, between the shallow area and the deeper part, will experience considerable amount of stress brought by strong wave action, as the waves start to break and shoal in this part. Hongo et al., (2011) conducted a study on the northern part of Ibaruma (about 1200 m away from this study's observation area), wherein he was able to simulate the effects of strong typhoons on coral communities under global warming condition. In his findings, an initial wave height with 10 m and 10 s period entering the reef areas will damaged the tabular corals located in the reef crest, while the massive corals located in the shallower lagoons will survive.

Some studies suggested that at certain point, coral reefs can tolerate high levels of hydrodynamic energy, i. e., Gillis et al., (2014) indicated that the usual threshold for coral reefs is 0.9 m wave height. In this study, the results showed that the significant wave height passing over the areas with high coral cover in the case of strong typhoon event ranges to 0.556 ~ 0.963 m which is still within the usual threshold for the corals to handle. However, those that are in the reef edge and reef crest with a simulated wave height of >1 m up to 6 m high, will suffer severe physical damage and breakage. The orbital velocity within the bottom is extremely high; hence, the possibility of sediment agitation and suspension to water column is very high. The same situation occurs for the total energy dissipation. Though as mention earlier, the increase in the total energy dissipation promotes an increase in the nutrient uptake of corals, this process might be hindered by high suspended-sediment concentration to the water column. The sediment particles, when present in high concentration, might disable the corals' mechanism to expulse sediment, and block the polyps from getting nutrients.

It is known that extreme weather events such as typhoon significantly influence the distribution and morphology of the coral reefs. However, this still depends on the frequency and severity of the typhoons as they do not occur all the time. Coral reefs maybe damaged up to certain extent, but depending on the frequency of the typhoon and the intervals, they will be able to recover given a sufficient time (Uhrin & Schellinger, 2011).

4.2.4 Sea surface temperature

The effects of sea-surface temperature to the corals are already well-documented. In most of the studies, it was reported that the optimum temperature for most coral reefs is 26–27 °C (79–81 °F). The findings of this study follow the same range of optimal temperature condition in which the temperature where high coral cover ranges to 27.1–27.3°C. It must be noted that since the observation area is a bit smaller, the distribution of SST tends to distribute evenly at the shallow lagoon area. Distinguished high temperatures (>=30°C) are observed near the coastline wherein during the period of summer season, thermal stress may occur to corals located near this area. For this reason, a heat stress map was prepared in order to determine which areas might suffer from extreme high temperatures. Using the temperature point data available in the observation area and the temperature distribution map, the areas exposed to >30°C were plotted in the map and the number of hours the corals are being exposed are counted. The results have indicated that the corals with 100% cover maybe exposed to heat stress for a total of 18 days during the hottest month (August) in Ibaruma. However, based on the temperature point data, the exposure is not continuous; the high temperature is experienced particularly during the mid-day. Moreover, prolonged exposure to high temperature can still be mitigated since this scenario can be regulated by wave action.

Taking a closer look on the distribution of SST in the coral reef area in Ibaruma, it is apparent that the temperature ranges are evenly distributed throughout the area. In this case, it might be difficult to distinguish the effects of SST in the case of Ibaruma, however it will still be subjected for statistical analysis in order to know its overall contribution to the coral reef distribution in the area.

4.3 Interpretation of Statistical Analysis Results

Quantifying the relationship of variables to each other provided an integrated overview of how one factor affects another. The information is useful in terms of ecological and engineering point of view, where one will have a full understanding on the factors that needed to be managed. Figure 47 shows the graphical relationship of each variables and the coral cover to each other. The blue tone gradient signifies negative correlation while the red represents positive correlation.

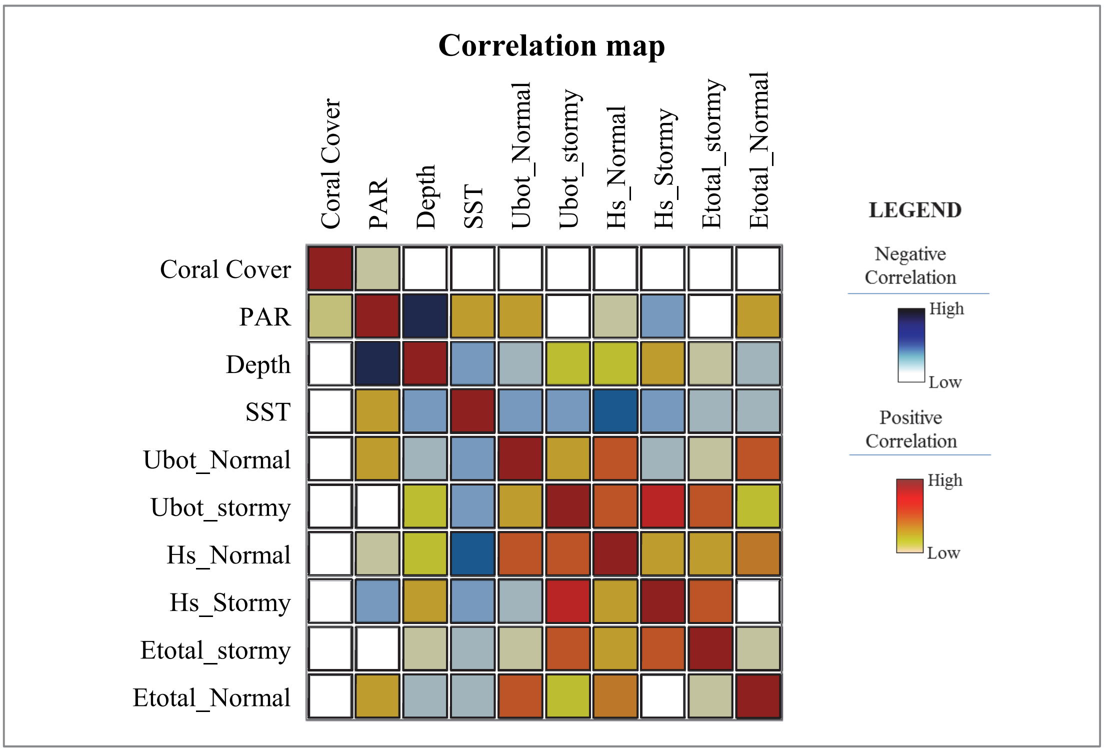

Figure 47. Correlation Map of %Coral cover and the different environmental variables employed in this study.

Figure 47 is the graphical representation of Table 7, the correlation matrix. It must be noted that a low significant correlation result were obtained between coral cover and among all the environmental variables considered in this study. It must be accounted to the relatively smaller ratio of the area of coral cover to the total observation area. Aside from this, the coral distribution tends to exist in clusters, or in patches, which is typical of a coral distribution in shallow lagoon areas. The “spaces”, or the “no coral” data points influence the final results in the regression analysis. Nonetheless, although low values for correlation were obtained, the factor which has the highest impact to the coral distribution was still obtained through the partial least square regression analysis.

For the correlation across the variables, there is a strong inverse relationship between depth and PAR. This result is quite obvious since as mentioned earlier, light intensity is a function of depth. The same is observed with SST, where temperature decreases with a decrease in depth. It must also be noted that under normal weather condition, the depth is negatively correlated with the total energy dissipation and orbital velocity near the bottom, while positively correlated during stormy weather condition.

For the total energy dissipation, studies have suggested that the energy dissipation mainly applies at the areas where wave breaking occurs (Sorensen, 2006); in this case, it is at the reef crest of the area. However, there is no direct argument that total energy dissipation is inversely associated with depth since energy dissipation primarily depends on the type of breaker, bottom roughness, and slope present in the area. Under the simulation of stormy weather conditions for the total energy dissipation, the positive correlation then can be explained by the high significant waves (that can be break when it reaches reef the crest) brought by the typhoon. The result of the simulation supported this assumption wherein a high-significant correlation is found between significant wave height and total energy dissipation during stormy weather condition.

A very weak correlation has been observed for orbital velocity near the bottom in relation with depth: a weak negative correlation during normal weather condition, and positive correlation during stormy weather condition. However though, as mentioned earlier, results of other studies have suggested that orbital velocity near the bottom is higher in shallower areas and is decreasing with depth. It must also be noted that orbital velocity near the bottom has strong correlation with significant wave height both during normal and stormy weather condition, and is just logical since theoretically, orbital velocities near the bottom are directly proportional to significant wave height and depend inversely with the depth (Wiberg & Sherwood, 2008).

The three parameters related with wave action are at some extent exhibit strong linear correlation with each other. Differences lie on the weather condition and other factors that primarily affect one factor more than the other such as bottom friction, slope, depth, and wavelength.

In the case of SST, it shows a relatively lower correlation with almost all other parameters except for the strong inverse relationship shown with the significant wave height during normal weather condition. This is understandable since high significant wave height are mainly observed first at the deeper part of the observation area, where SST is obviously lower, and then at the crest where a higher wave height is observed due to wave breaking. In this area, water is highly agitated because of water exchange caused by wave breaking, lowering the ambient temperature.

Lastly, in the case of PAR, aside from apparent inverse association with depth, shows an inverse relationship to significant wave height, total energy dissipation and orbital bottom velocity during stormy weather condition and a positive correlation during normal weather condition. Yet again, this result is just expected, since during stormy events, aside from thick cloud cover that lessen the solar radiation penetration; the water itself is highly agitated due to strong wave forces present in the ocean water, where possible turbidity may occur.

4.3.1 Controlling Factor

Quantifying the relationships of all variables with the coral cover and to each other has led to the determination of the controlling factor that is most influential to coral reef distribution in Ibaruma. The partial least square regression analysis, which is a type of multiple regression analysis designed for problems having highly-correlated variables, has successfully determined which among the factors considered in this study, is the most controlling factor. Based on the variable of importance to the projection of coral cover, the coral reef distribution in Ibaruma is mainly controlled by depth gradation. Since wave height and PAR are both a function of depth, it is understandable that depth, among any other variable, controls the reef distribution in the case of Ibaruma. The total energy dissipation is also somehow a function of depth because of its strong dependence to the roughness of the bottom. The SST is also generally dependent to depth. The least controlling factor that is found out in this study is the orbital velocity near the bottom during stormy weather condition. Although it is also related with depth, other factors might have been more dominant in the distribution of corals in the area.

CHAPTER 5: CONCLUSION AND RECOMMENDATION

The reef distribution is not always predominantly controlled by a single environmental factor, but it is dependent on the combination of different interacting environmental variables. Using a methodological approach which integrates field observation, GIS mapping, numerical-wave simulation and SST remote sensing, this study was able to determine the correlations between the range of environmental factors and coral reef distributions in Ibaruma Coast, Ishigaki Island Okinawa, Japan. The areas where the corals are most abundant, as well as the optimum conditions for corals were identified. Upon the course of identifying the optimum conditions for corals in the area, environmental stressors, such as possible heat stress occurrence and areas where corals will be most affected by extreme weather events such as typhoons, were identified. Ultimately, this study has identified the most controlling factor affecting the distribution of coral reefs in a local scale. Supported by the results of statistical analysis, series of simulations, and field observations, the most controlling factor among the environmental variables considered in this study, in the case of Ibaruma Coast, is the depth. Such information will be a useful management and monitoring tool in the current restoration and transplantation activities in the area.

While the findings of this study have underscored and confirmed the possibility of overlaying and mapping the various environmental factors in order to understand the complex interaction happening in a coral reef ecosystem on a local scale, there is still a need to improve the study design and include other environmental parameters such as other water quality parameters (salinity, nutrient loadings, turbidity), and tidal fluctuations. This will give a better understanding and holistic view of the synergistic and antagonistic effects of each environmental factor to the distribution of coral reefs. Moreover, for future works, using the suggested methods employed in this study, it is recommended to investigate and increase study sites for comparison (i.e., areas with adjacent outflows/rivers; enclosed bays), as well as include temporal data in addition to the spatial data available. Lastly, this study can be used as a first step for habitat suitability modeling in a local scale which can be practically applied to unsurveyed locations in order to compensate missing spatial information gaps.

REFERENCES

Ahmed, M, Chong, C.K., and Cesar, H., (eds). (2005). Economic Valuation and Policy Priorities for Sustainable Management of Coral Reefs. Second Edition. WorldFish Center Conference Proceedings 70, XX p.

Andréfouët, S., Muller-Karger, F. E., Robinson, J. A., Kranenburg, C. J., Torres-Pulliza, D., Spraggins, S. A., & Murch, B. (2006). Global assessment of modern coral reef extent and diversity for regional science and management applications: a view from space. In Proceedings of the 10th International Coral Reef Symposium (Vol. 2, pp. 1732-1745).

Baldock, T. E., Golshani, A., Callaghan, D. P., Saunders, M. I., & Mumby, P. J. (2014). Impact of sea-level rise and coral mortality on the wave dynamics and wave forces on barrier reefs. Marine pollution bulletin.

Barsi, J. A., Barker, J. L., & Schott, J. R. (2003a). An atmospheric correction parameter calculator for a single thermal band earth-sensing instrument. In Geoscience and Remote Sensing Symposium, 2003. IGARSS'03. Proceedings. 2003 IEEE International (Vol. 5, pp. 3014-3016). IEEE.

Barsi, J. A., Schott, J. R., Palluconi, F. D., Helder, D. L., Hook, S. J., Markham, B. L., & O'Donnell, E. M. (2003b). Landsat TM and ETM+ thermal band calibration. Canadian Journal of Remote Sensing, 29(2), 141-153.

Bauman, A. G., Feary, D. A., Heron, S. F., Pratchett, M. S., & Burt, J. A. (2013). Multiple environmental factors influence the spatial distribution and structure of reef communities in the northeastern Arabian Peninsula. Marine Pollution Bulletin, 72(2), 302-312.

Beger, M., & Possingham, H. P. (2008). Environmental factors that influence the distribution of coral reef fishes: modeling occurrence data for broad-scale conservation and management. Marine Ecology-Progress Series-, 361, 1.

Bellwood, D. R., Hughes, T. P., Folke, C., & Nyström, M. (2004). Confronting the coral reef crisis. Nature, 429(6994), 827-833.

Bello-Pineda, J., Ponce-Hernández, R., & Liceaga-Correa, M. A. (2006). Incorporating GIS and MCE for suitability assessment modelling of coral reef resources. Environmental monitoring and assessment, 114(1-3), 225-256.

Booij, N., Ris, R. C., & Holthuijsen, L. H. (1999). A third‐generation wave model for coastal regions: 1. Model description and validation. Journal of Geophysical Research: Oceans (1978‐2012), 104(C4), 7649-7666.

Bortone, S. A. (Ed.). (2014). Interrelationships Between Corals and Fisheries. CRC Press. p. 221.

Carrascal, L. M., Galván, I., & Gordo, O. (2009). Partial least squares regression as an alternative to current regression methods used in ecology. Oikos, 118(5), 681-690.

Connell, J. H. (1978). Diversity in tropical rain forests and coral reefs. Science, 199(4335), 1302-1310.

Couce, E., Ridgwell, A., & Hendy, E. J. (2012). Environmental controls on the global distribution of shallow□water coral reefs. Journal of Biogeography, 39(8), 1508-1523.

Dai, C.-F., (1993). Patterns of Coral Distribution and Benthic Space Partitioning on the Fringing Reefs of Southern Taiwan. Marine Ecology, 14: 185–204. doi: 10.1111/j.1439-0485.1993.tb00479.x

Davies, A. J., Wisshak, M., Orr, J. C., & Murray Roberts, J. (2008). Predicting suitable habitat for the cold-water coral *Lophelia pertusa* (Scleractinia). Deep Sea Research Part I: Oceanographic Research Papers, 55(8), 1048-1062.

Dollar, S. J. (1982). Wave stress and coral community structure in Hawaii. Coral Reefs, 1(2), 71-81.

Done, T. J. (1982). Patterns in the distribution of coral communities across the central Great Barrier Reef. Coral Reefs, 1(2), 95-107.

Done, T. (2011). Coral reef, definition. Encyclopedia of Modern Coral Reefs: Structure, Form and Process, 261-267.

Dunbar, R. B., Wellington, G. M., Colgan, M. W., & Glynn, P. W. (1994). Eastern Pacific sea surface temperature since 1600 AD: The δ18O record of climate variability in Galápagos corals. Paleoceanography, 9(2), 291-315.

Edmunds, P. J., & Gray, S. C. (2014). The effects of storms, heavy rain, and sedimentation on the shallow coral reefs of St. John, US Virgin Islands. Hydrobiologia, 734(1), 143-158.

English, S, C Wilkinson and V Baker (1997). Survey Manual for Tropical Marine Resources. Townsville, Australia, Australian Institute of Marine Science, Townsville Australia: pp. 378

Fabricius, K. E., De'Ath, G., Puotinen, M. L., Done, T., Cooper, T. F., & Burgess, S. C. (2008). Disturbance gradients on inshore and offshore coral reefs caused by a severe tropical cyclone. Limnology and Oceanography, 53(2), 690.

Fisher, J. I., & Mustard, J. F. (2004). High spatial resolution sea surface climatology from Landsat thermal infrared data. Remote Sensing of Environment, 90(3), 293-307.

Gates RD, Baghdasarian G, Muscatine L. (1992). Temperature stress causes host cell detachment in symbiotic cnidarians: implications for coral bleaching. Biol Bull 182:324-332

Gillis, L. G., Bouma, T. J., Jones, C. G., van Katwijk, M. M., Nagelkerken, I., Jeuken, C. J. L., & Ziegler, A. D. (2014). Potential for landscape-scale positive interactions among tropical marine ecosystems. Marine Ecology Progress Series, 503, 289-303.

Glynn, P. W., & Stewart, R. H. (1973). Distribution of coral reefs in the Pearl Islands (Gulf of Panama) in relation to thermal conditions. Limnol. Oceanogr, 18(3), 307-379.

Glynn, P. W., & Wellington, G. M. (1983). Corals and coral reefs of the Galápagos Islands. Univ of California Press.

Gourlay, M. R. (1996). Wave set-up on coral reefs. 1. Set-up and wave-generated flow on an idealised two dimensional horizontal reef. Coastal Engineering, 27(3), 161-193.

Graham, N. A., Chong-Seng, K. M., Huchery, C., Januchowski-Hartley, F. A., & Nash, K. L. (2014). Coral Reef Community Composition in the Context of Disturbance History on the Great Barrier Reef, Australia. PloS one, 9(7), e101204.

Green, E. P., Mumby, P. J., Edwards, A. J., & Clark, C. D. (2005). Remote sensing handbook for tropical coastal management.

Harvell, C. D. *et al.* (2002). Climate warming and disease risks for terrestrial and marine biota. Science 296, 2158−2162

Hasegawa, H., & Yamano, H. (2004). Ishigaki Island. Coral reefs of Japan. Ministry of the Environment, Tokyo, 212-218.

Hearn, C., Atkinson, M., & Falter, J. (2001). A physical derivation of nutrient-uptake rates in coral reefs: effects of roughness and waves. Coral Reefs, 20(4), 347-356.

Hill, J. and Wilkinson, C.R., (2004). Methods for Ecological Monitoring of Coral Reefs: A Resource for Managers. Australian Institute of Marine Science. 117 p.

Hoegh-Guldberg O., (2006). Complexities of coral reef recovery. Science 311:42-43.

Hongo, C., & Kayanne, H. (2009). Holocene coral reef development under windward and leeward locations at Ishigaki Island, Ryukyu Islands, Japan. Sedimentary Geology, 214(1), 62-73.

Hongo, C., Kawamata, H., & Goto, K. (2012). Catastrophic impact of typhoon waves on coral communities in the Ryukyu Islands under global warming. Journal of Geophysical Research: Biogeosciences (2005–2012), 117(G2).

Hongo, C., & Yamano, H. (2013). Species-specific responses of corals to bleaching events on anthropogenically turbid reefs on Okinawa Island, Japan, over a 15- year Period (1995–2009). PloS one, 8(4), e60952.

Hsu, T. J., Elgar, S., & Guza, R. T. (2006). Wave-induced sediment transport and onshore sandbar migration. Coastal Engineering, 53(10), 817-824.

Huston, M. A. (1999). Local processes and regional patterns: appropriate scales for understanding variation in the diversity of plants and animals. Oikos, 393-401.

International Navigation Association, & Environmental Commission. (2010). Dredging and Port Construction Around Coral Reefs (No. 108). PIANC.

Iryu, Y., Nakamori, T., Matsuda, S., & Abe, O. (1995). Distribution of marine organisms and its geological significance in the modern reef complex of the Ryukyu Islands. Sedimentary Geology, 99(3), 243-258.

Johnson, J.E. & PA Marshall (2007). Climate change the Great Barrier Reef: A vulnerability assessment. Great Barrier Reef Marine Park Authority. Townsville, Australia.

Jokiel, P. L., & Coles, S. L. (1977). Effects of temperature on the mortality and growth of Hawaiian reef corals. Marine Biology, 43(3), 201-208.

Kawana, T., and Nakata, T. (1994). Timing of late Holocene tsunamis originated around the southern Ryukyu islands, Japan, deduced from coralline tsunami deposits. 地學雜誌, 103(4), 352-376.

Kayanne, H. (1996). Response: coral reefs and carbon dioxide. Science, 271(5253), 1299-1300.

Kilar, J. A., & McLachlan, J. (1989). Effects of wave exposure on the community structure of a plant-dominated, fringing-reef platform: Intermediate disturbance and disturbance-mediated competition. Marine ecology progress series. Oldendorf, 54(3), 265-276.

Kleypas, J.A., McManus, J.W., Menez, L.A.B. (1999). Environmental limits to coral reef development: where do we draw the line? Am Zool 39:146-159.

Lesser, M.P. and Farrell, J.H., (2004). Exposure to solar radiation increases damage to both host tissues and algal symbionts of corals during thermal stress. Coral Reefs 23: 367-377.

Lewis, J. B. (1974). The importance of light and food upon the early growth of the reef coral *Favia fragum*. Journal of Experimental Marine Biology and Ecology, 15(3), 299-304.

Longuet-Higgins, M. S., & Stewart, R. W. (1964). Radiation stresses in water waves; a physical discussion, with applications. In Deep Sea Research and Oceanographic Abstracts (Vol. 11, No. 4, pp. 529-562). Elsevier.

Lowe, R. J., Falter, J. L., Bandet, M. D., Pawlak, G., Atkinson, M. J., Monismith, S. G., & Koseff, J. R. (2005). Spectral wave dissipation over a barrier reef. Journal of Geophysical Research: Oceans (1978–2012), 110(C4).

Lugo-Fernandez, A., Roberts, H. H., & Wiseman Jr, W. J. (1998). Tide effects on wave attenuation and wave set-up on a Caribbean coral reef. Estuarine, Coastal and Shelf Science, 47(4), 385-393.

Maina, J., Venus, V., McClanahan, T. R., & Ateweberhan, M. (2008). Modelling susceptibility of coral reefs to environmental stress using remote sensing data and GIS models. Ecological modelling, 212(3), 180-199.

Margolin, C. L., (2012). Interactive Effects of Water Flow and Light Levels with Decreasing pH on the Growth and Survival of Tropical Cnidarians. Open Access Dissertations. University of Miami Paper 919.

Massel, S. R., & Done, T. J. (1993). Effects of cyclone waves on massive coral assemblages on the Great Barrier Reef: meteorology, hydrodynamics and demography. Coral Reefs, 12(3-4), 153-166.

McCree, K. J. (1972). Test of current definitions of photosynthetically active radiation against leaf photosynthesis data. Agricultural Meteorology, 10, 443-453.

McCulloch, M., Fallon, S., Wyndham, T., Hendy, E., Lough, J., & Barnes, D. (2003). Coral record of increased sediment flux to the inner Great Barrier Reef since European settlement. Nature, 421(6924), 727-730.

Moberg, F., & Folke, C. (1999). Ecological goods and services of coral reef ecosystems. Ecological economics, 29(2), 215-233.

Mundy, C. N., & Babcock, R. C. (1998). Role of light intensity and spectral quality in coral settlement: implications for depth-dependent settlement?. Journal of Experimental Marine Biology and Ecology, 223(2), 235-255.

Raj, K. B. G., & Fleming, K. (2008). Surface Temperature Estimation from Landsat ETM Data for a part of the Baspa Basin, NW Himalaya, India. Bulletin of Glaciological Research, 25, 19-26.

Rinkevich, B., & Loya, Y. (1984). Does light enhance calcification in hermatypic corals?. Marine Biology, 80(1), 1-6.

Risk, M. J. (2014). Assessing the effects of sediments and nutrients on coral reefs. Current Opinion in Environmental Sustainability, 7, 108-117.

Rodolfo-Metalpa, R., Martin, S., Ferrier-Pagès, C., & Gattuso, J. P. (2010). Response of the temperate coral Cladocora caespitosa to mid-and long-term exposure to pCO2 and temperature levels projected for the year 2100 AD. Biogeosciences, 7(1), 289-300.

Roy, K. J., & Smith, S. V. (1970). Sedimentation and coral reef development in turbid water: Fanning Lagoon. Hawaii Institute of Geophysics Contribution, (358).

Sorensen, R. M. (2006). Basic coastal engineering (Vol. 10). Springer.

Spalding, M.D., C. Ravilious and E.P. Green. (2001). World atlas of coral reefs. UNEP World Conservation Monitoring Center, University of California Press, Berkeley, USA, 424 p.

Storlazzi, C. D., Field, M. E., Dykes, J. D., Jokiel, P. L., & Brown, E. (2002). Wave control on reef morphology and coral distribution: Molokai, Hawaii. In Waves 2001 Conference Proceedings (Vol. 1, pp. 784-793).

SWAN Team. (2013). User manual: SWAN Cycle III version 40.91ABC Available from http://swanmodel.sourceforge.net/online_doc/swanuse/swanuse.htm

Thomas CD, Cameron A, Green RE, Bakkenes M, Beaumont LJ, Collingham YC, Erasmus BFN, de Siqueira MF, Grainger A, Hannah L, Hughes L, Huntley B, van Jaarsveld AS, Midgley GF, Miles L, Ortega-Huerta MA, Townsend Peterson A, Phillips OL, Williams SE (2004) Extinction risk from climate change. Nature 427:145-148.

Trisakti, B., Sulma, S., & Budhiman, S. (2004, October). Study of Sea Surface Temperature (SST) using Landsat-7/ETM (in Comparison with sea surface temperature of NOAA-12 AVHRR). In Proceedings The Thirteenth Workshop of OMISAR (WOM-13) on Validation and Application of Satellite Data for Marine Resources Conservation. Denpasar.

Uhrin, A. V., & Schellinger, J. (2011). Marine debris impacts to a tidal fringing-marsh in North Carolina. Marine pollution bulletin, 62(12), 2605-2610.

Veron, J. E. (2011). Corals: biology, skeletal deposition, and reef-building. In Encyclopedia of Modern Coral Reefs (pp. 275-281). Springer Netherlands.

Wiberg, P. L., & Sherwood, C. R. (2008). Calculating wave-generated bottom orbital velocities from surface-wave parameters. Computers & Geosciences, 34(10), 1243-1262.

Wild, C., Huettel, M., Klueter, A., Kremb, S. G., Rasheed, M. Y., & Jørgensen, B. B. (2004). Coral mucus functions as an energy carrier and particle trap in the reef ecosystem. Nature, 428(6978), 66-70.

Wilkinson, C. (Ed.). (2008). Status of coral reefs of the world: 2008 (p. 298). Townsville: Global Coral Reef Monitoring Network.

Wloczyk, C., Richter, R., Borg, E., & Neubert, W. (2006). Sea and lake surface temperature retrieval from Landsat thermal data in Northern Germany. International Journal of Remote Sensing, 27(12), 2489-2502.

Yamano, H., Kayanne, H., Yonekura, N., Nakamura, H., & Kudo, K. (1998). Water circulation in a fringing reef located in a monsoon area: Kabira Reef, Ishigaki Island, Southwest Japan. Coral Reefs, 17(1), 89-99.

Yamano, H., Kayanne, H., Yonekura, N., & Kudo, K. (2000). 21-year changes of backreef coral distribution: causes and significance. Journal of coastal research, 99-110.

Yoshioka, P. M., & Yoshioka, B. B. (1989). Effects of wave energy, topographic relief and sediment transport on the distribution of shallow-water gorgonians of Puerto Rico. Coral Reefs, 8(3), 145-152.